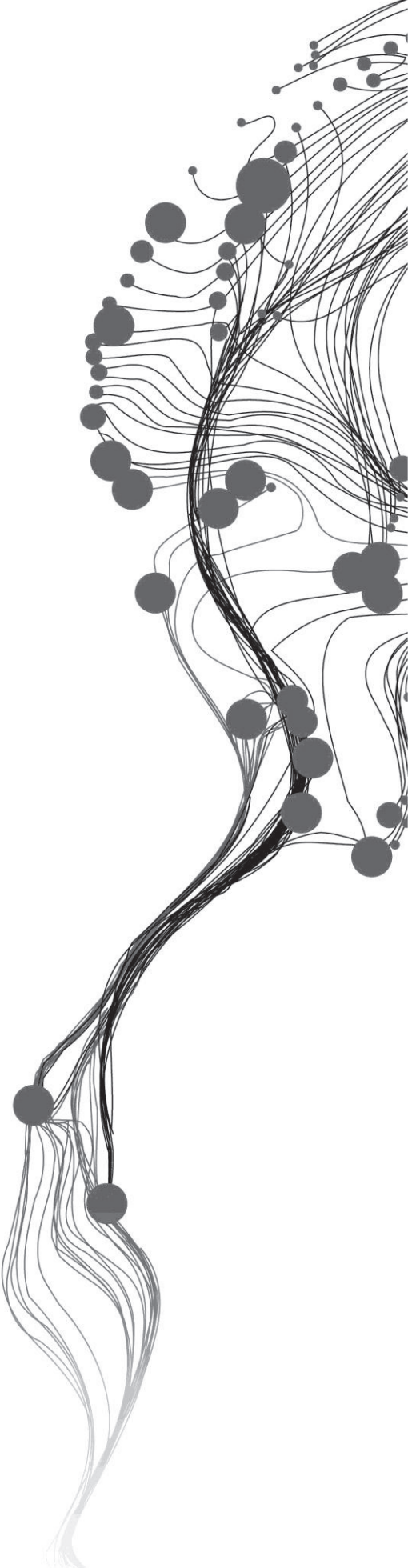


FOREST INVENTORY PARAMETERS AND CARBON MAPPING FROM AIRBORNE LIDAR

VINOD KUMAR
February, 2012

SUPERVISORS:
Dr. Yousif Hussin
Dr. H.A.M.J. Hein van Gils



FOREST INVENTORY PARAMETERS AND CARBON MAPPING FROM AIRBORNE LIDAR

VINOD KUMAR

Enschede, The Netherlands, February, 2012

Thesis submitted to the Faculty of Geo-Information Science and Earth Observation of the University of Twente in partial fulfilment of the requirements for the degree of Master of Science in Geo-information Science and Earth Observation.

Specialization: Natural Resources Management

SUPERVISORS:

Dr. Yousif Hussin

Dr. H.A.M.J. Hein van Gils

THESIS ASSESSMENT BOARD:

Dr. A.G. Toxopeus

Dr. Ir. R. van der Velde (ITC)

DISCLAIMER

This document describes work undertaken as part of a programme of study at the Faculty of Geo-Information Science and Earth Observation of the University of Twente. All views and opinions expressed therein remain the sole responsibility of the author, and do not necessarily represent those of the Faculty.

ABSTRACT

Sustainable decision making incorporating biological, ecological, social and economic component of forestry is reliant on precision forestry. As forest covers extensive landholdings, accurate, timely, repeatable, detailed and spatially explicit forest inventory characterisation and structural information are highly desirable for precision forestry needs. Light detection and ranging (LiDAR), a relatively recent active remote sensing technology, can provide accurate appraisal of vertical forest canopy structure. Individual tree and stand-level physical attributes such as height, vertical structure, canopy closure, and density can be retrieved from LiDAR data. In the present research, a novel method to precisely detect individual trees from high density airborne LiDAR point cloud data has been tested. Tree Canopies are delineated using object based image analysis and a new approach of Thiessen polygons. Further an array of important tree parameters such as tree height, canopy projection area (CPA), canopy base height, canopy volume, canopy density, canopy gaps, local tree density and canopy inclination have been extracted from the LiDAR point cloud data to prepare geospatial forest inventory. The research also deals with tree species classification based on query method on structural tree parameters in inventory database. Lastly, the sequestered forest carbon in the study area has been assessed by developing regression equation from the extracted parameters. Tree peaks were detected with high accuracy of 96 %, while best crown segmentation accuracy for Region growing segmentation approach was 84 % with 93.5 % one to one (1:1) correspondence. Thiessen polygon segmentation approach proved to be a good estimator of CPA with 94.2 % 1:1 correspondence and it could explain reference CPA with $R^2=0.9$, $RMSE=3.2$ m². Tree height was extracted with $R^2=0.86$, $RMSE=0.86$ m while canopy base height was extracted with an accuracy of $R^2=0.73$, $RMSE=0.86$ m. Species classification was achieved with an overall accuracy of 97 %. The best carbon model using extracted parameters had accuracy of $R^2=0.78$, $RMSE=0.23$ kg. In this research, LiDAR has emerged as a potential technology to fulfil the needs of precision forestry.

Key words: Forest inventory, Tree crown delineation, Region growing, Thiessen polygon, Object based image analysis

ACKNOWLEDGEMENTS

I would like to express my sincere gratitude to Forest department, Haryana, India for permitting me to join MSc course and upgrade my skills. I hope the skills gained here would be an asset to the department in effective forest management. I am sincerely thankful to Ministry of Personnel and Training, Government of India for providing funds for this course.

I am especially thankful to my first supervisor Dr. Yousif Hussin for introducing me the subject and for his untiring support, guidance and encouragement throughout the research work. Thanks go to my second supervisor Dr. H.A.M.J. Hein van Gils for thought provoking discussions and valuable suggestions during my research. I will remain indebted to both my supervisors for the time, space and energy given to me for the successful completion of this thesis.

My sincere thanks to Dr. M. J.C. Weir, Course Director, NRM for his cooperation and support throughout the course. I am thankful to Mr. Grigorijs Goldbergs for his kind help and guidance in ortho-rectification of the aerial photographs. My sincere gratitude to Dr. M. W. Menno Straatsma for sharing some valuable discussions. A special thanks to Mr. Khamarrul Azahari Razak for his kind help and support during the field campaign.

To my fellow NRM students Ameya Gode, Fatemeh Hatami, Wouter Beukema, Nguyet Dang, Yogendra Karna, Pema Wangda and all others, it has been a pleasure and memorable experience working with you and sharing diverse cultures from all around the world. I am thankful to my friend Remi Chandran for his encouragement and support during my stay here.

Finally, my deepest gratitude to my parents for their constant care and affection during my stay in Enschede. My wife Dr. Anshu needs a special mention as it was her boundless love and care that I am able to complete this research. Last but not the least, my deepest love to my sweet daughters Avi and Vaani for patiently waiting for me. I missed you a lot.

TABLE OF CONTENTS

1.	INTRODUCTION.....	1
1.1.	Background.....	1
1.2.	Overview of LiDAR technology	3
1.3.	LiDAR for biomass.....	4
1.4.	Conceptual framework for carbon estimation	5
1.5.	Problem Statement and justification	6
1.5.1.	Individual tree delineation	6
1.5.2.	Delineation using LiDAR data.....	7
1.5.3.	Forest Inventory.....	7
1.5.4.	New approaches.....	8
1.5.5.	Justification	8
1.6.	Research Objectives	8
1.6.1.	Main Objective	8
1.6.2.	Specific Objectives.....	8
1.7.	Research Questions.....	9
1.8.	Hypothesis	10
1.9.	Thesis outline	10
2.	Description of the study area.....	11
2.1.	Climate.....	11
2.2.	Land Cover	11
2.3.	Trees & Forests.....	11
2.3.1.	<i>Pinus nigra</i> Arnold (Le Pin noir)	11
2.3.2.	<i>Pinus sylvestris</i> L. (Le Pin sylvestre)	11
2.3.3.	<i>Pinus uncinata</i> Mill. ex Mirb.(Le Pin à crochet).....	12
2.3.4.	<i>Picea abies</i> L. (Karsten)	12
2.3.5.	<i>Larix decidua</i> Miller	12
2.4.	Geology and Geomorphology	12
3.	Description of methods and data used	14
3.1.	Dataset.....	14
3.2.	LiDAR data	15
3.3.	Field material.....	17
3.4.	Processing software.....	17
3.5.	Sampling design	17
3.6.	Methodology	18
3.7.	Grid size for Digital Elevation Models.....	20
3.8.	DSM, DTM, nDSM and normalized point cloud generation	20
3.8.1.	DSM.....	21
3.8.2.	DTM	21
3.8.3.	Normalised point cloud	21
3.8.4.	CHM	22
3.9.	Tree Peak identification.....	23
3.9.1.	Smooth CHM.....	23
3.9.2.	Smooth CHM with varying degree of smoothness	24
3.9.3.	Finding local maxima in CHM using ArcGIS.....	24
3.9.4.	Selecting local maxima for tree locations	24

3.9.5. Validation of Tree peak identification	25
3.10. Preparing inter canopy gaps mask	25
3.10.1. Method.....	25
3.11. Tree Crown Segmentation	26
3.11.1. Tree crown delineation using Region growing approach in eCognition.....	26
3.11.2. Thiessen polygons segmentation.....	27
3.11.3. Method.....	27
3.12. Validation of tree crown delineation.....	28
3.12.1. Visualising segmented trees in point cloud.....	29
3.13. Tree Parameter extraction for geospatial forest inventory.....	29
3.13.1. Tree Height.....	29
3.13.2. CPA.....	31
3.13.3. Canopy Volume.....	32
3.13.4. Canopy Base Height (CBH).....	34
3.13.5. Canopy tilt.....	34
3.13.6. Canopy Orientation.....	35
3.13.7. Canopy density.....	36
3.13.8. Elevation, Slope and Aspect.....	37
3.13.9. Average CPA height.....	37
3.13.10. Canopy diameter.....	37
3.13.11. Perimeter, Semi Major and Minor axis.....	37
3.13.12. Centroid of the crown segment.....	37
3.13.13. Local tree density.....	38
3.13.14. Local canopy gaps (LCG).....	39
3.13.15. Canopy Shape.....	40
3.13.16. Landuse.....	40
3.13.17. Stable and Unstable area.....	41
3.14. Species Classification.....	41
3.15. Allometric Equation.....	41
3.16. Regression analysis.....	41
4. RESULTS.....	43
4.1. Descriptive Analysis of field data.....	43
4.2. Peak detection.....	44
4.3. Tree Crown delineation.....	46
4.3.1. Tree crown delineation using Region growing approach in eCognition.....	46
4.3.2. Tree crown delineation using Thiessen polygons.....	47
4.3.3. Comparison of delineated crowns from Region growing and Thiessen polygons approaches.....	48
4.3.4. Species classification.....	48
4.4. Tree Height.....	51
4.5. Canopy Base Height.....	51
4.6. CPA.....	52
4.7. Canopy tilt.....	52
4.8. Application of inventory data.....	53
4.8.1. Open canopies.....	53
4.8.2. Close canopies.....	54
4.8.3. Canopy tilt.....	56
4.8.4. Variation in tree parameters due to aspect.....	56

4.9.	Descriptive statistics of study area from inventory data.....	59
4.10.	Tree height profile in the study area	59
4.11.	Regression analysis	60
4.11.1.	Model 1 (CPA and Height).....	60
4.11.2.	Model 2 (Canopy Volume and Height)	61
4.11.3.	Model 3 (CPA, Height, LTD).....	63
4.11.4.	Selecting best model for Carbon estimation.....	64
5.	Discussion.....	66
5.1.	Tree Peak identification.....	66
5.1.1.	Fixed size window.....	68
5.1.2.	Variable size window.....	68
5.1.3.	Reasons for good accuracy.....	68
5.1.4.	Limitation of the method	68
5.1.5.	Sources of error.....	69
5.2.	Delineation of tree crowns	69
5.2.1.	Visualising segmented trees in point cloud.....	70
5.3.	Species classification	70
5.3.1.	Limitation	71
5.4.	Extracted parameters	72
5.4.1.	Height	72
5.4.2.	CPA.....	73
5.4.3.	Canopy Volume.....	73
5.4.4.	Canopy base height.....	73
5.4.5.	Canopy tilt.....	73
5.5.	Forest inventory.....	74
5.5.1.	Open canopies.....	74
5.5.2.	Close canopies	75
5.6.	Descriptive statistics of extracted parameters	75
5.7.	Carbon Modelling.....	75
6.	Conclusions and recommendations.....	77
6.1.	Conclusion.....	77
6.2.	Recommendation	78

LIST OF FIGURES

Figure 1. LiDAR scanning (Source: USGS)	3
Figure 2. Conceptual diagram for biomass/ carbon estimation using high density airborne LiDAR data.....	5
Figure 3. 3D visualization of the study area terrain	12
Figure 4. Study area, Bois noir, Barcelonnette, France.....	13
Figure 5 . Cross sectional view of LiDAR point cloud over a water stream.	14
Figure 6. Sample aerial photograph of the study area.....	14
Figure 7. 3D view of LiDAR point cloud of the study area	15
Figure 8. Flowchart of research methodology	19
Figure 9. 3D Digital Terrain Model (DTM) of part of the study area.	22
Figure 10. 3D Digital Surface Model (DSM) of part of the study area.....	22
Figure 11. (a) CHM, (b) Point Cloud & Normalised point cloud	23
Figure 12 (a)Thiessen polygons Segmentation of tree crowns,	27
Figure 13. Difference in CHM peak and Smooth CHM peak	30
Figure 14. Canopy surfaces	32
Figure 15. (A) Tree point cloud, (B) Canopy top enveloping surface, (C) Tree with its enveloping surface	32
Figure 16. (A) Tree point cloud, (B) Canopy bottom touching surface, (C) Tree with its bottom touching surface.....	33
Figure 17. Canopy Base Height (CBH).....	34
Figure 18 Schematic diagram of a tilted tree.....	35
Figure 19 Location of tree peak (point P) and centroid on CPA (Point C).....	36
Figure 20 Local tree density	38
Figure 21. Canopy gap percentage around 1m buffer	39
Figure 22. Descriptive statistics of sampled trees.....	43
Figure 23. Frequency of the sampled tree species.....	43
Figure 24. Tree Parameters Distribution (a) DBH, (b) Height, (c) Crown Diameter, (d) Carbon	44
Figure 25. (a) sCHM3 (3.9.2), (b) sCHM9 (3.9.2), (c) Peaks detected in sCHM9, (d) Final peaks	45
Figure 26. (a) Region growing segmentation on pre-determined tree peaks, (b) Polygon smoothing on segmentation.....	46
Figure 27. A subset of tree point cloud of 1000 randomly selected trees from segments of Region growing approach.....	47
Figure 28. (a) Thiessen segmentation on the CHM, (b) Thiessen segmentation overlay on the ortho-image.....	48
Figure 29. Delineated crowns of Region Growing (a) and Thiessen polygons (b) approaches.....	48
Figure 30. Species classification in Bois noir forests, Barcelonnette, France.	49
Figure 31. Tree species distribution in the study area.....	50
Figure 33. R ² for LiDAR derived CBH.....	51
Figure 32. Scatter plot for CHM height.....	51
Figure 34. Relation of Region Growing CPA with manually delineated CPA	52
Figure 35. Scatter plot of canopy tilt and field measured tree tilt at 2 m from base of tree.....	53
Figure 36. Extracted point cloud of tilted trees with canopy tilt < 70 degree.....	53
Figure 37. Open canopies in landslide and non-landslide zones	54
Figure 38. Close canopies in landslide and non-landslide zones.....	55

Figure 39. Distribution of tilted trees.....	57
Figure 40. Variation in tree parameters due to aspect	58
Figure 41. Tree height profile of the study area.....	59
Figure 42. Reference and predicted carbon in training and validation data sets (Model 1).....	61
Figure 43. Reference and predicted carbon in training and validation data sets (Model 2).....	63
Figure 44. Reference and predicted carbon in training and validation data sets (Model 3).....	64
Figure 45. Carbon map for <i>Pinus uncinata</i> and <i>Pinus sylvestris</i>	65
Figure 47. Point cloud visualisation on the basis of elevation, returns, classification and intensity	67
Figure 46. <i>Larix</i> tree with 55,654 LiDAR hits	67
Figure 48. (a) Region growing segmentation (b) Thiessen segmentation.....	69
Figure 49. (a) Thiessen segmentation (b) Region growing segmentation	70

LIST OF TABLES

Table 1 ASPRS Standard LiDAR point classes	16
Table 2 Summary of LiDAR point cloud for the study area	16
Table 3. List of software used in this research.....	17
Table 4. List of tree parameters extracted for forest inventory	30
Table 5. Tree canopy shape and Volume. <i>Source</i> : USGS	40
Table 6. Number of peaks detected in smooth CHM with varying degree of smoothness.....	45
Table 7. D Values (Segmentation error) for Region growing and Thiessen polygons segmentation	46
Table 8. 1:1 correspondence for segmentation accuracy of Region growing and Thiessen polygons.....	47
Table 9. Species classification accuracy.....	Error! Bookmark not defined.
Table 10. R ² for LiDAR derived heights	51
Table 11. Accuracies of CPA obtained from Region growing and Thiessen polygons segmentation approaches	52
Table 12. Open canopy distribution.....	54
Table 13. Distribution of trees with close canopies.....	56
Table 14. Distribution of tilted trees	56
Table 15. Mean height and CPA of trees in Northern and Southern aspect.....	56
Table 16. Descriptive Statistics of extracted parameters in the study area.....	59
Table 17. Summary statistics of parameters used in the model 1.	60
Table 18. Correlation matrix (Model 1)	60
Table 19. Goodness of fit statistics (Model 1).....	60
Table 20. Model 1 Parameters	61
Table 21. Summary statistics of parameters used in the model 2.	62
Table 22. Correlation matrix (Model 2)	62
Table 23. Goodness of fit statistics (Model 2).....	62
Table 24. Model 2 Parameters	62
Table 25. Goodness of fit statistics (Model 3).....	63
Table 26. Model 3 parameters.	64
Table 27. Carbon estimation of Pines in the study area.....	65

LIST OF APPENDICES

Appendix 1. Barcelonnette catchment, (B). Location of field plots for tree sampling in Bois noir forests, Barcelonnette, France. I to VI: Field photographs (source: (Azahari Razak et al., 2010))	88
Appendix 2. Ruleset for Region Growing in eCognition.....	89

LIST OF ACRONYMS

Acronym	Definition
AGB	Above Ground Biomass
ALS	Airborne laser scanning
CAMPINO	Collapsing and merging procedures in octree-graphs
CBH	Canopy Base Height
CD	Canopy Diameter
CHM	Canopy Height Model
CO ₂	Carbon dioxide
CPA	Canopy Projection Area
CS	Canopy Shape
CV	Canopy Volume
DBH	Diameter at breast height
DEM	Digital Elevation Model
DSM	Digital Surface Model
DTM	Digital Terrain Model
FAO	Food And Agriculture Organization
FARSITE	Fire behaviour and fire growth simulator
GIS	Geographic Information Systems
GLAS	Geoscience Laser Altimeter System
GLONASS	Global Navigation Satellite System
GPS	Global Positioning System
HDAL	High Density Airborne LiDAR
IMU	Inertial Measurement Unit
InSAR	Interferometric Synthetic Aperture Radar
IPCC	Intergovernmental Panel On Climate Change
ISPRS	International Society for Photogrammetry and Remote Sensing
LAS	LASer File Format
LiDAR	Light Detection And Ranging
LTD	Local Tree Density
LCG	Local Canopy Gaps
MAPE	Mean Absolute Percentage Error
MSE	Mean Square Error
MSS	Mean Sum of Squares
NASA	National Aeronautics And Space Administration
nDSM	Normalised Digital Surface Model
NSIDC	National Snow And Ice Data Center
OBIA	Object based image analysis
ONF	Office National des Forêts
R ²	Coefficient of determination
REDD	Reducing carbon emission form deforestation and forest degradation
RMSE	Root Mean Square Error
SAR	Synthetic Aperture Radar
SkelTre	Tree skeletonization software

LIST OF ACRONYMS (contd.)

SPSS	Statistical Package for the Social Sciences
TLS	Terrestrial Laser Scanning
UNFCCC	United Nations Framework Convention on Climate Change
USGS	United States Geological Survey
VHF	Very High Frequency
VHR	Very high resolution

1. INTRODUCTION

1.1. Background

Forests, which occupy 31 per cent of the total land area of the world, sequester about 289 giga tonnes (Gt) of atmospheric carbon to their biomass alone (FAO, 2010). Deforestation and forest degradation alone account for 30% of the anthropogenic carbon emission (Goetz et al., 2009). The role of forest in reducing the atmospheric level of CO₂ has been emphasised in United Nations Framework Convention on Climate Change (UNFCCC) and its Kyoto Protocol, which requires signatory countries to quantify their carbon stocks and its changes. The United Nations REDD (Reducing Emissions from Deforestation and Forest Degradation) programme offers incentives for developing countries to reduce emissions from forested lands by creating a financial value for the carbon stored in forests. Thus, with increasing commitment to climate change initiatives, there exists a greater requirement for precise estimates of biomass and forest productivity (Patenaude et al., 2005).

Conventionally, the biomass has been estimated by field measurement based methods such as destructive sampling, allometric equations or conversion from volume to biomass (Houghton, 2005; Lu, 2006). These methods are the most accurate ways of biomass estimation but they require sufficient number of field measurements for developing above ground biomass estimation models (Houghton, 2005; Lu, 2006). However, these approaches are time consuming, labour intensive, highly expensive and destructive. Moreover, they are difficult to implement in remote and inaccessible areas; also they are unsuitable for providing biomass distribution over large areas. GIS based methods, using ancillary data like elevation, slope, soil, precipitation, etc. are also difficult in absence of good quality ancillary data, and because of the indirect relationship between ancillary data and biomass, and the comprehensive impact of environmental factors on biomass accumulation (Brown & Gaston, 1995; Lu, 2006). Remote sensing based biomass estimation has increasingly attracted scientific interest because of provision of systematic, repetitive and consistent data collection, a synoptic view in a digital format allowing fast processing of large data and the presence of correlations between spectral bands and vegetation parameters (Lu, 2006; Patenaude et al., 2005).

Radar system can collect Earth feature data irrespective of weather or light conditions which makes it very suitable for the areas persistently covered by cloud (Lu, 2006). Radar has been used for biomass assessment since late 1980 especially with L and P-band and cross polarized images. Previous research has shown the potential of radar data in estimating AGB (Castel et al., 2002; Hussin et al., 1991; Santos et al., 2002; Sun et al., 2002; Treuhaft et al., 2004). Different radar data have their own characteristics in relating to forest stand parameters (Leckie & Ranson, 1998). For example, radar backscatter in the P and L bands

is highly correlated with major forest parameters, such as tree age, tree height, DBH, basal area, and AGB. In particular, SAR L-band data have proven to be valuable for AGB estimation (Luckman et al., 1997; Sader, 1987; Sun et al., 2002). However, low or negligible correlations were found between SAR C-band backscatter and AGB (Le Toan et al., 1992). Beaudoin et al. (1994) found that the HH-polarised return was related to both trunk and crown biomass, and the VV and HV-polarised returns were linked to crown biomass. Radar data collected over mountainous area with steep slopes provides much higher backscattering on slopes facing the radar antenna than with same cover type in flat terrain. However, the radar data suffers from saturation problem which depends on wavelength, polarization, vegetation stand structural characteristics and ground conditions.

Light detection and ranging (LiDAR) is a relatively recent active remote sensing technology that operates in the visible or near infrared portion of the electromagnetic spectrum (Heritage et al., 2009). LiDAR data can provide accurate appraisal of vertical forest canopy structure (Lim et al., 2003), but are somewhat limited in the two-dimensional spectral domain (Kebiao et al., 2010). Passive optical data provide extensive coverage of generalized structural classes in the horizontal plane but are relatively insensitive to measure individual structural components in a vertical plane (Goetz et al., 2009). Individual tree and stand-level physical attributes such as height, vertical structure, canopy closure, and density can be generated from LiDAR data (Kebiao et al., 2010; Lim et al., 2003) and correlated with density and horizontal canopy parameters from high-resolution optical data.

No single sensor data is capable of giving infallible assessment for forest biomass (Goetz et al., 2009), especially in areas with complex forest stand structures and environmental conditions (Lu, 2006). The combination of high-resolution data from optical imagers and LiDAR systems permits individual tree and canopy height information to be extracted along with the species, health, and other biophysical tree attributes (Kim et al., 2010; Lim et al., 2003; Pilger, 2008). A relationship of vertical forest structure, obtained from LiDAR, with digital spectral values of optical images over species specific validation sites may then be extrapolated from local to regional and finally to national coverage (Li, 2009), substantially reducing the cost associated with field validation sites and improving on existing inventory methods.

Space borne LiDAR system is a reality. The Geoscience Laser Altimeter System (GLAS) on the NASA Ice, Cloud and land Elevation Satellite (ICESat) launched in 2003 has provided a view of the Earth in three dimensions with unprecedented accuracy (Schutz et al., 2005). The GLAS laser transmits short pulses (4 nanoseconds) of infrared light at 1064 nm and visible green light at 532 nm 40 times per second and collects data at full waveform. The spatial resolution of the disk illuminated by the laser is 70 meters in diameter and spaced at 170-meter intervals along the Earth's surface (NSIDC, 2011). ICESat/GLAS has also been used to derive biomass parameters and canopy height for large areas (Kebiao et al., 2010; Lefsky et al., 2005; Pang et al., 2006). In near future commercial space borne LiDAR, providing global coverage

may be a reality, reducing the cost of LiDAR data substantially (Hudak et al., 2002; Lefsky et al., 2002). It is envisaged that the models developed for estimation of biomass using high density airborne LiDAR (HDAL) then become an important and practical tool for low cost accurate biomass assessment for large forest area.

1.2. Overview of LiDAR technology

LiDAR (Light Detection And Ranging) is one of the active optical remote sensing technologies to collect topographic data. It works similar to Radar (Radio Detection and Ranging) but instead of radio waves, LiDAR systems emit laser light. LiDAR transmits laser pulses to the ground surface; the pulses are reflected from the surface back to the laser system. Based on the speed of light, the distance to the ground hit point can be calculated. LiDAR can provide highly accurate measurements of both forest canopy and the ground surface. It provides data that make it possible to detect and isolate individual trees and calculate attributes describing their size and form of individual trees. Airborne laser scanning systems have four major hardware components: (1) laser scanner, (2) differential global positioning systems (GPS;

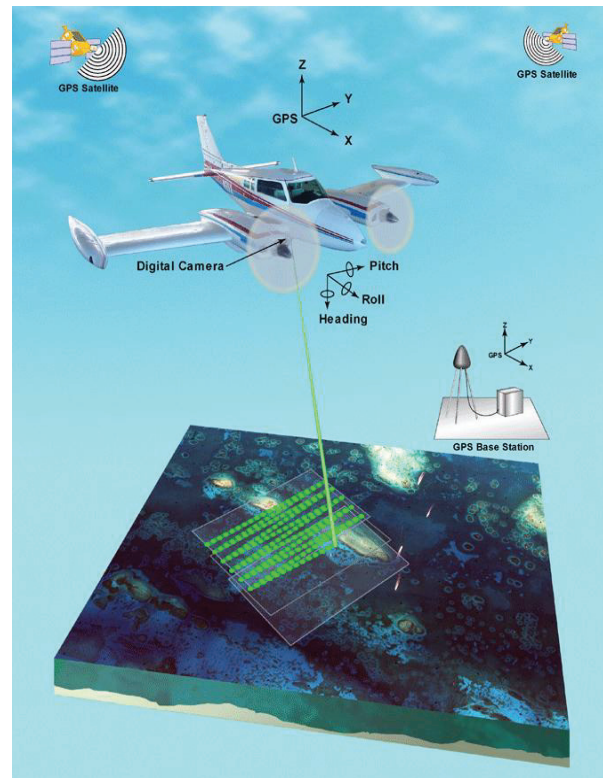


Figure 1. LiDAR scanning (Source: USGS)

aircraft and ground units), (3) a highly sensitive inertial measurement unit (IMU) attached to the scanning unit, and (4) on-board computer to control the system to store data from the first three components (Figure 1). The position and attitude of the scanner at the time each pulse is emitted are determined from data collected by the GPS and IMU units. LiDAR systems used for topographic mapping applications usually operate in the near infrared range of the spectrum (700-1200 nm). The most commonly used lasers system emits light is at a wavelength of 1064 nm. Most systems have the capability of acquiring multiple measurements (i.e., 2-5 per laser pulse). The scan angle is typically limited to 15 - 20 degrees off-nadir allowing systems to acquire measurements along a “swath” beneath the aircraft (Figure 1). LiDAR systems have a beam divergence of approximately 0.25- 4 mrad; therefore, the “footprint” of the LiDAR pulse when it reaches the ground (or canopy surface) is approximately 15 - 90 cm in diameter, depending upon flying height. For topographic mapping applications, LiDAR data are acquired in leaf-off conditions to maximize the percentage of pulses that reach the ground surface. For canopy mapping or studying forest

attributes, data are acquired in leaf-on conditions to maximize laser returns from tree crowns and forest structures (McGaughey & Carson, 2003).

Scanning laser systems may be mounted on different platforms: on a tripod (terrestrial LiDAR system), on aircraft (airborne LiDAR system), or on satellite (space-borne LiDAR system) (Heritage et al., 2009). Ground-based laser scanning is used to capture very high-resolution data describing architectural details in construction projects. Ground-based laser scanning systems have been used in forestry research, and they can provide detailed reconstructions of trunk, branch and leaf distribution from which tree locations, diameter and height, timber volume and canopy gap fraction can be quantified (Danson et al., 2008; Hopkinson et al., 2004; Li, 2009; Litkey et al., 2008), but the complexity of forest scenes makes analysis very complicated. Space-borne LiDAR system have often been used in atmospheric research and a few large-scale ecosystem studies (Boudreau et al., 2008; Large et al., 2009; Lefsky et al., 2002). Due to limited data availability and coarse resolution, there are not many studies that apply space-borne LiDAR data for forest inventory (Pflugmacher et al., 2008). Airborne LiDAR systems are commercially available and have been used to map and model terrain elevation. In the past two decades, airborne LiDAR systems have been used to model forest canopy structure and function, mostly in the scientific research projects (Andersen et al., 2003; Drake et al., 2001; Holmgren & Persson, 2004; Lefsky et al., 1999; Lefsky et al., 2002; Lim et al., 2003; Means et al., 1999; Naesset et al., 2004). There are also some efforts to promote airborne LiDAR system in operational forest inventory, especially in Scandinavia counties (Næsset, 2007).

1.3. LiDAR for biomass

An overview on the status of small footprint, multiple point or fullwave form of LiDAR data for general forest applications is provided by (Hyypä et al., 2009), (Koch, 2010) as well as by (Mallet & Bretar, 2009). They show that the information related to height or structure of forests can be extracted with high quality. There exist several approaches to estimate biomass from LiDAR data. One of the pioneering studies is from (Nelson et al., 1988) using the tree height as a LiDAR derived parameter. Most authors concentrate on the above-ground biomass (Lefsky et al., 1999). Lefsky et al (2001) explained 84% of the aboveground biomass variance by regression from the LiDAR measured canopy structure. Overall, the study gives a good overview for large-area carbon storage estimation. (Popescu, 2007) managed to explain 93% of the biomass using individual tree metrics. The only known study focusing on the below-ground biomass is from (Naesset et al., 2004), in which they used regression methods to explain 86% of the below-ground and 92% of the above-ground biomass. For biomass estimation from LiDAR data, the indirect approach is often chosen. This means that tree heights are first calculated from LiDAR (Nelson et al., 1988), and then wood volume is modelled based on this (Straub et al., 2009) and finally expansion factors are applied to estimated biomass. (Maltamo et al., 2009) combined LiDAR in a two-stage stratified sampling, showing an RMSE of 18% for biomass and carbon estimation.

1.4. Conceptual framework for carbon estimation

Assessment of biomass/carbon estimation of the forest has recently gained more importance in the wake of global warming issues, UNFCCC's Kyoto protocol and emerging carbon trade (Rosenqvist et al., 2003). The emphasis has shifted to 'accuracy' of carbon estimation when sequestered forest carbon has monetary value in international carbon markets. Remote sensing techniques to estimate forest carbon had been quite helpful to assess forest biomass/carbon estimation for large areas. Gibbs et al. (2007) reviewed the uncertainties in estimation of biomass for different methods such as forest inventory, biomes averages, optical remote sensing, Radar and LiDAR based active remote sensing. LiDAR and high resolution optical images have shown low to medium level of uncertainty (Gibbs et al., 2007). Fusion of LiDAR with VHR optical image has shown to give promising results of biomass estimation (Chen & Chiang, 2005; Deng et al., 2007; Erdody & Moskal, 2010; Heinzel et al., 2008; Huber et al., 2003; Kebiao et al., 2010; Kim et al., 2010; Mumtaz & Mooney, 2008; Popescu et al., 2004; Zaremba & Gougeon, 2006). The present research becomes relevant here for assessing the accuracy of carbon estimation from high density airborne LiDAR data. The conceptual diagram showing relevance of proposed research is given in Figure 2.

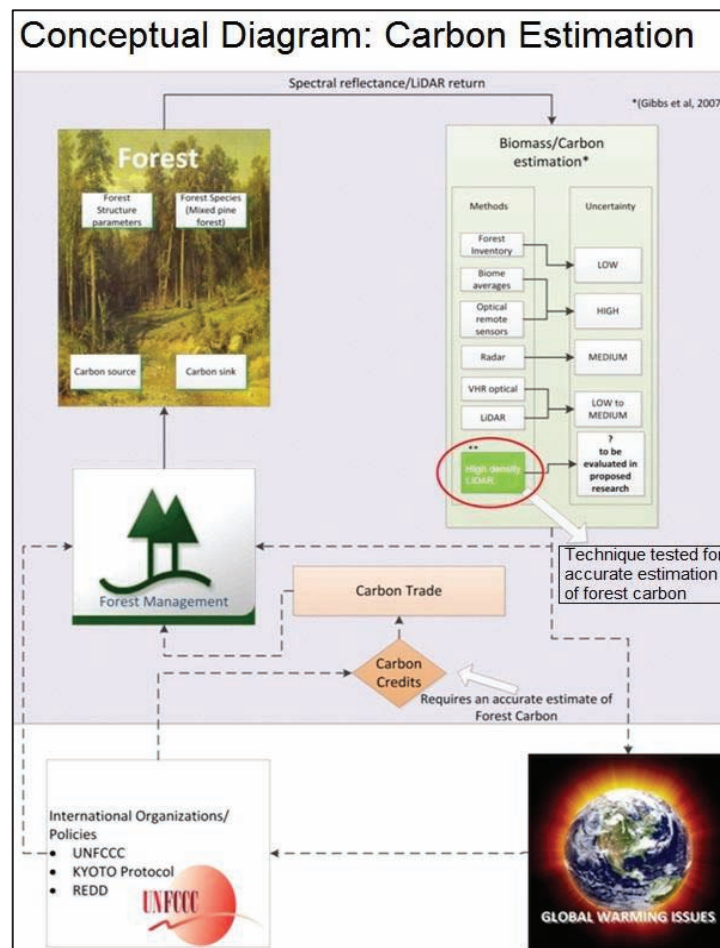


Figure 2. Conceptual diagram for biomass/carbon estimation using high density airborne LiDAR data..

1.5. Problem Statement and justification

Structural descriptions of forests, such as plant height, canopy width, canopy cover, biomass, vertical and horizontal heterogeneity, are essential to understand how forest ecosystems function and help to advance studies of the global carbon cycle (Means et al., 1999). Moreover, these structural parameters are critical to study biogeochemical cycles, water budgets, sun radiation energy transfer in the forest system. (Lefsky et al., 2002; Lim et al., 2003). LiDAR technology has been demonstrated to permit such three-dimensional measurements of the forest canopy (Lim et al., 2003) with accuracies rivalling those of field based measurements. Accurate forest inventory is crucial to forest resource management and wildlife habitat assessment (Innes & Koch, 1998; Lefsky et al., 2002). An accurate assessment of forest biomass and carbon is a pressing requirement for many countries due to developing carbon trade and international obligation of United Nations Framework Convention on Climate Change (UNFCCC) and its Kyoto Protocol. Before airborne LiDAR became available, aerial photogrammetry and InSAR had been used to extract forest structural information at various scales ranging from individual trees to landscapes (Sheng et al., 2001; Sun et al., 2002). However, these methodologies require matching multi-angular images and it is often difficult to obtain reliable results especially in hilly areas.

1.5.1. Individual tree delineation

The individual tree-based delineation approach was introduced by Samberg and Hyypä (1999) using multispectral images (Kim et al., 2010; Koch et al., 2006). Many algorithms for delineation of individual tree crowns were developed using high resolution spectral images (Brandtberg et al., 2003; Gougeon, 1995; Wulder et al., 2000) such as the valley-following method (Gougeon, 1995), multiple scale edge segmentation (Brandtberg & Walter, 1998), template matching (Pollock & Woodham, 1996), watershed segmentation (Schardt et al., 2002) and local maxima filtering (Dralle & Rudemo, 1996). Wulder et al. (2000) adopted local maximum filtering approach to locate trees on high resolution imagery. Among these methods, watershed segmentation, as proposed by Beucher and Lantuejoul (1979), is a well-known method that incorporates the advantages of many other image segmentation methods, such as the Region growing and edge detection methods (Soille, 2003). However, in these cases, the accuracy of delineating individual trees is relatively low due to the broad variation of spectral values in forest areas on the satellite images (Schardt et al., 2002). Although simple smoothing methods, such as Gaussian filtering, can reduce the depth of pits and small peaks, the technique remains unable to fully remove commission or omission errors. Therefore, for these methods, over-segmentation problems remain (Chen et al., 2006). To avoid the problem of over-segmentation, Meyer and Beucher (1990) introduced marker-controlled watershed segmentation, as a technique well-fitted for tree isolation (Chen et al., 2006). Images indicating the locations of markers are named as marker functions, and images for producing watersheds are named segmentation functions (Chen et al., 2006). With appropriate markers and segmentation functions, marker-controlled watershed segmentation can be used to delineate the boundaries of individual tree crowns. Wang et al. (2004) used a marker controlled watershed segmentation technique to extract crown

size and detect treetops based on high spatial resolution aerial imagery. These methods are based on optical imagery and assumed that treetops and crowns have higher reflected radiation because they expose more sunlit surface. However, treetop reflectance is dependent on Sun angle and weather conditions, therefore under cloudy imaging conditions or with dense canopy closure, treetops are difficult to identify, even visually.

1.5.2. Delineation using LiDAR data

LiDAR is an active ranging technique that can directly measure 3D forest canopy coordinates at laser illuminated locations. The high density LiDAR point cloud of the forest area contain rich forest structural information (Hyypä et al., 2008). Popescu (2003) explored the feasibility of LIDAR data for estimating tree crown diameters using variable window size techniques as well as other LiDAR measured parameters such as tree height and number of trees, and used a regression model to retrieve crown diameter to estimate forest biomass and stand volume. Bortolot (2006) adopted an object-oriented method using tree clusters as objects to assess canopy cover and density. Koch et al. (2006) used a pouring algorithm to delineate crown shape based on treetops detected by local maximum filtering algorithm. Chen et al. (2006) adopted watershed segmentation to isolate individual trees and proposed an improved watershed segmentation algorithm with a distance-transformed image to reduce inadequate segmentation. In most cases, individual tree-based research using laser data focused on estimating forest parameters (Persson et al., 2002; Popescu et al., 2003). All of these methods rely on computer vision techniques based on two dimensional optical image processing. The low density of the LiDAR point cloud is the limiting factor to the accuracy of crown shape delineation. There has still been limited research on tree crown delineation and extraction of forest parameters using high density airborne LiDAR data.

1.5.3. Forest Inventory

Sustainable decision making incorporating biological, ecological, social and economic component of forestry is reliant on precision forestry. As forest covers extensive landholdings, accurate, timely, repeatable, detailed and spatially explicit forest inventory characterisation and structural information are highly desirable for precision forestry needs. Advance remote sensing technologies have emerged as viable and effective monitoring tool to fulfil the needs of precision forestry. In recent years, the remote sensing technology has progressed towards making use of monitoring methodologies as the fundamental geospatial database deliverable for decision support tools. Such tools are needed in production forestry, wildlife and forest health management, estimating sequestered carbon, understanding efficient and optimal water interception, distribution of wildlife habitat (Moskal et al., 2008). Among other remote sensing technologies, LiDAR technology has emerged as a promising method to estimate tree structural biophysical parameters because of its ability to provide reconstruction of vertical canopy structure. Therefore, the use of LiDAR technology for generating individual tree based geospatial forest inventory is pertinent to the need of precision forestry.

1.5.4. New approaches

All these methods discussed so far, do not provide information about 3D canopy shape and volume despite the fact that high density LiDAR data contains valuable information about it. Very little research has so far been done to extract the ground feature directly from the point cloud data. Working on 3D point cloud is computationally complex and requires new algorithms, research and software to support it. Bucksch (2008) generated tree skeletons directly from the point cloud using Terrestrial Laser Scanning (TLS) data employing CAMPINO (Collapsing and merging procedures in octree-graphs) method. Lefsky (1999), Harding (2001), and Andersen (2003) using large-footprint LiDAR data with continuous waveform, estimated vertical canopy structure of forest through group of regression equations based on field investigations. A majority of the algorithms for single tree delineation are based on Digital Surface Model (DSM) where trees are delineated according to the features of the crowns on the DSM, therefore trees in the understory may not be detected. It is of interest for forest managers to assess the regeneration success in the understory. Wang et al. (2008) developed a procedure for both vertical canopy structure analysis and 3D single tree modelling based on a LiDAR point cloud. In this method, understory trees can also be detected and their canopy volume could be assessed. Pyysalo and Hyyppa (2002) have provided a process of reconstruction of tree crowns with prior knowledge of tree location and crown size. Furthermore, a new full-waveform based algorithm to detect single tree has been presented by Reitberger et al. (2007).

1.5.5. Justification

In view of the above research methodologies, an investigation into developing an appropriate individual tree based methodology for extraction of tree parameters and assessment of forest biomass/carbon in the study area using high density airborne LiDAR is proposed.

1.6. Research Objectives

1.6.1. Main Objective

The main objective of this research is to develop methods to extract tree biophysical structural parameters for generation of geospatial forest inventory and to accurately estimate biomass/carbon stocks in the Bois noir forests in the French Alps using high density airborne LiDAR data.

1.6.2. Specific Objectives

Individual Tree Delineation

- a) To develop a method and assess its accuracy for individual tree Peak identification from LiDAR point cloud data.
- b) To assess the accuracy of CPA (Canopy Projection Area) estimation by delineating tree canopies using Thiessen polygons segmentation and Region growing segmentation method in eCognition

with prior knowledge of tree peaks locations using LiDAR derived CHM (Canopy height Model) as a basic input.

Forest Inventory

To prepare individual tree based geospatial inventory of the study area by developing methods to extract tree structural parameters such as tree height, CPA, canopy diameter, canopy base height, canopy volume, canopy density, canopy tilt from high density LiDAR point cloud data.

Species classification

To develop a method to classify *Larix deciduas*, *Pinus uncinata*, *Pinus sylvestris* in the study area using extracted tree structural parameters and to assess the accuracy of classification.

Biomass/Carbon

- a) To develop regression models for biomass/carbon estimation using (CPA + Height) and (Canopy Volume + Height) as pair of explanatory variables.
- b) To check whether inclusion of additional explanatory variables such as local tree density, local canopy gaps around each tree improve the regression model significantly.
- c) To estimate total above ground biomass/carbon of Pines in the study area and prepare a geospatial map of above ground carbon for pines in the study area.

1.7. Research Questions

1. How accurately the tree peaks can be detected in a Canopy Height Model of high density airborne LiDAR data?
2. What is the difference in segmentation methods by Object based image analysis and Thiessen polygons using airborne LiDAR data with prior knowledge of tree peaks and inter canopy gaps.?
3. How accurately the tree structural parameters such as tree height, CPA, canopy base height, tree tilt can be estimated from LiDAR point cloud data?
4. What is the accuracy of Biomass/carbon obtained from (CPA + Height) and (Canopy Volume + Height) as pair of explanatory variables in regression analysis?
5. What is the accuracy of Biomass/carbon obtained from CPA, height with additional variables such as local tree density and local canopy gaps?
6. What is the accuracy of species classification in the study area?
7. What is the relationship between CPA, height and biomass/Carbon?
8. What is the relationship between canopy volume, height and biomass/Carbon?
9. What is the amount of biomass/carbon stock of pines in the study area?

1.8. Hypothesis

1. It is possible to identify individual trees by locating tree peak points in LiDAR point cloud data.
2. Thiessen polygons can provide a significantly accurate estimation of CPA with prior knowledge of tree peaks and inter canopy gaps.
3. It is possible to extract tree structural parameters such as tree height, CPA, canopy base height, canopy volume, canopy density, canopy tilt and canopy shape from the LiDAR point cloud data with significant accuracy.
4. *Larix decidua*, *Pinus uncinata* and *Pinus sylvestris* in the study area can be isolated using tree structural parameters with significant accuracy.
5. There is a significant relationship of carbon with a pair of variables (CPA, height) and (canopy volume, height).
6. Tree canopy volume and height are better explanatory variables than CPA and height to estimate biomass/carbon.

1.9. Thesis outline

In Chapter 1, the LiDAR technology and conceptual framework for use of LiDAR data for carbon stock modelling has been introduced along with a background of application of remote sensing for biomass and carbon stock estimation. Thereafter, the research problem and research interest of this thesis have been described.

Chapter 2 briefly describes the relevant topographic, climate and vegetation characteristics of the study area.

Methods used in this research to answer research questions and achieve the research objectives are described briefly in Chapter 3. The chapter also provides information about data and materials used.

Chapter 4 consists of the results of tree peak detection, tree crown delineation approaches and its quantitative comparisons, outcomes of species classification, extraction of forest structural parameters and regression modelling for carbon from extracted parameters.

The results are discussed in Chapter 5 and conclusions from the discussion linked to research objectives and questions are drawn in Chapter 6.

2. DESCRIPTION OF THE STUDY AREA

The study area for the present MSc thesis is Bois noir (Black Wood) situated in Barcelonnette basin in the south French Alps (Figure 4). The area is characterised by irregular topography (Figure 3) with slope gradient ranging between 10° and 35°, having 92 % of forest cover of the total surface area and consisting predominantly *Pinus uncinata* with some deciduous trees (Thiery et al., 2007). Predisposing geomorphic and climatic influences triggered various types of landslides in the area mostly covered by deciduous and coniferous forests. Trees are damaged and stand distorted by recurrent landslides in this area.

2.1. Climate

The climate is characterized by strong inter-annual rainfall variability and is influenced by the dry and mountainous Mediterranean intra-Alpine zone. It has an annual rainfall which varies between 400 and 1100 mm

2.2. Land Cover

The Bois noir is mostly covered by coniferous forest (76%) followed by bare land (9%) in the South Eastern part, broad leaved forest (6%) in the Northern part, pastures (6%), and natural grassland (3%) spread over the whole area.

2.3. Trees & Forests

The details of tree species in the study area were collected from Dr. H.A.M.J. Hein van Gils during personal communication. The description of the dominant tree species is as follows.

2.3.1. *Pinus nigra* Arnold (Le Pin noir)

The Black pine (*Pinus nigra* Arnold) is indigenous in the Eastern and Central Alps, Balkan, Apennines and Corsica, where it constitutes mostly monospecific forests. The Flora Europaea does not mention The French Alp as part of the *Pinus nigra* Arnold distribution area. Plantations of Black pine, mostly for land rehabilitation, are common within and outside its natural distribution area, including the (French) Western Alps and sand dunes in the Netherlands. From plantations Black pine spontaneous disperses into the surroundings occasionally as high as the alpine tree line. The Black pine has five subspecies of which two are native in France subsp. *salzmannii* (Cevennes and Pyrenees) and subsp. *laricio* (Corsica), but are not native in the French Alps.

2.3.2. *Pinus sylvestris* L. (Le Pin sylvestre)

The Scotch pine (*Pinus sylvestris* L.) is indigenous in, among others, the montane forest belt (<1700 m a.s.l.) of the dry inner-alpine valleys and the (dry) Western Alps, mostly as a monospecific forest. The Scotch pine is distinguished from other pines by its orange and peeling bark in the upper half of the stem. The

Scotch pine in the Alps is locally infested with *Viscum album* L. In Barcelonnette this infestation is quite dramatic.

2.3.3. *Pinus uncinata* Mill. ex Mirb. (Le Pin à crochet)

The Mountain pine (*Pinus uncinata*) is found naturally at the tree line and from there down slope in scree slopes in the Pyrenees and the Western Alps. *Pinus uncinata* is aka is subspecies of *Pinus mugo*, the later found in the Central- to Eastern Alps and the Balkan in similar sites. Plantations of *Pinus uncinata* are used for land rehabilitation in France. *Pinus uncinata* is distinguishable from the other pines by the hooked bracts (scales) of its cone ('uncinata'= hooked). We have collected extremely hooked cones in pine plantations in the research area.

2.3.4. *Picea abies* L. (Karsten)

The spruce (*Picea abies*) is indigenous in Northern Europe and throughout the Alps in the montane belt often up to the tree line. It is widely planted outside its native distribution area.

2.3.5. *Larix decidua* Miller

The larch (*Larix decidua*) is a deciduous coniferous tree indigenous in the Alps and found often up to the alpine timberline also at the pass heights close to the Barcelonnette research area.

2.4. Geology and Geomorphology

The Quaternary deglaciation of Pleistocene age has contributed to the formation of the hummocky topography in the Barcelonnette basin (Hippolyte & Dumont, 2000; Thiery et al., 2003). Mass wasting processes and the formation of badlands configure the landscape in the Barcelonnette Basin (Maquaire, et al., 2003). Furrowed badlands are present in the North-West of Bois noir area (Thiery et al., 2003).

In Bois noir, two litho-morphological zones can be distinguished, the Northern zone which shows mainly black marls overlaid by morainic deposits of vary thickness up to 15 m, and the Southern zone which is formed by limestone outcrops, weathered marls, flysch, and screes (Thiery et al., 2003). The southern zone is characterized by steep slopes of up to 70° with extensive screes near the bottom.



Figure 3. 3D visualization of the study area terrain

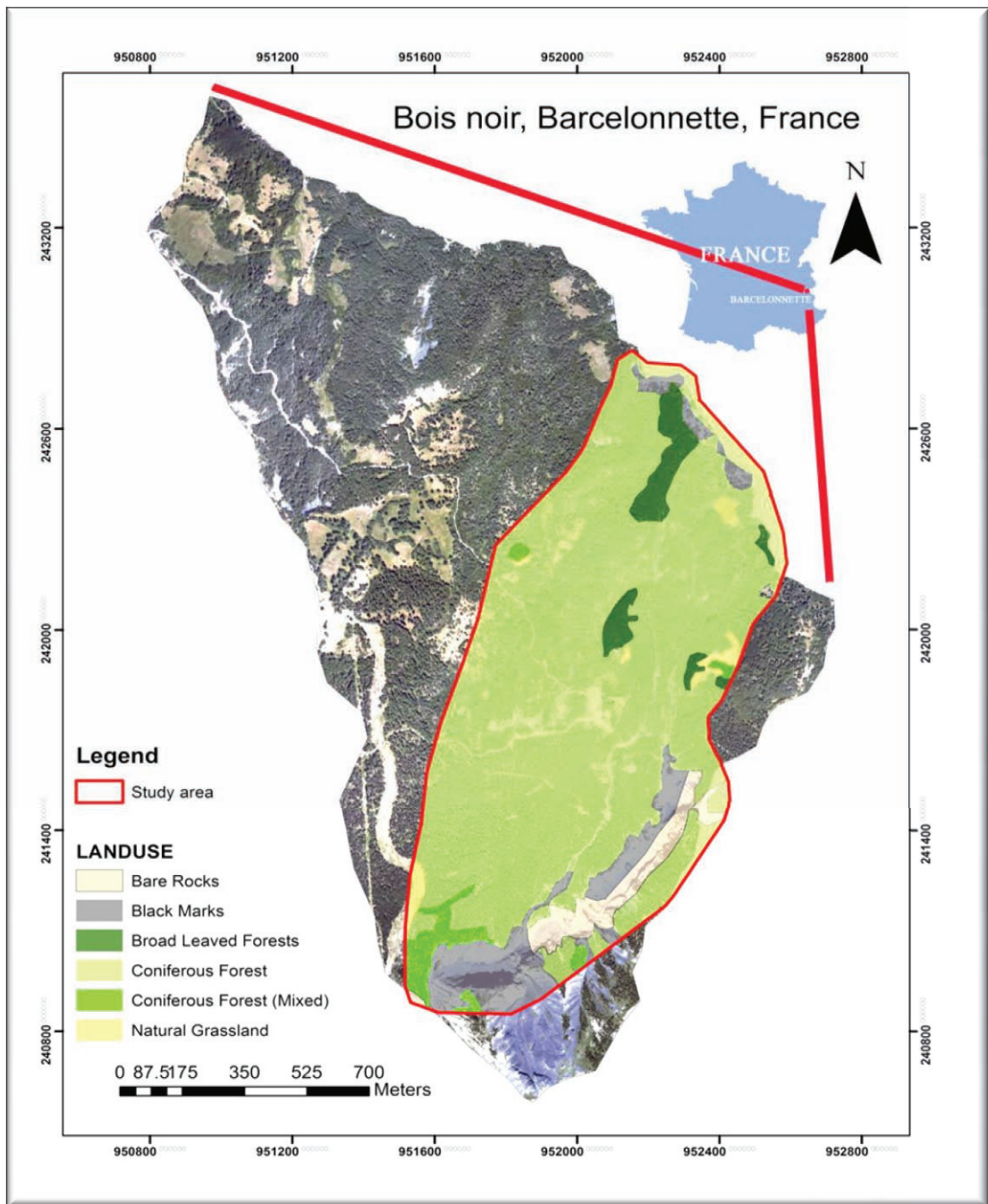


Figure 4. Study area, Bois noir, Barcelonnette, France

3. DESCRIPTION OF METHODS AND DATA USED

3.1. Dataset

The active remote sensing LiDAR data and aerial photographs for the study area were acquired in July 2009 under snow-free conditions using a helicopter flying at an altitude of 300 m above the ground. An airborne hand-held laser scanner from the Helimap Company was used during the Airborne LiDAR Scanning (ALS) campaign. This scanner has been developed specifically for the mapping over mountainous



Figure 6. Sample aerial photograph of the study area.

forested areas (Vallet and Skaloud, 2004). A RIEGL VQ-480 laser scanner with a pulse repetition rate of up to 300 kHz was used to record the LiDAR data. Spatial positioning was done using a Topcon Legacy GGD capable of tracking GPS and GLONASS positioning satellites. The orientation of the aircraft was determined using the iMAR FSAS inertial measurement unit (IMU) (see Table 1 for details). In order to increase the point density seven flight lines were flown resulting in 50 million points, with resultant mean density of 164 points/m². The last return of LiDAR pulse data had 35 million points with a mean density of 140 points/m². The aerial photographs of 30 cm resolution (Figure 6) were co-captured with the LiDAR data. The dataset was primarily acquired for the study of the landslide activities in the study area. A sample visualization of the LiDAR data is shown in Figure 5 & Figure 7.

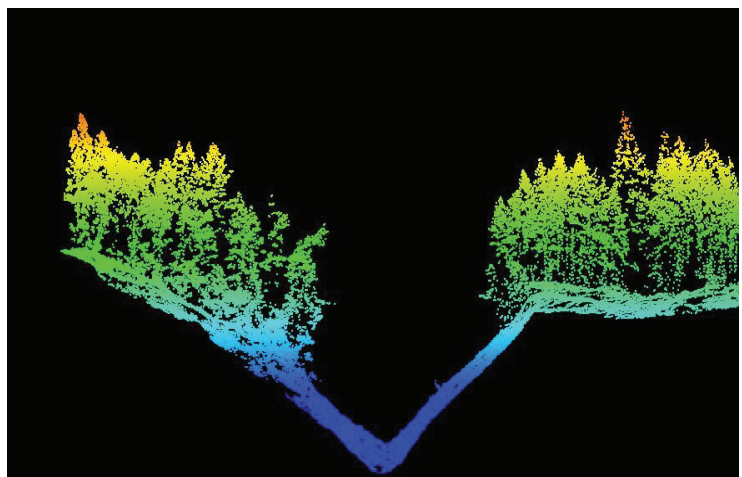


Figure 5 . Cross sectional view of LiDAR point cloud over a water stream.

Table 1: Metadata for the airborne LiDAR campaign

Acquisition (month/year)	Jul-09
Laser scanner	RIEGL VQ480i
IMU system	IMAR FSAS (record up to 500 Hz)
Positional system	Topcon legacy (record up to 5Hz)
Laser pulse repetition rate	300 kHz
Beam divergence	0.3 mrad
Laser beam footprint	75 mm at 250 m
Field of view	60°
Scanning method	Rotating multi-facet mirror

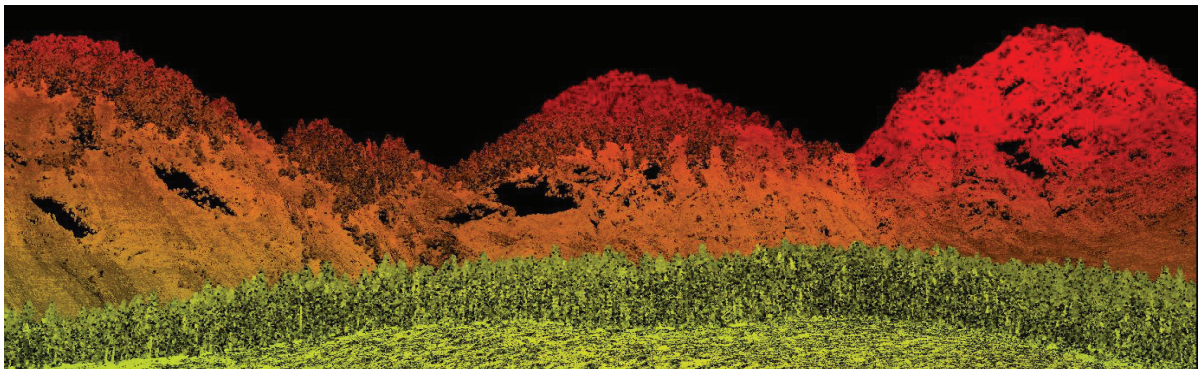


Figure 7. 3D view of LiDAR point cloud of the study

3.2. LiDAR data

The raw LiDAR data for the study area was obtained from the vendor in LAS1.2 format. The LiDAR flight data as obtained from the field was first pre-processed by the vendor using TerraScan software which combines GPS, IMU and laser pulse range data to produce (X,Y,Z) point data in LAS1.2 format. The intention of the data format is to provide an open format that allows different LiDAR hardware and software tools to output data in a common format (ASPRS, 2008). The format contains binary data consisting of a header block, variable Length Records, and point data. The header block consists of generic data such as point numbers and coordinate bounds. The variable Length Records contain various types of data including projection information and user application data. The point data contains (X,Y,Z) coordinates, intensity, return number, scan direction, edge of flight line, classification, scan angle rank, point source ID and GPS time. The classification values are standardised by the ASPRS (American Society of Photogrammetry and Remote Sensing) as shown in the

Table 1 ASPRS Standard LiDAR point classes

Classification	Meaning
0	Created, never classified
1	Unclassified
2	Ground
3	Low Vegetation
4	Medium Vegetation
5	High Vegetation
6	Building
7	Low Point (noise)
8	Model Key-point (mass point)
9	Water
10	Reserved for ASPRS definition
11	Reserved for ASPRS definition
12	Overlap points
13-31	Reserved for ASPRS definition

The LiDAR data acquired from the vendor included the classification for ground and non-ground points with classification values 2 and 0 respectively. The data was provided in 17 subsets for the study area in LAS file format. The summary of LAS data for the study area is given in Table 2.

Summary LiDAR data						
LiDAR points	Area (m ²)	Point density (points/m ²)	Ground points	Non-ground points	Ground points %	No. of returns
212,894,997	1,298,996	164	9,366,984	203,528,013	4.60	Up to 5

Table 2 Summary of LiDAR point cloud for the study area

3.3. Field material

Instruments used for field work are: iPAQ and Leica differential GPS system 1200, Suunto compass, measuring tape, slope- meter, Suunto PM5, Laser alti-meter, Caliper, increment borer and fieldwork datasheet.

3.4. Processing software

Software required for data analysis and thesis writing are given in Table 3

Table 3. List of software used in this research

<i>Software</i>	<i>Purpose of usage</i>
LAStools v111006	DSM, DTM, CHM and normalised point cloud generation
Lasutility	Generating LAS file from XYZ points
SAGA_GIS v2.0.8	Surface Interpolation methods
Quick Terrain Modeler (INTL) v7.1.4	LAS visualization
LASViewer v1.0.0	
MARS v7.0 (32-bit)	LAS visualization with shape files
LP360	Overlaying LAS with raster datasets and feature classes
LPS	Ortho-rectification of aerial photographs
ArcGIS_10	GIS (Analysis)
Erdas Imagine 10	Image processing
ENVI 4.7.2.	
R	Statistical analysis
SPSS	
XLSTAT	
Word, Excel, Powerpoint, Visio and End note	Thesis writing and editing

3.5. Sampling design

The study area is highly undulating with steep slopes and frequent landslides. Therefore, the sampling design was made to ensure access to the sampling plots. The sampling design strategy was based on plot sampling. Plots were selected on a purposive basis for taking readings in both landslide affected (unstable) and non-landslide (stable) areas in close proximity. A total of 13 plots were sampled, 6 in the unstable

areas, 7 in stable areas. The plots were evenly spread out throughout the study area leaving out broadleaved forests. Plots are shown in the **Error! Reference source not found.** The plot based sampling was done to measure tree structural attributes, namely height, diameter at breast height (DBH), canopy width, canopy base height, tree tilt, orientation and type of deformation, disease if any. These tree structural attributes were measured primarily to validate LiDAR derived tree parameters and regression models using these parameters as explanatory variable. To get the age of trees, the increment borer was used on 6 trees per plot. The borer holes were carefully filled up and sealed for the protection of the tree. Canopy width was measured in North – South direction and East to West direction with a measuring tape. Tree height and Canopy base height were measured with the laser rangefinder. DBH was measured with the help of tree caliper. Inclination and orientation of tilted trees were measured by inclinometer and compass respectively. Differential GPS, in combination with the total station was used to get the precise location coordinates of the base of the sample trees. Since Differential GPS needs open space to get enough satellite signals to work accurately, a base station in the closest open space from the plot was selected. From the base station, additional points were selected for placement of the total station with unobstructed visibility. The location of each total station point was also recorded by Differential GPS for calibration of total station readings. Each differential GPS reading took 3 hour to 12 hour to reach mm accuracy. Therefore changing the location of the total station was restricted to one to two points per plot. Consequently, trees selected for sampling were limited to clear range of visibility from the total station.

3.6. Methodology

Ortho image of the study area was prepared from mosaicking aerial photographs and ortho-rectifying in LPS plugin of Erdas Imagine 10 using LiDAR derived DTM. The obtained image was used for reference purposes. DTM, DSM and normalised point cloud were generated from processing of LiDAR data. Canopy Height Model (CHM) was obtained from subtracting DTM from DSM. Identification of tree peaks and delineation of inter canopy gaps were obtained using CHM and smooth CHM. Segmentation was done using Region growing and Thiessen Polygon approaches on the CHM by supplying information of tree peak locations and inter canopy gaps. Tree parameters were extracted from LiDAR derived layers within delineated tree crown segments. Species classification was achieved on the basis of structural and spatial differences of trees. Finally, the carbon modelling was done using selected extracted parameters as explanatory variables. The methodology for this research is described in the flowchart given in Figure 8. The detailed description is provided in the following sections.

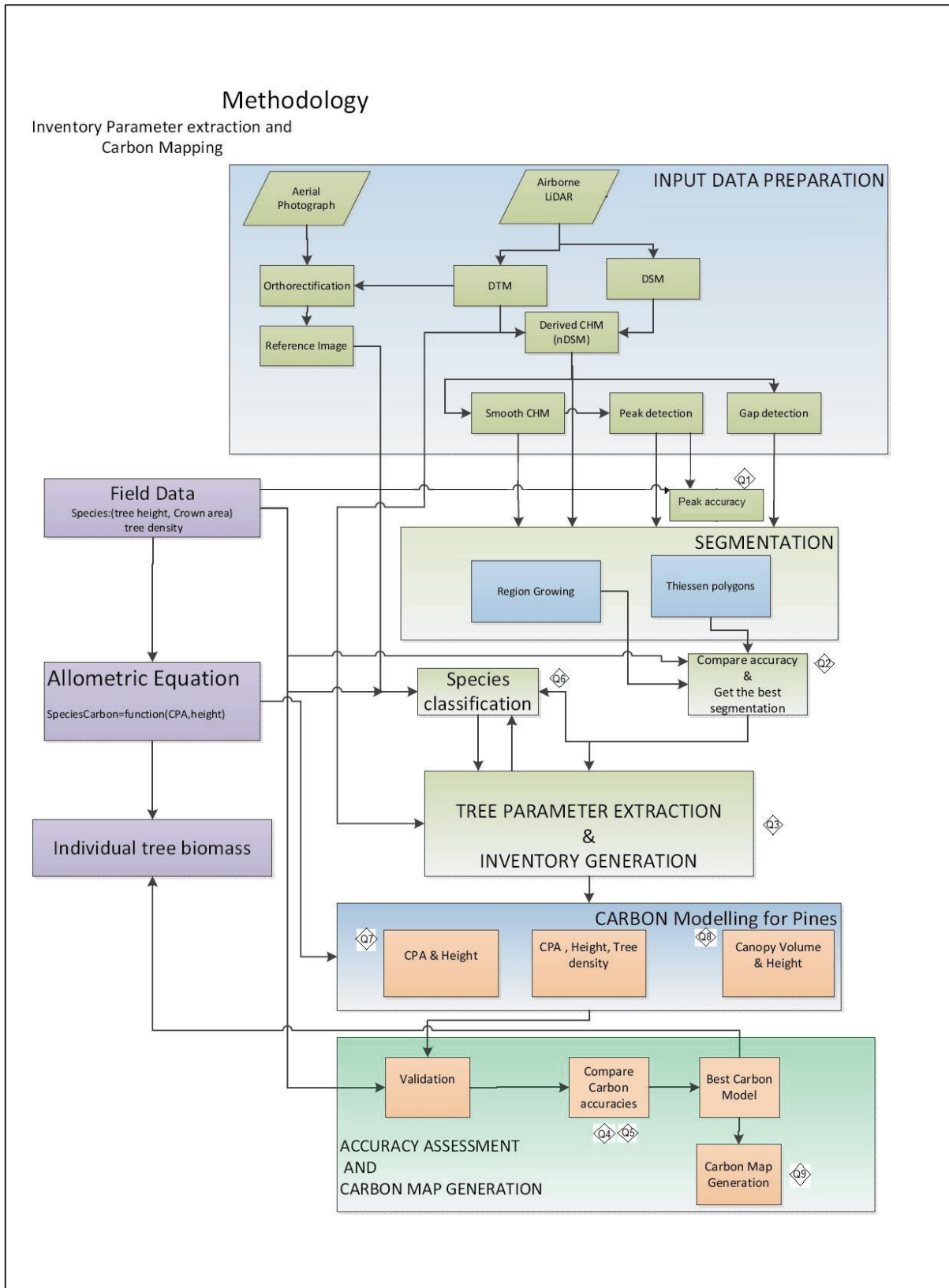


Figure 8. Flowchart of research methodology

3.7. Grid size for Digital Elevation Models

Before generating any LiDAR derived Digital Elevation Model (DEM), selection of grid size for DEM raster layer is crucial for minimizing the data loss during conversion. The optimized DEM resolution must match the density of LiDAR data and be able to reflect the variability of the terrain surface to represent the majority of terrain features (Liu, 2008). McCullagh (1988) suggested that the number of grids should be roughly equivalent to the number of LiDAR points in the covered area. The grid size (S) of a DEM can be estimated by:

$$S = \sqrt{\frac{A}{n}}$$

Where n is the number of terrain points and A is the covered area ((Hu et al., 2003)). This means that the DEM resolution should match the sampling density of the original terrain points. Average point density for the LiDAR data is 164 points/m² (Table 2).

$$S = \sqrt{\frac{1}{164}} = .078 \text{ m}$$

The grid size obtained is the minimum size of grid where the numbers of grids are equal to number of LiDAR points. In practice, LiDAR points are vertically distributed, therefore many grids will have more than one LiDAR points implying several grids with no LiDAR points. The grid size of .078 m is not practical to use because of huge storage requirement and long processing time. Another researcher (Pouliot et al., 2002) suggested that ratio of crown dia with grid size should be sufficient to define crown shape. A grid size of 0.15 m was found appropriate as for smallest measured crown (1 m dia) in the field; total number of grids used to define the crown shape is 36. Therefore, in this research for rasterizing point cloud data, 0.15 m grid size was used.

3.8. DSM, DTM, nDSM and normalized point cloud generation

The Digital Surface Model (DSM) and Digital Terrain Model (DTM) were generated using LAStools software. DSM (Figure 10) is a raster image obtained from the elevation attribute of the first return of LiDAR point cloud data, the intermediate pixels are interpolated. Interpolation is a general process of estimating the elevation at a specified grid node from measurements at surrounding point locations (El-Sheimy et al., 2005). Global interpolation methods use all of the known elevations at the reference points to estimate the unknown elevation at the reference point. Examples of global methods are: Trend surface analysis, Fourier analysis, and Kriging. DTM (Figure 9) was similarly generated from the elevation attribute of the last return of LiDAR point cloud data. Dense forest canopy do not allow full penetration of LiDAR signals to the ground, therefore all the last returns are not necessarily from the ground. Filtering is used to generate DTM, with the assumption that terrain does not change abruptly but gradually. DTM pixels are

interpolated on the basis of LiDAR return points hitting the ground by selecting minimum elevation points in a grid. The influence of forest parameters on LiDAR derived DTM has been investigated by Reutebuch et al.(2003). LiDAR data is in the form of discrete point clouds of ground features having X,Y,Z coordinates of all the points. The Z values in the LAS data contain elevation of each point. In the raw LAS file the elevation data (Z values) correspond to height from the mean sea level while in the normalised point cloud the elevation is absolute height of the point as measured from the bare ground surface. Normalised DSM (nDSM) is often referred as Canopy Height Model (CHM) (Figure 11a). It gives the absolute height of trees and was obtained through gridding normalised point cloud. Alternatively, it could also be obtained through subtracting DTM from DSM. The normalized point cloud is analogous to nDSM in the 3D cloud giving the absolute height of the ground feature (trees) on the Z-axis and was generated using lasheight tool provided in the LAStools software (Figure 11b). The detail procedure to prepare these layers is as follows;

3.8.1. DSM

Perform lasgrid in LAStools with grid size 0.15 m on point cloud data, keeping first returns and selecting highest option on elevation. →DSM (‘→’ indicates the layer generated from the operation)

3.8.2. DTM

- i. Perform lasground (LAStools) on point cloud data, selecting forest or hills option. → LasGrnd, This step will identify the ground points and classify them as value 2 in the Las file.
- ii. Perform las2dem or bast2dem in LAStools on elevation values with grid size 0.15 m on LasGrnd by selecting kill triangles > 20 and keeping classification value 2 (ground points only). →DTM

3.8.3. Normalised point cloud

- i. Perform lasheight (LAStools) on LasGrnd by selecting classification value 2 and choosing replace z option. →nLas
- ii. Perform lasheight (LAStools) on nLas by selecting classification value 2 and choosing drop points with height below 0 and height above 40 (to remove noise). → nLasCorr

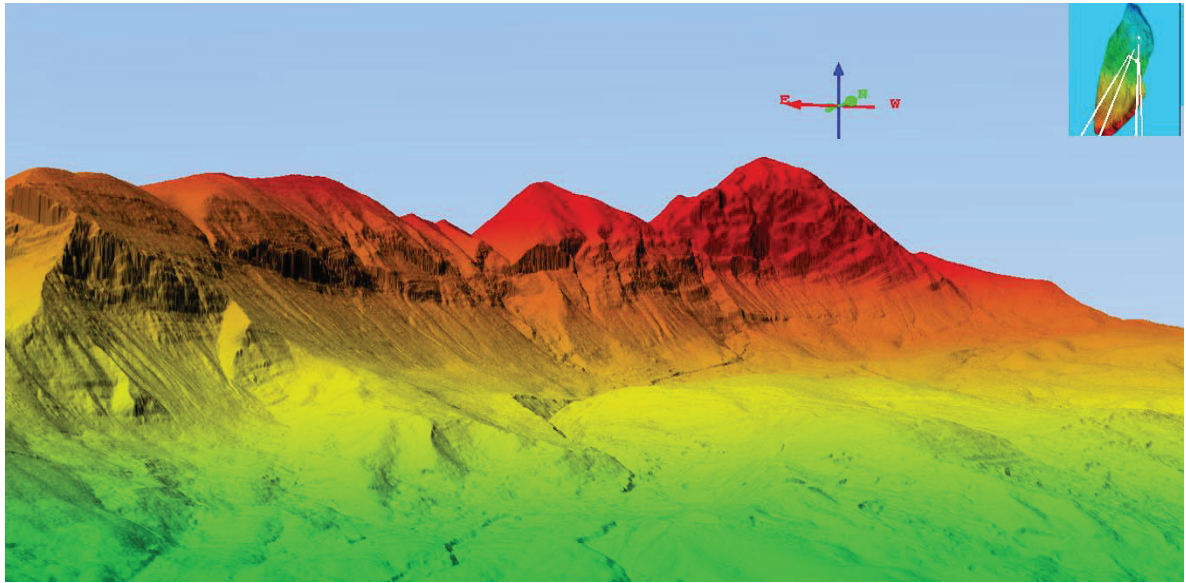


Figure 9. 3D Digital Terrain Model (DTM) of part of the study area.

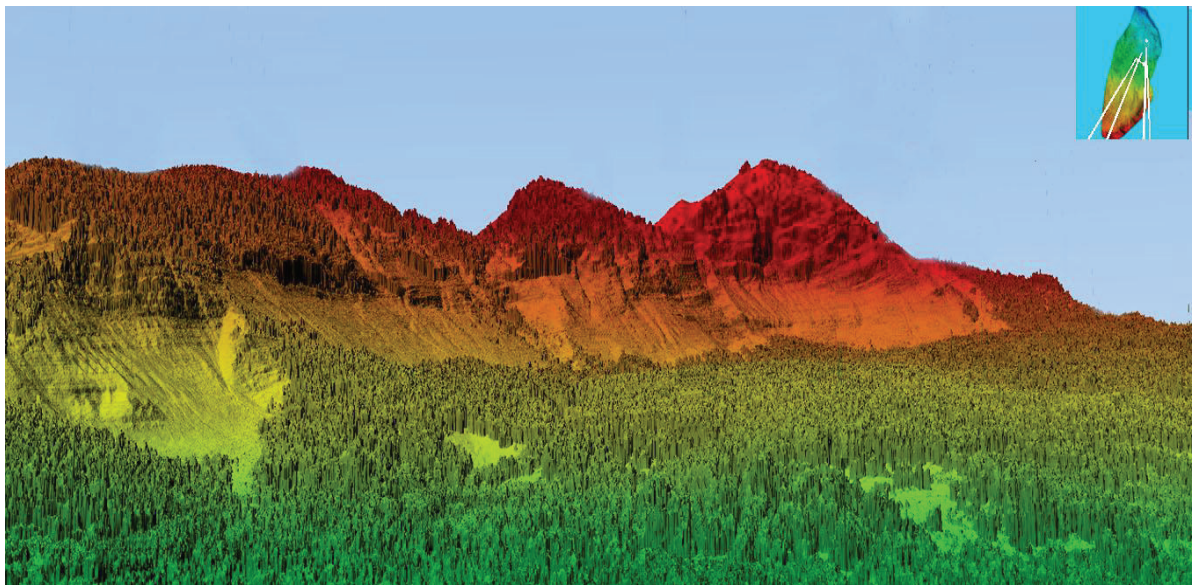


Figure 10. 3D Digital Surface Model (DSM) of part of the study area.

3.8.4. CHM

CHM was obtained from the normalised point cloud through gridding operation by selection of highest elevation within each grid of the first return with fill value of 6 pixels. CHM prepared in this way does not suffer from the aberration of the highest elevation values from corresponding values in the normalised point cloud.

Method

- i. Perform lasgrid (LAStools) with grid size 0.15 m on nLasCorr (3.8.3), keeping first returns and selecting highest option on elevation with fill of value 6 pixels. → CHM
- ii. Alternatively, subtract DTM from DSM in raster calculator (ArcGIS). → CHM

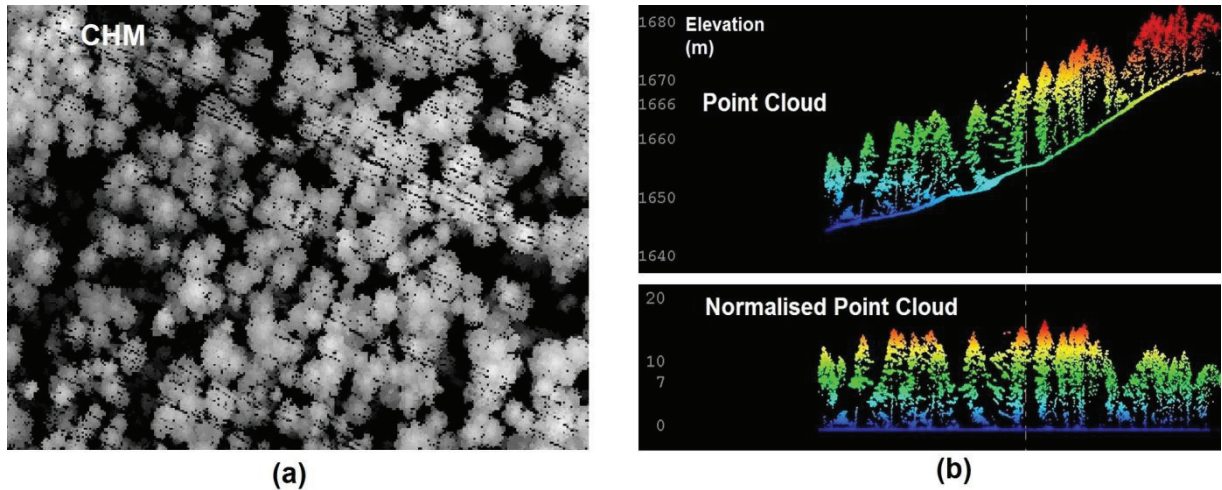


Figure 11. (a) CHM, (b) Point Cloud & Normalised point cloud

3.9. Tree Peak identification

Tree identification in the LiDAR data is crucial for tree crown segmentation and for the extraction of biophysical structural parameters of trees. In most of the cases, tree detection and crown delineation are based on local maxima of the CHM (Brandtberg et al., 2003; Hyyppä et al., 2004; Popescu et al., 2003). Popescu, et al (2003) used variable size search window based on tree height to identify local maxima. Pitkänen et al (2004) used smooth CHM with degree of smoothing defined by the heights of the pixels for finding local maxima. Rahman and Gorte (2009) used densities of high points from the high density airborne LiDAR for individual tree crown delineation. In this research, a novel adaptive method of tree detection based on variable smoothing with height retaining local maxima of CHM using fixed size search window is presented. The CHM was smoothed using Gaussian mean filter and the degree of the smoothing was defined by heights of the pixels. After the smoothing, all the pixels which experience a drop in height values were identified and replaced back with their original values before successive filtering. The smooth CHM obtained was a convex hull surface, passing through tree crown boundary points smoothly. The detail procedure adopted is as follows;

3.9.1. Smooth CHM

Following procedure was adopted to make smooth CHM with height retaining local maxima.

- i. Prepare CHM raster layer (3.8.4).

- ii. Perform focal statistics (mean) on CHM in ArcGIS by rectangular window size 3 (pixels). → CHMfs3
- iii. Compare CHMfs3 to CHM and select all the pixels in CHMfs3 which drop in their values (pixel value decreased => higher value pixel in the neighbourhood) and replace back these pixels to CHM values using command line `con(CHMfs3<CHM,CHM,CHMfs3)` in raster calculator (ArcGIS). →CHMfs3corr
- iv. Perform step (ii) and (iii) in succession 6 times using output raster of (iii) as input raster in (ii).
- v. Let the final raster be called sCHM

3.9.2. Smooth CHM with varying degree of smoothness

- i. Perform focal statistics (mean) on sCHM (3.9.1(v)) in ArcGIS by rectangular window size 3 (pixels) one time. → sCHM3
- ii. Perform focal statistics (mean) on sCHM in ArcGIS by rectangular window size 5 and 3 (pixels) in succession. → sCHM5
- iii. Perform focal statistics (mean) on sCHM in ArcGIS by rectangular window size 7 and 3 (pixels) in succession. → sCHM7
- iv. Perform focal statistics (mean) on sCHM in ArcGIS by rectangular window size 9 and 3 (pixels) in succession. → sCHM9
- v. Add a random value of the order of 10^{-4} m to all these raster layers to get sCHM3R, sCHM5R, sCHM7R, sCHM7R and sCHM9R.

3.9.3. Finding local maxima in CHM using ArcGIS

- i. Perform focal statistics (maximum) on sCHM3R (3.9.2(v)) in ArcGIS by rectangular window size 3 (pixels) → sCHM3Rmx
- ii. Perform command line, `setnull(sCHM3Rmx<2, setnull(sCHM3Rmx!=sCHM3R, sCHM3Rmx))` in raster calculator (ArcGIS) → Peaks_rast3R
- iii. Convert Peaks_rast3R to point feature to get local maxima point shape file. →Peaks3
- iv. Perform set of operations (i, ii & iii) on sCHM5R, sCHM7R, sCHM7R and sCHM9R (3.9.2(v)) to get local maxima shape files, Peaks5, Peaks7, Peaks9 respectively.

3.9.4. Selecting local maxima for tree locations

To get true peaks from Peaks3, Peaks5, Peaks7 and Peaks9 (3.9.3), we adopted the following procedure.

- i. Perform segmentation in eCognition on layer CHM (3.9.1(i)) taking peaks3 (3.9.3(iv)) as thematic layer for region grow. → seg3 (polygon shape file)
- ii. Similarly, get seg5, seg7, seg9 taking peaks5, peaks7, peaks9 (3.9.3(iv)) as thematic layers for region grow on CHM raster layer in eCognition.
- iii. Select all peaks > 20 in Peaks9 and make a layer of selection → Peaks9Gr20

- iv. Select all segments in seg9 containing Peaks9Gr20 and a make a layer of selection → seg9Gr20
- v. Delete all points of Peaks7, Peaks5, Peaks3 falling in seg9Gr20 and make new layers with remaining points. → Peaks7Lte20, Peaks5Lte20, Peaks3Lte20
- vi. Select all peaks > 16 in Peaks7Lte20 and make a layer of selection → Peaks7Gr16Lte20
- vii. Select all segments in seg7 containing Peaks7Gr16Lte20 and a make a layer of selection → seg7Gr16Lte20
- viii. Delete all points of Peaks5, Peaks3 falling in seg7Gr16Lte20 and make new layers with remaining points. → Peaks5Lte16, Peaks3Lte16
- ix. Select all peaks > 11 in Peaks5Lte16 and make a layer of selection → Peaks5Gr11Lte16
- x. Select all segments in seg5 containing Peaks5Gr11Lte16 and a make a layer of selection → seg5Gr11Lte16
- xi. Delete all points of Peaks3 falling in seg5Gr11Lte16 and make a new layer with remaining points. → Peaks3Lte11
- xii. Join layers Peaks9Gr20, Peaks7Gr16Lte20, Peaks5Gr11Lte16 and Peaks3Lte11 to get final tree peaks shape file. → **FinalPeaks**

3.9.5. Validation of Tree peak identification

The validation of tree peak identification was done on one to one (1:1) correspondence with reference tree peaks. Identified peaks which were completely contained within manually delineated reference segments of field observed tree crowns, were selected using spatial selection method in ArcGIS. Tree peaks were found matching only if there was a single peak within the reference crown segment corresponding to reference crown peak.

3.10. Preparing inter canopy gaps mask

The methodology used for preparation of canopy gaps was first to repair canopies in CHM for missing pixels by generating a smooth surface passing through the boundary points of tree crown (convex hull) and then selecting a cut-off limit (2 m) on elevation to identify gaps.

3.10.1. Method

- i. Get normalised point cloud gridded with highest elevation and clipping on z axis by 2 m without interpolating for nodata pixels. Interpolation is not used as it will have an effect of growing the size of canopies adjacent to gaps due to clipping on z axis. → Rast1.
- ii. To fill the nodata pixels in canopies, we prepared smooth CHM from Rast1 (3.9.1). → Rast2
- iii. Set the pixel value to zero for all pixels in Rast2 which are less than 2 meter. → Rast3.
- iv. A binary gap raster was prepared by putting value 0 to all pixels with elevation less than 2 m in Rast3 and value 1 for the remaining pixels.
- v. To get shape file for gaps, convert Rast3 to polygon shape file.

3.11. Tree Crown Segmentation

3.11.1. Tree crown delineation using Region growing approach in eCognition

For the delineation of individual tree crowns, object based image analysis (OBIA) is used to create objects that roughly approximated the size and shape of the individual tree crown area (Kim et al., 2009). Region growing is a bottom-up approach of object segmentation, it starts with one pixel objects and subsequently merges pairs of adjacent objects into larger objects based on the smallest growth of heterogeneity, which may be defined through spectral variance and geometry of the object (Definiens 2009). Region growing also can be done using specified seed points using rule based algorithms in eCognition. Starting at potential seed pixels, neighbouring pixels are examined sequentially and added to the growing region if they are sufficiently similar to the seed pixels (Ke & Quackenbush, 2008). In case of tree crown delineation, local maxima are used as seed to grow and local minima are used as a restriction for growing region (Culvenor, 2002).

Method

The detail rule set is given in **Error! Reference source not found.**

We used CHM (3.8.4) and sCHM5 (3.9.2) as basic raster layers for Region Grow segmentation. Final Peaks (3.9.4) shape file was used as thematic layer for tree seeds while inter canopy gaps mask (3.10) was used as another thematic layer for gap delineation. The rule set was developed to delineate tree crowns upto 2 m height. eCognition was unable to perform chessboard segmentation at the resolution of the CHM layers (15 cm) due to large requirement of memory and processing power. The best we could get was 4 pixel chessboard (60 cm) segmentation. The rule set was accordingly modified to work at finer resolution (upto 15 cm) only on edges of objects (crown and gap boundaries) where it was needed most. Gaps objects were modified gradually in eCognition from the imported objects in thematic layer by identifying pixels less than 2m in CHM. The gaps modification was required as gaps were imported from 15 cm original pixel resolution to 60 cm object resolution in eCognition, consequently making the gap edges coarser. Frequent merging of new gap objects was done to save on memory. The main steps of algorithm are as follows;

We initially allowed small tree (2-4 m) seeds to grow with gap identified in CHM for pixels less than 0.5 m before importing inter canopy gaps mask (for CHM pixel < 2 m) as thematic layer. Then all tree objects were grown from the seeds (3.9.4) with direction of grow based on homogeneity criteria in sCHM5 (3.9.2). Minima were used to control the relative growth of tree objects adjacent to it by stopping tree growth for two growth iterations. Later minima were converted back to candidate object to prevent neighbouring

objects intruding into others space. The process was stopped when there was no available candidate object to merge into growing object.

3.11.2. Thiessen polygons segmentation

Thiessen polygons define the area that is closest to each point relative to all other points. They are mathematically defined by the perpendicular bisectors of the lines between all points. Using Thiessen polygons for crown delineation is a new topic of research. In this research the hypothesis was tested that Thiessen polygons segmentation could be a significant estimator of CPA. If we take tree peaks as nodes to create Thiessen polygons, it means that within each polygon any branch or leaf of the tree is closest to its own tree trunk than any surrounding tree trunk.

3.11.3. Method

- i. Create Thiessen polygons from tree peaks shape file (3.9.4) in ArcGIS.
- ii. Clip Thiessen polygons by study area boundary.
- iii. Update polygons by inter canopy gaps shape file (3.10)using update function in ArcGIS.
- iv. Use smooth polygon in ArcGIS by setting tolerance limit to 1m and 2m in succession.

The Figure 12 shows the steps in Thiessen polygons segmentation.

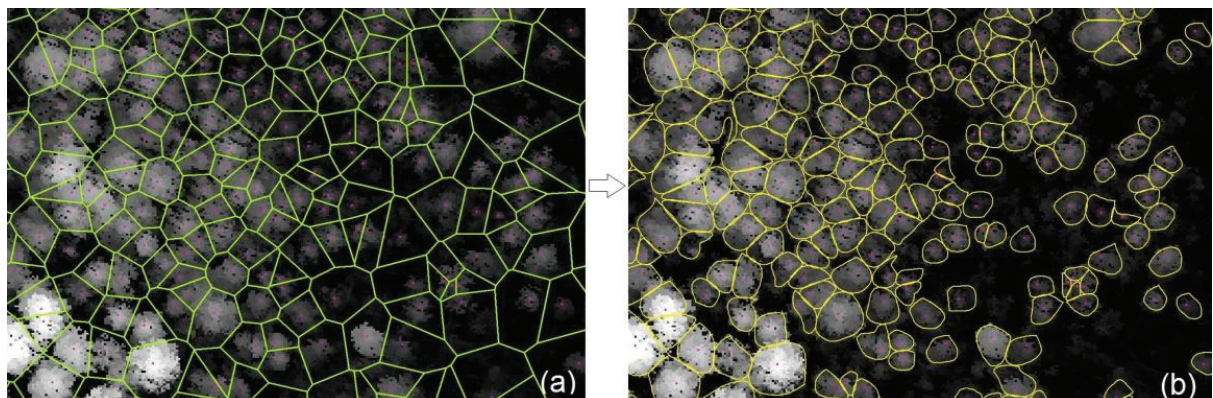


Figure 12 (a)Thiessen polygons Segmentation of tree crowns,
(b) Thiessen segmentation after updating with gaps and applying polygon smoothing

3.12. Validation of tree crown delineation

The quality of segmentation is related to quality of data (noise, spatial and spectral resolution) and the optimal customization of parameter settings, which enables the adaptation of segmentation results on target objects (Möller *et al.*, 2007). Validation of segmentation can be interpreted as ‘an issue of matching objects’ (Zhan *et al.*, 2005) where at least two hierarchical object-levels have to be considered in terms of their topological and geometrical relationships (Möller *et al.*, 2007). Topological relationships of interests are ‘containment’ and ‘overlap’, whereas; geometric relationships can be determined by the comparison of object positions.

For segmentation validation, following approaches have been used by the researchers,

- i. Relative area of intersection between segmented objects and reference objects (Möller *et al.*, 2007)
- ii. Distance between the centroids (Ke *et al.*, 2010)
- iii. 1:1 spatial correspondence (Gougeon & Leckie, 2006; Z Li *et al.*, 2009)
- iv. Total number of pixel that segmented correctly (Coillie *et al.*, 2008; Wang *et al.*, 2004) are commonly used for validation of segmentation of tree crowns.

Clinton *et al.* (2010) summarized different segmentation accuracy measures by many researchers and modified relative area metrics by Möller *et al.* (2007). Over segmentation and under segmentation as defined by Clinton *et al.* (2010) are described as follows (Equation 1 and 2):

$$\text{Over segmentation}_{ij} = 1 - \frac{\text{area}(x_i \cap y_j)}{\text{area}(x_i)} \quad \dots 1$$

$$\text{Under segmentation}_{ij} = 1 - \frac{\text{area}(x_i \cap y_j)}{\text{area}(y_j)} \quad \dots 2$$

Where x_i is a reference object and y_j is a corresponding segmented object.

The value range of over segmentation and under segmentation is between 0 and 1, where 0 value means a perfect segmentation. Closeness of fit, D is a measure of error in segmentation (Clinton *et al.*, 2010). (see Equation 3).

$$D = \sqrt{\frac{\text{over segmenation}^2 + \text{under segmenation}^2}{2}} \quad \dots 3$$

Value of D ranges from 0 to 1 where D equals to 0 implies zero error or a perfect segmentation.

For the purpose of detecting better tree crown delineation in this case, relative area measures modified by Clinton *et al.* (2010) and 1:1 spatial correspondence were selected as measure of accuracy. These accuracy measures were calculated for delineated tree crowns. For 1:1 spatial correspondence, overall accuracy was calculated by comparing the number of 1:1 corresponding tree crowns of the reference and delineated tree crowns and total number of reference tree crowns.

The reference objects were manually delineated on the image as adopted in many tree crown delineation studies (Erikson & Olofsson, 2005; Gougeon & Leckie, 2006; Leckie et al., 2005; Wang et al., 2004). Manual delineation of tree crowns was done using CHM (3.8.4) image and tree peaks (3.9) shape file.

3.12.1. Visualising segmented trees in point cloud

To further assess the accuracy of Region growing crown segmentation, point cloud of 1000 randomly selected tree crown segments was extracted from LiDAR point cloud data using lasclip for visual interpretation.

3.13. Tree Parameter extraction for geospatial forest inventory

For generation of geospatial forest inventory from LiDAR data, several biophysical structural parameters of tree were extracted (Table 4). Parameters listed in the first column of the Table 4 were obtained using LiDAR point cloud data or LiDAR derived elevation models. Parameters listed in column 2 were derived from column 1 parameters while parameters in third column were extracted from readymade layers. The detailed methodology for extraction of inventory parameters is given in the following sections.

3.13.1. Tree Height

In the present research, the tree height has been estimated in four ways to assess their variability and accuracy. Following is a brief description of their extraction methodology.

3.13.1.1. Smooth CHM Height

The smooth CHM height of a tree is defined as the highest elevation of the tree points in the smooth CHM (3.9.1). It was obtained by extracting pixel values in smooth CHM (3.9.1) corresponding to tree peak locations (3.9.4).

Parameters extracted for inventory database		
From point cloud	Derived from 1st column	Other data layers
1 Height	15 Canopy dia	24 Landuse
2 CPA	16 Perimeter CPA	25 Landslide zone (Stable/Unstable)
3 Canopy Volume	17 Major & minor axis CPA	
4 Canopy base height	18 Local tree density	
5 Canopy tilt	19 Local canopy gaps %	
6 Canopy orientation	20 Canopy Shape	
7 Canopy density	21 Tree species	
8 Elevation	22 Biomass	
9 Slope	23 Carbon	
10 Aspect		
11 Location of Peak (cloud)		
12 Location of Peak (CHM)		
13 Location centroid of CPA		
14 Average CPA height		

Table 4. List of tree parameters extracted for forest inventory

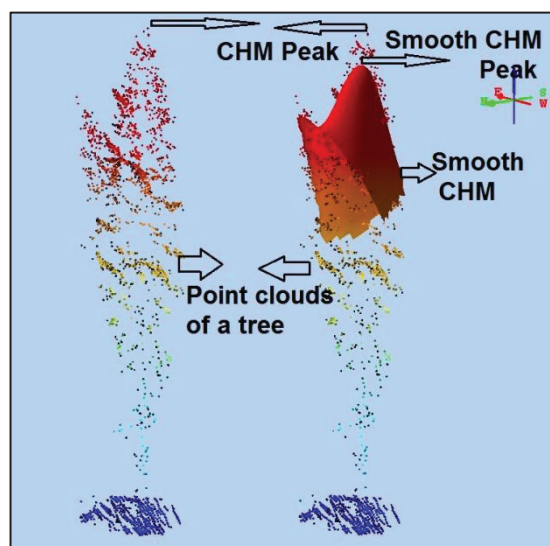


Figure 13. Difference in CHM peak and Smooth CHM peak

3.13.1.2. CHM Height

CHM height of a tree is defined as the highest elevation of the tree points in the CHM (3.8.4). Since in the CHM, the highest elevation corresponding to a tree is the same as that in the LiDAR normalised point cloud, the LiDAR highest hit for a tree can be extracted from the CHM more easily than from the LiDAR point cloud. It was observed that location of smooth CHM height and CHM height do not exactly overlap and the shift depended on the crown shape and degree of smoothing (Figure 13). This happens because smooth CHM makes a smooth convex hull of the crown points culminating at apex point (smooth CHM peak) where calculation of all points in CHM including apex point is based on neighbourhood points (filtering window size). Therefore to get CHM height, a buffer around the tree peak point location (3.9.4(xii)) was created. The maximum value of CHM pixel within the buffer was taken as the CHM height. The detail procedure is as follows;

- i. For each tree peak (3.9.4), calculate the distance of nearest peak using near function in ArcGIS, then create variable buffers with size [nearest peak distance]*0.25. Here a factor of 0.25 is taken to ensure that buffers completely fall within its tree crown segment avoiding overlapping with neighbouring tree crowns.
- ii. Now for extracting CHM height and finding its location, use Zonal Statistics selecting maximum as statistics type on CHM raster with buffer shape file as zone feature. → Rast1
- iii. Use raster calculator with command line
- iv. Setnull(Isnull(CHM), setnull(CHM!=Rast1,Rast1)) → Rast2
- v. This will generate a raster of maximum pixel in CHM within each buffer polygon, all other pixels will be null.
- vi. Convert Rast2 to point feature. This point feature corresponds to CHM height location with height values in its attribute table.

3.13.1.3. eCognition smooth CHM Height

The eCognition smooth CHM Height is defined as maximum pixel value in the smooth CHM within tree crown boundary obtained through eCognition segmentation. This height is extracted from smooth CHM (3.9.1) layer in eCognition by creating a feature class for maximum pixel in tree crown objects.

3.13.1.4. eCognition CHM Height

eCognition CHM Height is defined as maximum pixel value in CHM within tree crown boundary obtained through eCognition segmentation. This height is extracted from CHM layer in eCognition by creating a feature class for maximum pixel in tree crown objects.

3.13.2. CPA

This is extracted by using calculate geometry (Area) of eCognition segmentation shape file in ArcGIS.

3.13.3. Canopy Volume

Canopy Volume (CV) is defined as volume contained within canopy top enveloping surface and canopy base touching surface (Figure 14). The Canopy top enveloping surface is defined as smooth surface, enveloping canopy boundary points as visible from the top of the canopy in 3D. Canopy base touching surface is defined as the smooth surface passing through the lowest points of canopy.

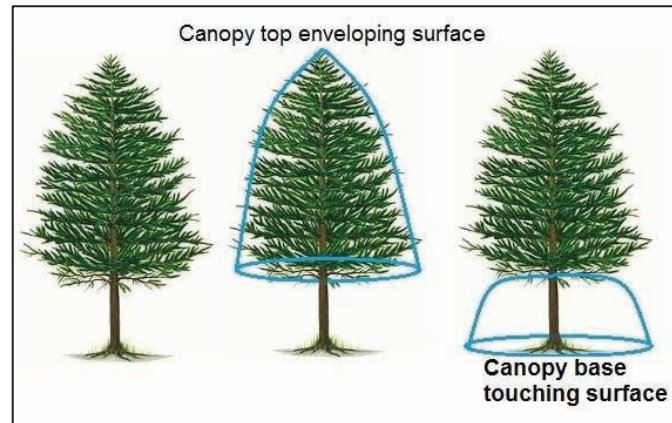


Figure 14. Canopy surfaces

Preparing canopy top enveloping surface

- i. Get sCHM (3.9.1(v)).
- ii. Perform Focal statistics (mean) on sCHM by rectangular window size 3 once. → TopRast.

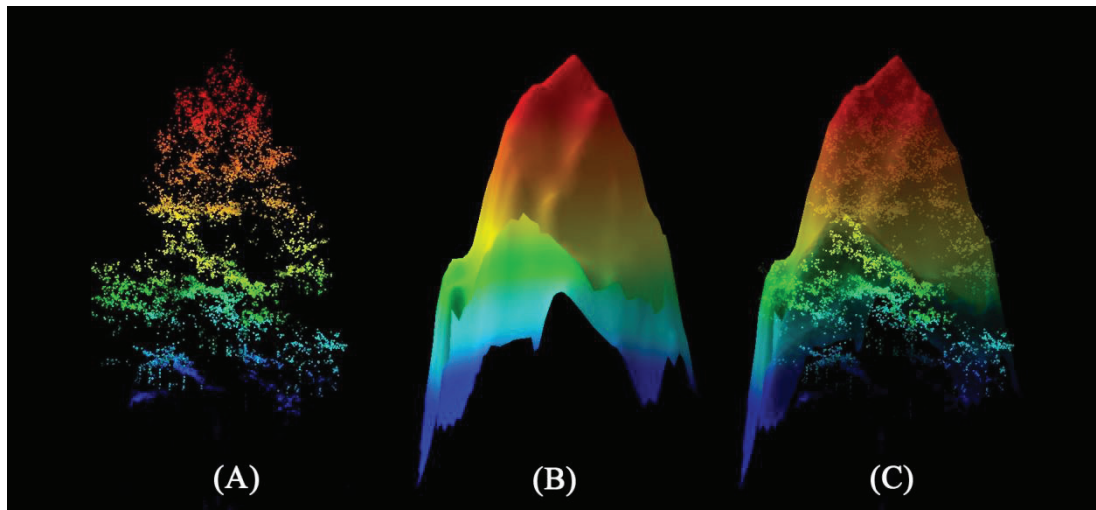


Figure 15. (A) Tree point cloud, (B) Canopy top enveloping surface, (C) Tree with its enveloping surface

Canopy base touching surface

- i. Prepare CHM of 15 cm grid size by gridding operation on normalised point cloud in LAStools taking the lowest elevation point in the grid, dropping single returns, keeping zero fill and clipping on the Z axis below 2 m. → CHM_low

- ii. Convert zero value pixels (missing grid values) to nodata by the raster calculator. Keeping zero will otherwise allow these pixels to participate in the operation performed in step (iii) and jeopardise selection of minimum value.
- iii. Perform Focal statistics (minimum) in ArcGIS by rectangular window size 3 (pixels) two times.
- iv. Perform Focal statistics (mean) by rectangular window size 3 (pixels) two times.
- v. Missing pixels will be filled by now if not repeat above step one more time.
- vi. Select all the pixels which have gained height (z value increased => lowest point in the neighbourhood) during minimizing and averaging operations by comparison to CHM_low (step (i)) and replace these pixels to their original values in the CHM_low of step(i) using raster calculator in ArcGIS.
- vii. Perform Focal statistics (mean) by rectangular window size 3 two times. → BaseRast

Calculation of Canopy volume

- i. Subtract canopy top enveloping surface layer TopRast from canopy base touching layer (BaseRast) using raster calculator. Let this layer be Raster3.
- ii. Calculate the sum of pixel values of Raster3 within each eCognition tree crown segmentation using Zonal Statistics as table tool in ArcGIS.
- iii. Multiply by square of grid size (i.e. 0.15×0.15) to sum value of each segmentation to get volume in cubic meter

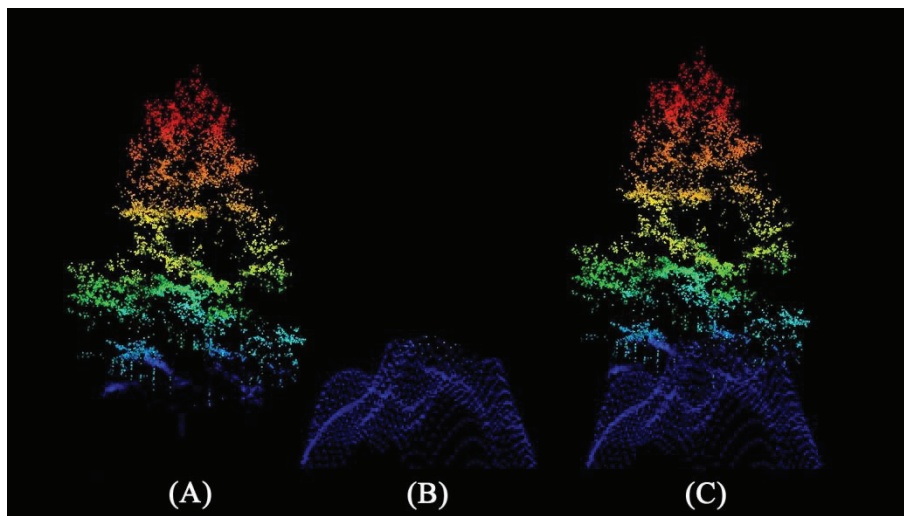


Figure 16. (A) Tree point cloud, (B) Canopy bottom touching surface, (C) Tree with its bottom touching surface

3.13.4. Canopy Base Height (CBH)

CBH is defined as the lowest height above the ground above which there is sufficient canopy fuel to propagate fire vertically (Scott & Reinhardt, 2002). CBH is a parameter in fire behaviour models such as FARSITE (Finney & Station, 1998).



Figure 17. Canopy Base Height (CBH)

CBH Calculation

CBH is estimated from canopy base touching surface.

$CBH \cdot CPA = \text{Volume of canopy base touching surface}$

$$= (\text{grid size})^2 \cdot (\text{sum of pixel values})$$

Or $CBH = (\text{grid size})^2 \cdot (\text{sum of pixel values}) / CPA \quad \dots 4$

$CPA = (\text{grid size})^2 \cdot (\text{Count of pixels})$

Therefore, $CBH = \text{sum of pixel values} / \text{count of pixels}$

$$= \text{Average pixel value in Raster2 within tree crown segmentation}$$

Now use Zonal Statistics as table tool in ArcGIS on Raster2 taking eCognition segmentation shape file to define zones to get average pixel value for each zone (tree crown segmentation)

3.13.5. Canopy tilt

Canopy tilt was calculated on the basis of the coordinates of tree peaks in the smooth CHM (3.9) and the centroid of the CPA (3.13.12). It was assumed that trees are symmetrical objects, where tree trunk coincides with the centroid of CPA at canopy base height. The minimum height for the peak observation was 2m from the ground (3.9). Completely fallen trees or any tree having peak height less than 2m therefore, are not accounted for. If $P(X_1, Y_1, Z_1)$ and $C(X_2, Y_2, Z_2)$ are coordinates of the DSM peak and the centroid of the CPA respectively and θ be the canopy tilt from horizontal plane (Figure 18) then,

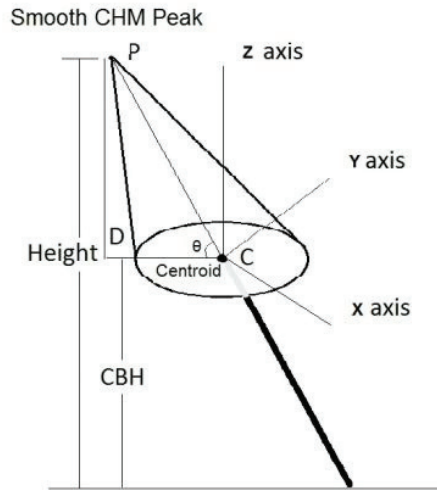


Figure 18 Schematic diagram of a tilted tree

$$PD/DC = \tan\theta,$$

PD = (Height - CBH) and DC is the distance between P(X₁, Y₁) and C(X₂, Y₂) in XY plane

$$DC = \sqrt{(X_1 - X_2)^2 + (Y_1 - Y_2)^2}$$

$$\text{Or } \tan\theta = (\text{Height} - \text{CBH}) / \sqrt{(X_1 - X_2)^2 + (Y_1 - Y_2)^2}$$

$$\text{Or Canopy tilt, } \theta = \tan^{-1} (\text{Height} - \text{CBH}) / \sqrt{(X_1 - X_2)^2 + (Y_1 - Y_2)^2}$$

$$\text{Or Canopy tilt, } \theta = \tan^{-1} (Z_1 - Z_2) / \sqrt{(X_1 - X_2)^2 + (Y_1 - Y_2)^2} \quad \dots 5$$

The coordinates of the CHM peak are obtained in the tree peak detection routine as discussed in section (3.9). The coordinates of centroid of CPA were determined by converting CPA polygon into point using feature to point tool in ArcGIS (3.13.12).

3.13.6. Canopy Orientation

Canopy orientation is the canopy tilt direction measured from North in a XY plane. Therefore, canopy orientation can be measured by the slope of the smooth CHM peak, P(X₁, Y₁) and centroid of CPA, C(X₂, Y₂) in the XY plane (Figure 19). A linear transformation on the slope angle would be required to correct the direction of measurement of the slope angle. As in the map coordinates, the X axis points towards East and the slope of a line in XY plane is measured from East in anti-clockwise direction, whereas orientation is measured from North in the clockwise direction. If the slope of the line PC in XY plane be φ then,

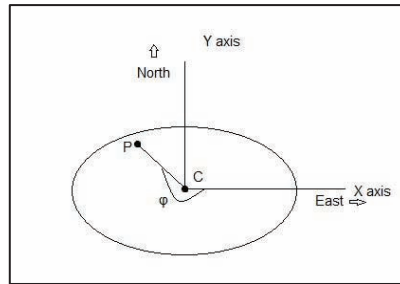


Figure 19 Location of tree peak (point P) and centroid on CPA (Point C)

$$\text{Slope} = \tan \varphi = (Y_2 - Y_1) / (X_2 - X_1)$$

or,

$$\varphi = \tan^{-1} (Y_2 - Y_1) / (X_2 - X_1), \dots 6$$

or,

$$\text{Canopy orientation} = \text{Mod}[(90 - \varphi) + 360, 360] \dots 7$$

3.13.7. Canopy density

Canopy density (CD) is defined as the number of LiDAR hits per unit volume. It is a measure of biomass density and gives an indication of tree vigour and growth. If a forest is of same species and age, areas with poor soils are easily identified by the proportion of biomass.

Method

- i. CD is calculated using lasgrid in LAStools at a grid size of 0.15m as highest and 'item' as density. It prepares a raster of the total number of LiDAR hits within the grid.
- ii. Get the sum of pixel values in the raster obtained in step 1 by Zonal Statistics as table tool in ArcGIS with eCognition segmentation shape file (cross-reference) as defining zones.
- iii. Divide the sum (step 2) by canopy volume for each tree crown segmentation (3.11.1) to get the canopy density for each tree.
- iv. The LiDAR point cloud density in the study area was increased by taking multiple flights over the same area. Therefore, this canopy density was normalised by dividing canopy density of a tree by count of different source ID used for a tree point cloud data. Source ID is an attribute in LAS file which keeps the detail of flight tack ID for each point cloud data.

3.13.8. Elevation, Slope and Aspect

- i. Use Zonal Statistics as table tool in ArcGIS on DTM prepared in Section 3.8.2 with eCognition segmentation shape file (3.11.1) as defining zones to get average elevation for each tree crown segmentation.
- ii. Prepare slope raster from DTM using Slope tool in ArcGIS. Now use Zonal Statistics as table tool in ArcGIS on slope raster with eCognition segmentation shape file (3.11.1) as defining zones to get average slope for each tree crown segments.
- iii. Prepare aspect raster from DTM using Aspect tool in ArcGIS. Now use Zonal Statistics as table tool in ArcGIS on aspect raster with eCognition segmentation shape file (3.11.1) as defining zones to get average aspect for each tree crown segmentation.

3.13.9. Average CPA height

The average CPA height is in between height and CBH and is a point around which maximum biomass is concentrated on the vertical axis. This parameter is used to determine fire behaviour.

Method

Use Zonal Statistics as table tool in ArcGIS on CHM (3.8.4) with eCognition segmentation shape file ((3.11.1)) as defining zones to obtain average height for each tree crown segment.

3.13.10. Canopy diameter

It was calculated from CPA in two ways.

- i. As diameter of circle with equal area of CPA (3.13.2)
- ii. As sum of semi-major and semi-minor axis of inscribed ellipse of CPA (3.13.11)

3.13.11. Perimeter, Semi Major and Minor axis

Use Zonal geometry tool in ArcGIS on CHM (3.8.4) with eCognition segmentation shape file as defining zones to get perimeter of the crown segmentation, the semi major and minor axis of the fitting ellipse of the crown segmentation for each tree. The sum of semi major and minor axis gives the estimation of crown diameter. They are also used to calculate eccentricity of the ellipse to identify elongated crown segments and slivers.

3.13.12. Centroid of the crown segment

Centroid of the tree crown segment was obtained by converting crown segmentation (3.11.1) to points using feature to point tool in ArcGIS.

3.13.13. Local tree density

The local tree density (LTD) is defined as the number of trees per unit area (in Ha) falling within a buffer of 3 meter around tree crown segments. This parameter is calculated to investigate the impact of local tree density on tree growth. The selection of the buffer dimension is based on average crown size in the study area (6.7 m²). The idea is to obtain a minimum size buffer to cover all neighbouring trees around a tree.

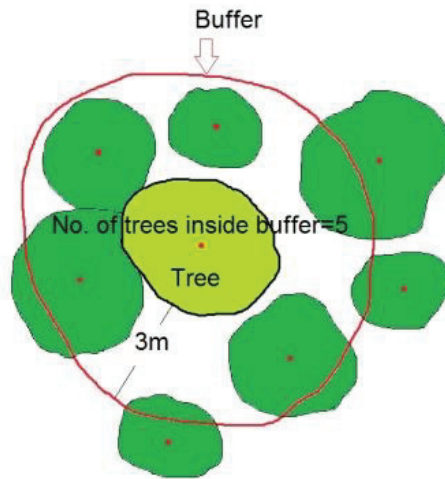


Figure 20 Local tree density

Method

- i. Create buffer of 3 meter around eCognition segments using the buffer tool in ArcGIS.
- ii. Perform spatial join in buffer shape file with the centroid of tree crown segment shape file (3.11.1).
- iii. The count field in the Joined file gives the number of trees falling within each buffer.
- iv. Calculate area of each buffer by calculate geometry in ArcGIS on buffer shape file.
- v. Divide number of trees within the buffer (step iii) by buffer area (step iv) to get local tree density in number of trees per m².
- vi. Multiply the result of step (v) by 10000 to get the density in number of trees per hectare.

3.13.14. Local canopy gaps (LCG)

LCG is defined as percentage of gaps in annular buffer of 1m around tree crown segments.

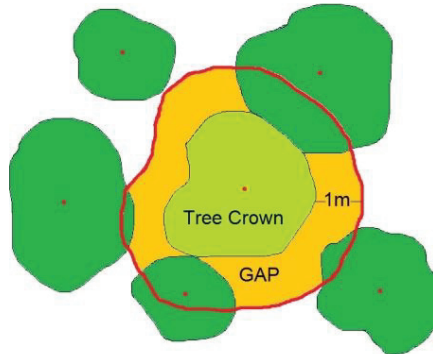


Figure 21. Canopy gap percentage around 1m buffer

Method

- i. Create buffers of 1m around eCognition segmentations using buffer tool in ArcGIS. → Buff1m.
- ii. Convert inter canopy gaps mask shape file as prepared in Section 3.10 from 0.15m grid size to 1m size. Let this layer be called Rast1
- iii. The buffers obtained in step (i) are overlapping for being around a tree crown segment. Unfortunately, the Zonal Statistics tool in ArcGIS does not work on overlapping zones, therefore, this tool cannot be used. In fact, there is no easy way to get gap percentage in buffer polygon through ArcGIS. Therefore, resolution of gap raster is decreased to 1 meter and gap raster is converted to point shape file. To avoid the point shape file going very big, resolution of gap file was reduced to 1m (step ii). Each point now represents an area of 1 m² of gap. These points now can be counted within buffer to assess gap percentage.
- iv. Rasterize buffer layer on attribute 'val' having value 1, let it be called Rast2
- v. Use raster calculator in ArcGIS with command line, Setnull(Isnull(Rast2), Rast1). This is done to reduce the size of gap raster to exclude gaps which are falling outside the buffer. Let this raster be called Rast3.
- vi. Now convert Rast3 to point using raster to point tool in ArcGIS. Let this shape file be called Rast3toPoint.
- vii. Spatial join Buff1m with Rast3toPoint in ArcGIS selecting SUM statistics. This took about an hour of processing in ArcGIS.
- viii. Look for Count or Sum attribute in the joined field of Buff1m. This is actually an area of gaps in m².
- ix. Subtract the area of crown segment from its buffer area to get the area of annular buffer.

- x. Get the gap percentage by dividing gaps in buffer (step viii) by total area of annular buffer (step ix) and multiplying by 100.

3.13.15. Canopy Shape

Canopy shape (CS) is defined as the ratio of the canopy diameter with canopy height (USGS). Canopy shape volume may also be estimated from the volume formula for given shape (

Table 5). Canopy shapes were determined for all segmented trees based on the shape value, primarily to investigate whether Canopy shape may be indicative of species type. Further to know whether extreme shapes are indicative of wrong crown segmentation.

Canopy height=Tree height-Canopy base height

Shape Value=Canopy diameter/Canopy height

Now based on shape value, shapes may be assigned to tree canopies.

Table 5. Tree canopy shape and Volume. *Source:* USGS

Value	Name	Volume Formula
1	Cylinder	$a \cdot 0.7854$
0.875	Rounded-edge cylinder	$a \cdot 0.6872$
0.75	Elongated spheroid	$a \cdot 0.5891$
0.667	Spheroid	$a \cdot 0.5236$
0.625	Expanded parabolic	$a \cdot 0.4909$
0.5	Parabolic	$a \cdot 0.3927$
0.375	Fat Cone	$a \cdot 0.2945$
0.333	Cone	$a \cdot 0.2619$
0.25	Neiloid	$a \cdot 0.1964$
0.125	Thin Neiloid	$a \cdot 0.0982$

$$a = (\text{Canopy diameter})^2 \cdot \text{Canopy Height}$$

3.13.16. Landuse

The landuse information for the study area was provided by the ONF (Forest department, France). The landuse has 8 classes namely broad leaved forests, coniferous forests, coniferous mix forests, natural grassland, pastures, bare rocks, black marks, urban fabric. Landuse was entered in landuse field for selected trees in the attribute table.

3.13.17. Stable and Unstable area

A shape file delineating landslide active (Unstable) and non-landslide (Stable) area was provided by doctoral researcher Mr. Khamarrul A. Razak working in the study area on landslides. This field was added in the attribute table of eCognition crown segments. Stable/Unstable was entered in the Landslide field for selected trees in the attribute table.

3.14. Species Classification

Tree species classification was done by the query method on extracted parameters. LiDAR data has rich structural information, therefore tree species structurally different from other may be identified and suitably classified. To achieve this, first identifying differences among species were examined from descriptive statistics of extracted parameters such as canopy volume, CPA, height, CBH, elevation, canopy density. The next step was to formulate a suitable query on individual tree based geospatial inventory database on structural and spatial parameters. Distribution of *Pinus uncinata* and *Pinus sylvestris* was found to have dependence on elevation while *Larix decidua* was found structurally distinct from Pines in shape, canopy volume, height and CPA. These facts were converted to a query to get the classification.

Query

Larix

CPA>15 m²

Height>12 m

Canopy Volume>130 m³

P. uncinata: Elevation>1600 m

P.sylvestris: Elevation<=1600 m

3.15. Allometric Equation

We could not find any allometric equation for *Pinus uncinata* and *Pinus sylvestris* for France. The following allometric equation for *Pinus nigra* (Netherlands) was used for the estimation of carbon for pines in the study area (Hale et al., 2004).

$$\text{Stem Volume (dm}^3\text{)} = (\text{dbh}^{1.89192}) \cdot (\text{height}^{0.95374}) \cdot e^{-2.72505}$$

$$\text{Carbon (kg)} = 0.25(\text{dbh}^{1.89192}) \cdot (\text{height}^{0.95374}) \cdot e^{-2.72505} \dots 8$$

3.16. Regression analysis

The objective of regression analysis in remote sensing based data is to quantify the relationship between response variable (measured in field or derived from measured parameters through allometric equations) and one or more explanatory variables which are derived from remote sensing data sets. Quantitative

relationship is expressed by an equation and its graphic representation (Husch et al., 2003). The coefficient of determination (R^2) gives the proportion of variance of one variable that is predictable from the other variable or in other words is the ratio of the explained variation to the total variation.

Regression modelling is commonly used for biomass estimation studies (Lu, 2006). In this research three regression models were developed for prediction of biomass/carbon. Three sets of explanatory variables used were (CPA, height), (Canopy Volume, height), (CPA, height, Local tree density). Allometric equation for biomass was based on DBH and height. After calculating aboveground carbon stock using field measured DBH and height information in allometric equation, relationship of aboveground carbon stock and explanatory variables were analysed using regression analysis.

Tree crowns that had 1:1 spatial correspondence with reference and delineated tree crowns having less error in terms of the relative area (less than 6 m²) were used for modelling. The significance and the strength of this relationship was determined using evaluation dataset, which was 30 % of field dataset.

4. RESULTS

4.1. Descriptive Analysis of field data

In total, forest stand parameters data of 275 trees was collected from 13 plots spread over the study area. All the sampled trees were manually delineated on CHM after locating the tree with the help of the tree base coordinates collected during the field campaign. The accuracy of differential GPS for base stations coordinates was 4 mm horizontally (XY plane) and 7mm vertically (Z axis). The sample data comprised of mainly three species namely *Pinus uncinata*, *Pinus sylvestris* and *Larix decidua*. One tree of *Picea abies* was also sampled. The descriptive statistics of sampled trees is given in Figure 22. Frequency distribution of sampled trees species is shown in Figure 23. The distribution of the measured tree parameters are illustrated in Figure 24 .

Figure 22. Descriptive statistics of sampled trees

Variable	n	Min	Max	Mean	Std. deviation
DBH (cm)	200	9.1	41	19.57	4.34
Height (m)	200	5.2	17.8	11.14	2.59
Canopy dia (cm)	192	1	6.7	3.15	0.90
<i>Pinus sylvestris</i>					
Variable	n	Min	Max	Mean	Std. deviation
DBH (cm)	51	11	36	24.11	5.83
Height (m)	51	6.5	15	10.85	2.35
Canopy dia (m)	50	2.25	6.9	4.68	1.14
<i>Larix decidua</i>					
Variable	n	Min	Max	Mean	Std. deviation
DBH (cm)	23	15	61	31.24	12.35
Height (m)	23	12	21.2	15.21	2.50
Canopy dia (m)	23	3.05	8.95	6.22	1.70

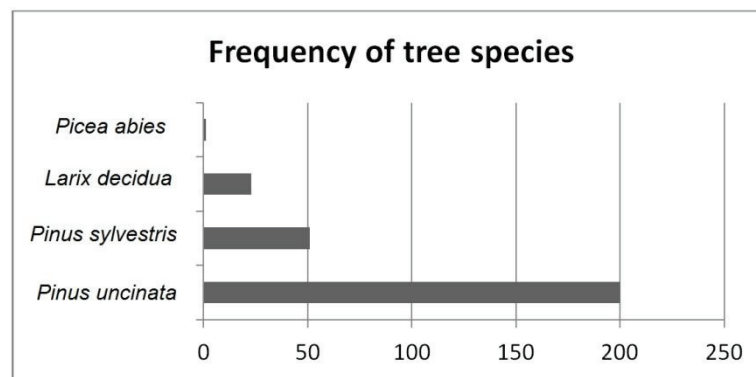


Figure 23. Frequency of the sampled tree species

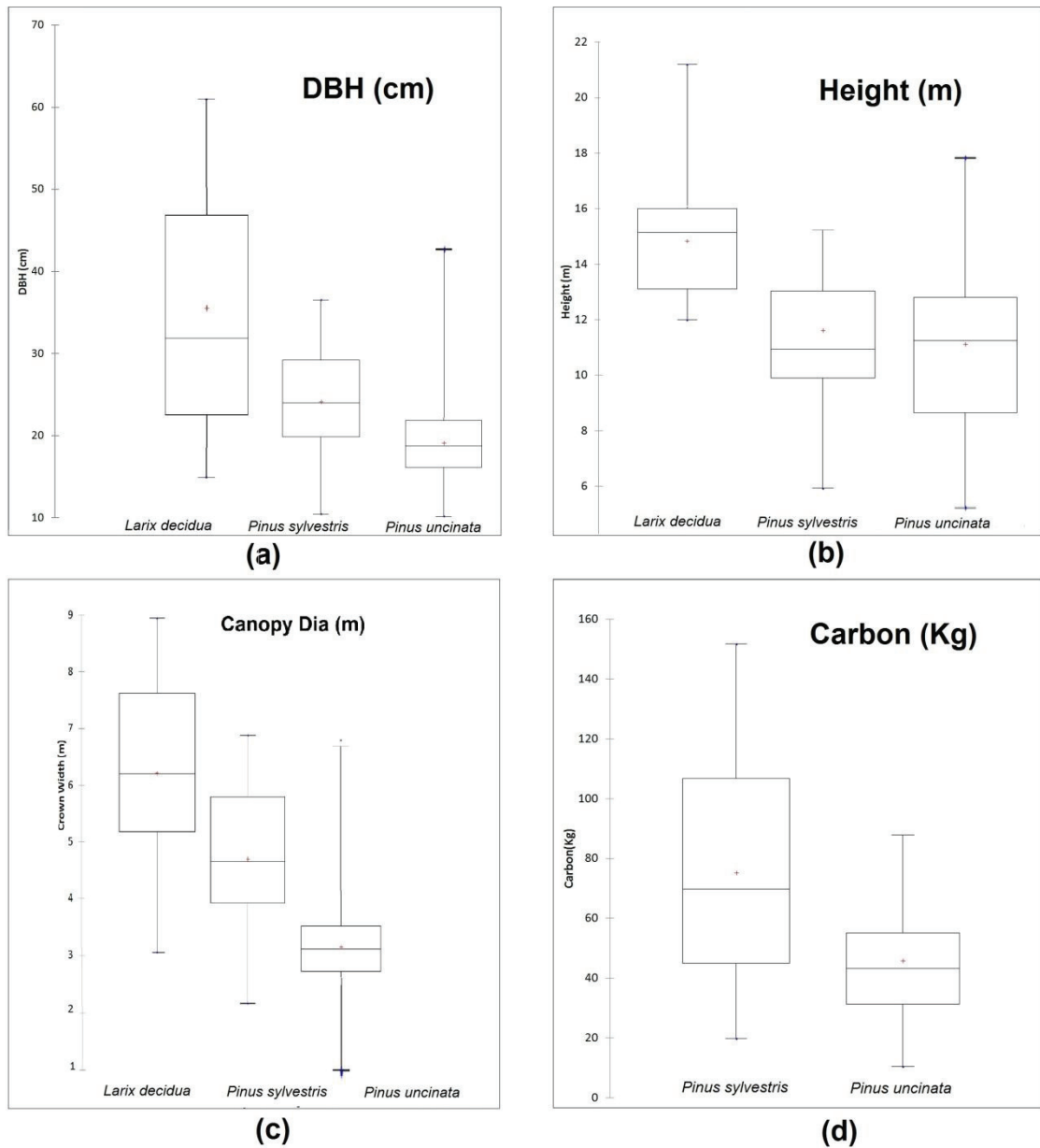


Figure 24. Tree Parameters Distribution (a) DBH, (b) Height, (c) Crown Diameter, (d) Carbon

4.2. Peak detection

Tree peaks were detected as explained in Section (3.9.4). Out of 275 sample trees, peaks of 264 trees could be detected. Therefore, the accuracy of tree peak detection was 96 %. The accuracy obtained relates with the tree peak detection only and it is not the accuracy of tree identification. Trees were identified in the crown delineation procedure as explained in Section (3.11). For the whole study area, in total 128,918 tree peaks were detected.

Table 6 shows the number of peaks identified in the CHM with varying degree of smoothness and the number of final peaks after removing false peaks, based on height criteria as explained in Section (3.9.4).

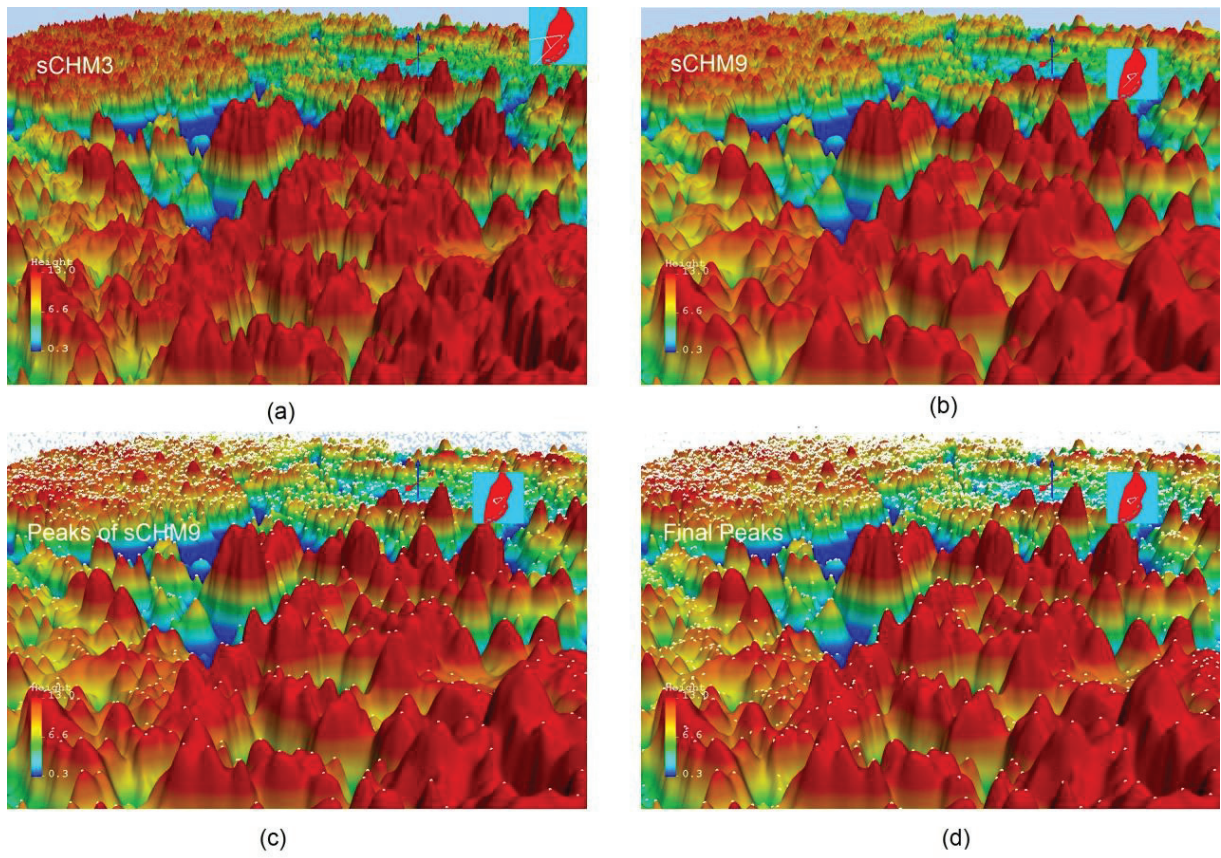


Figure 25. (a) sCHM3 (3.9.2), (b) sCHM9 (3.9.2), (c) Peaks detected in sCHM9, (d) Final peaks

Table 6. Number of peaks detected in smooth CHM with varying degree of smoothness

Smooth CHM	Tree peaks detected	Final Peaks
sCHM3	164,787	128,918
sCHM5	92,867	
sCHM7	72,609	
sCHM9	54,194	

4.3. Tree Crown delineation

4.3.1. Tree crown delineation using Region growing approach in eCognition

The result of individual tree crown delineation using Region growing approach in eCognition is given in Figure 26. Table 7 shows accuracy measures of D of delineated crowns. Overall for the whole study area, over segmentation error was 16.5 %, under segmentation error was 21.5 % and total delineation of tree crowns was 81 % accurate (19 % error). When polygon smoothing was done on the Region growing segmentation, there was improvement in the overall segmentation accuracy by 3 %. With smooth segmentation, over segmentation error was 15 %, under segmentation error was 17 % and total delineation of tree crowns was 84 % accurate (16 % error). For the accuracy measure of 1:1 correspondence, 93.5 % of the total reference crowns were matching to the Region growing crown delineation with 1:1 correspondence (Table 8).

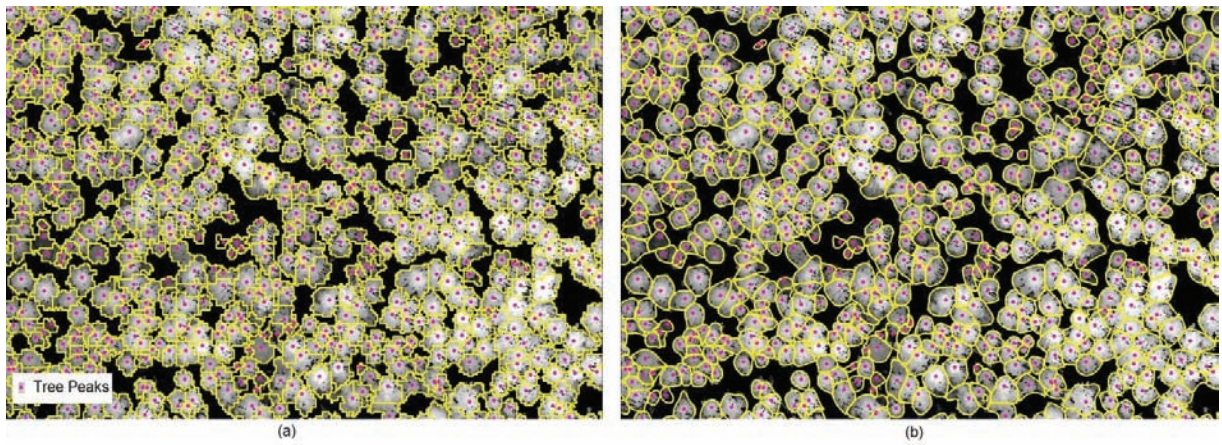


Figure 26. (a) Region growing segmentation on pre-determined tree peaks, (b) Polygon smoothing on segmentation

Table 7. D Values (Segmentation error) for Region growing and Thiessen polygons segmentation

D Value (Segmentation error fraction)	Region growing Segmentation		Region growing Segmentation (Smooth)		Thiessen Segmentation		Thiessen Segmentation (Smooth)	
	fraction	%	fraction	%	fraction	%	fraction	%
Over Segmentation	0.165	16.5	0.15	15	0.189	18.9	0.197	19.7
Under Segmentation	0.215	21.5	0.168	16.8	0.242	24.2	0.218	21.8
Overall	0.192	19.2	0.16	16	0.217	21.7	0.208	20.8

Table 8. 1:1 correspondence for segmentation accuracy of Region growing and Thiessen polygons.

Tree species	reference	1:1 correspondence		accuracy %	
		Region growing	Thiessen polygons	Region growing	Thiessen polygons
<i>Pinus uncinata</i>	200	187	188	93.5	94.0
<i>Pinus Sylvestris</i>	51	48	49	94.1	96.1
<i>Larix decidua</i>	23	21	21	91.3	91.3
<i>Picea abies</i>	1	1	1	100	100.0
Total	275	257	259	93.5	94.2

Visualising segmented trees in point cloud

The result of Region growing crown segmentation extracted from LiDAR point cloud as explained in Section 3.12.1 for visual interpretation is shown in Figure 27.

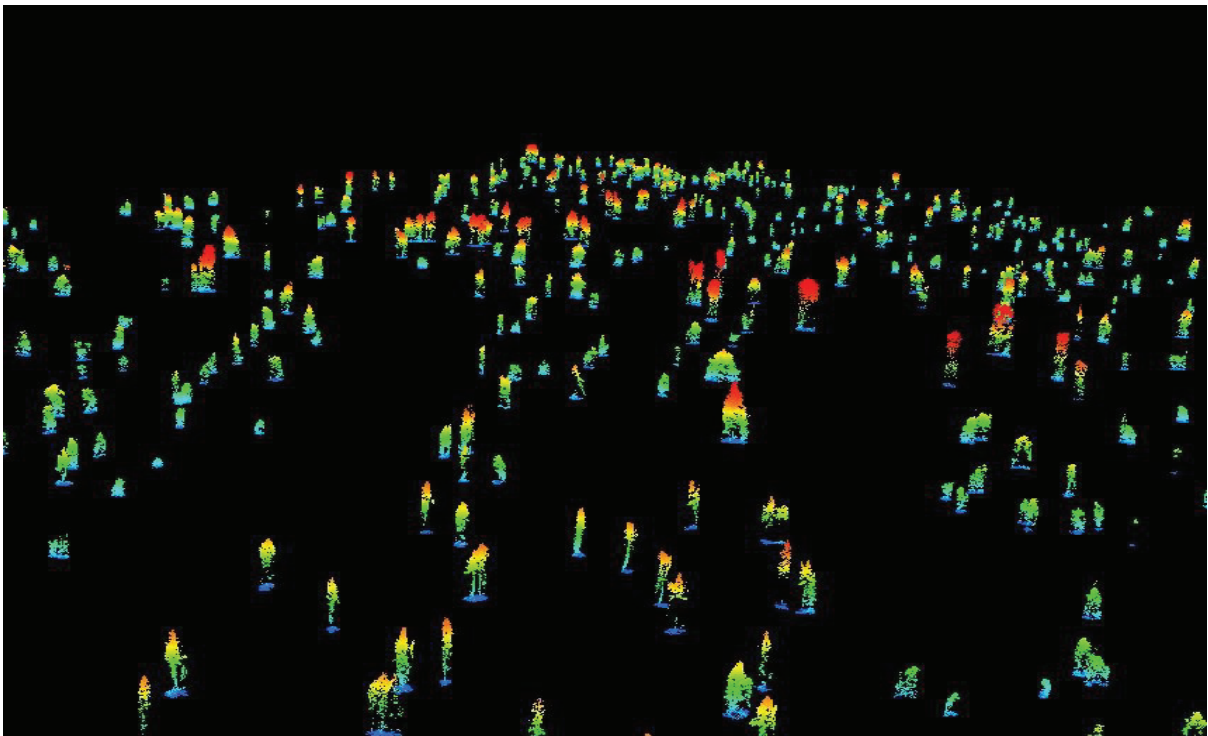


Figure 27. A subset of tree point cloud of 1000 randomly selected trees from segments of Region growing approach.

4.3.2. Tree crown delineation using Thiessen polygons

The result of individual tree crown delineation using Thiessen polygons is given in Figure 26. Table 7 shows accuracy measures of D of delineated crowns. Overall for the whole study area, over segmentation error was 19 %, under segmentation error was 24 % and total delineation of tree crowns was 78 % accurate (22 % error). With polygon smoothing, the Region growing segmentation was improved by

marginally by 1 % in overall accuracy. With smooth segmentation, over segmentation error was 20 %, under segmentation error was 22 % and total delineation of tree crowns was 79 % accurate (21 % error). For the accuracy measure of 1:1 correspondence, 94.2 % of the total reference crowns were matching to the Region growing crown delineation with 1:1 correspondence (Table 8).

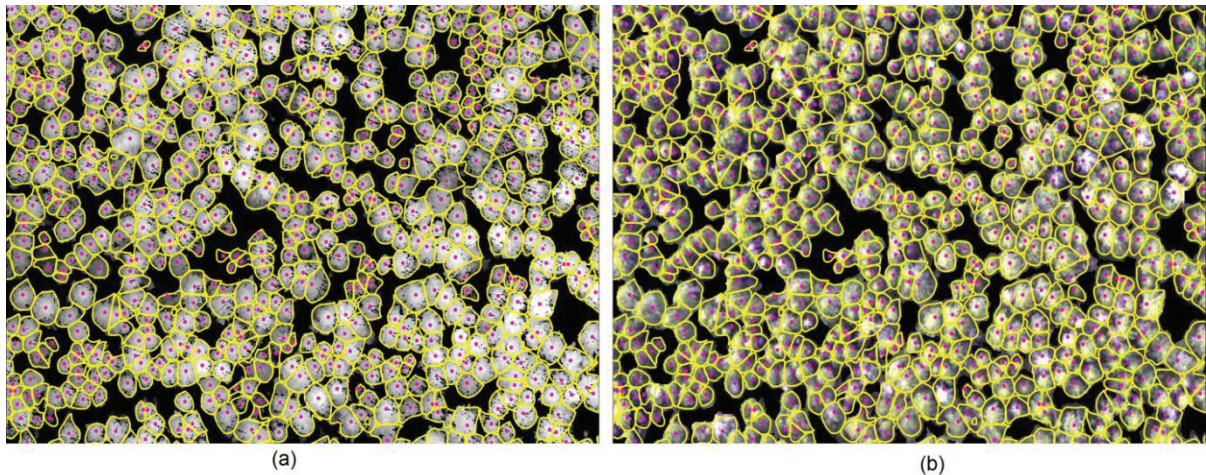


Figure 28. (a) Thiessen segmentation on the CHM, (b) Thiessen segmentation overlay on the ortho-image

4.3.3. Comparison of delineated crowns from Region growing and Thiessen polygons approaches

Figure 29 shows delineated crowns of Region growing and Thiessen polygons approaches (reference tree crowns in red and delineated tree crowns of Region growing in blue and that of Thiessen polygons in yellow. Tree peaks are shown in pink).

Overall D value of Region growing and Thiessen polygons approaches was 0.19 and 0.22 respectively, while application of polygon smoothing on these segmentation resulted D value of 0.16 and 0.21 respectively (Table 7).

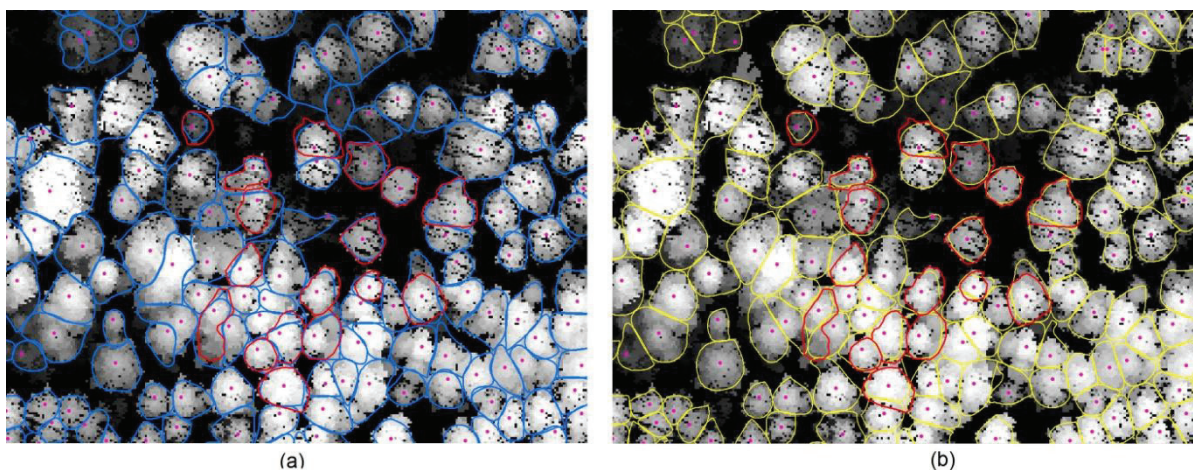


Figure 29. Delineated crowns of Region Growing (a) and Thiessen polygons (b) approaches.

4.3.4. Species classification

Delineated tree crowns of Region growing approach were classified into four species types namely *Larix deciduas*, *Pinus uncinata*, *Pinus sylvestris* and broadleaved with the help of a query approach on extracted

parameters. The accuracy of species classification is given in Table 9. The count of classified species is given in Figure 31.

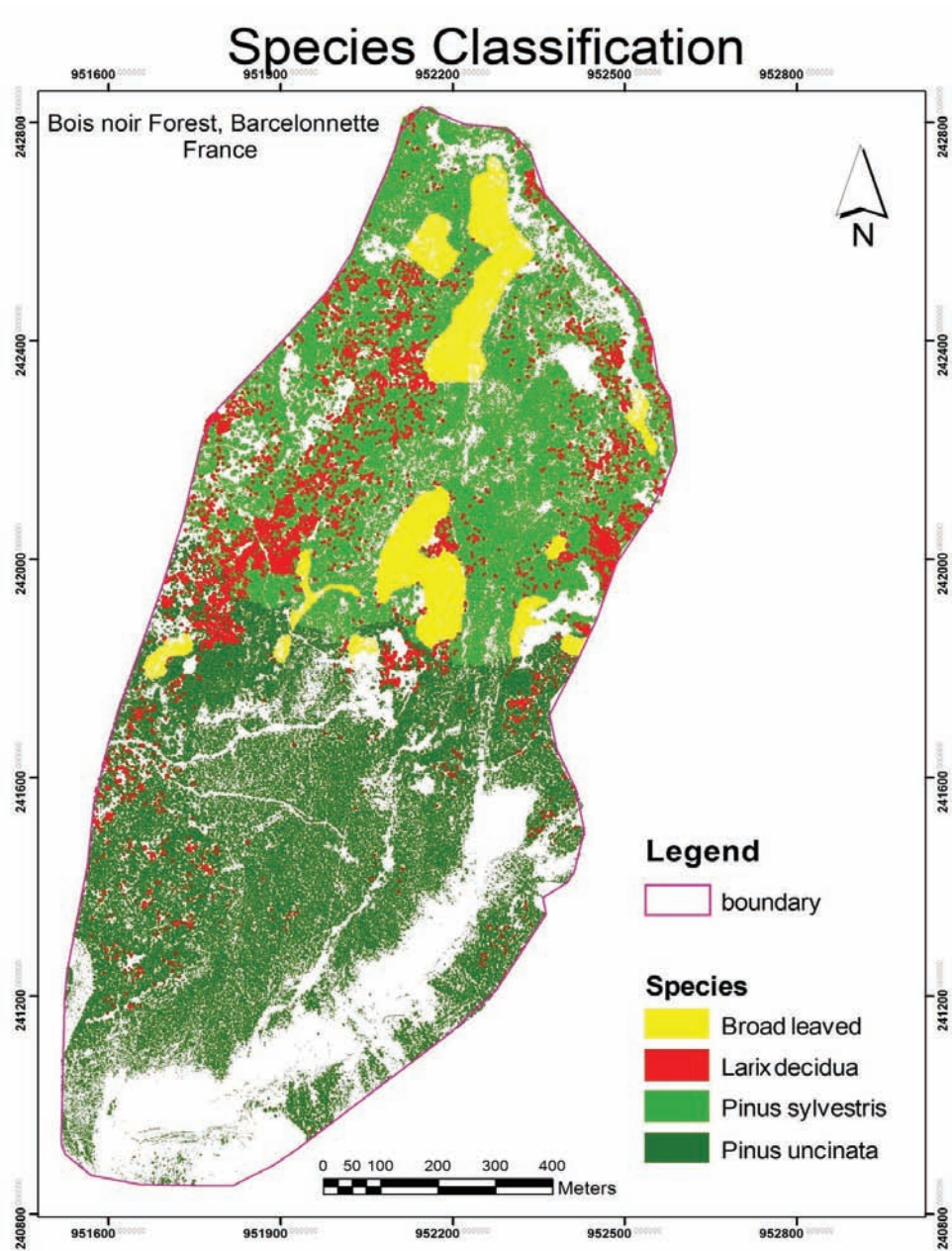


Figure 30. Species classification in Bois noir forests, Barcelonnette, France.

Table 9. Species classification accuracy

Classified		Reference						
	Species	Larix	<i>P. uncinata</i>	<i>P. Sylvestris</i>	<i>Picea abies</i>	n	Error commission	User accuracy %
	<i>Larix decidua</i>	20	5	0	1	26	23	77
	<i>P. uncinata</i>	3	195	0	0	198	2	98
	<i>P. Sylvestris</i>	0	0	51	0	51	0	100
	<i>Picea abies</i>	0	0	0	0	0	0	100
	total	23	200	51	1	275		
	Error Omission	13	3	0	100			
	Producer accuracy %	87	98	100	0		Overall accuracy	97

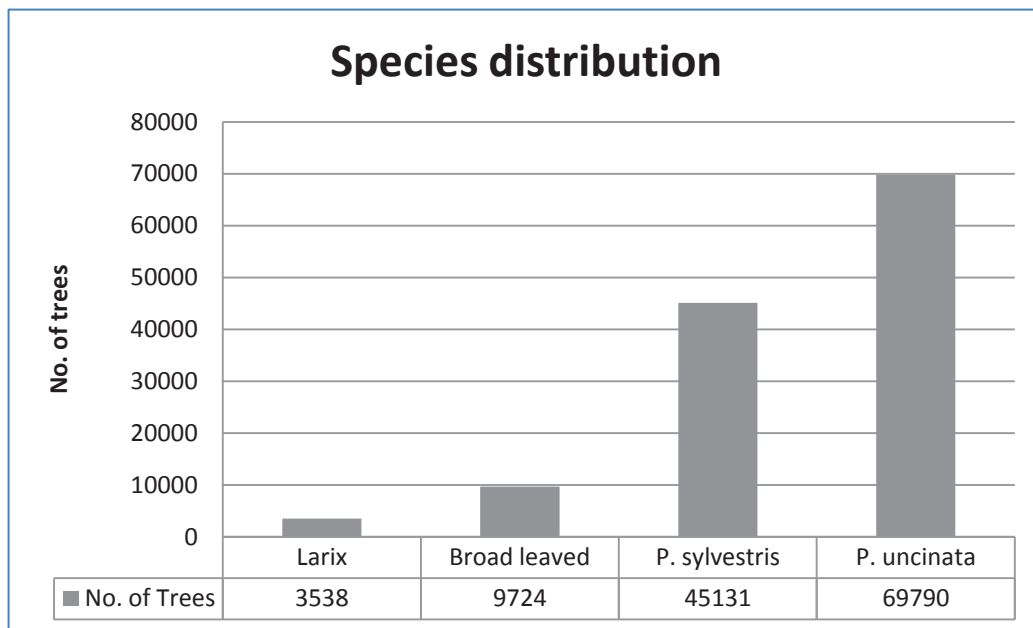


Figure 31. Tree species distribution in the study area

4.4. Tree Height

Tree height was estimated in four ways as described in Section 3.13.1. The coefficient of determination, R^2 and RMSE of these heights with field measured height is given in Table 10. Scatter plot for CHM height is given in Figure 32.

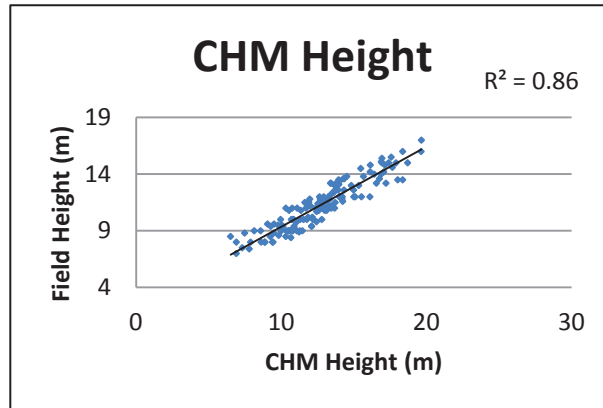


Figure 32. Scatter plot for CHM height

Table 10. R^2 for LiDAR derived heights

Height	R^2	RMSE (m)
CHM Height	0.86	0.8
Smooth CHM Height	0.85	0.83
eCognition CHM Height	0.81	0.93
eCognition smooth CHM Height	0.81	0.93

4.5. Canopy Base Height

Scatter plot of field measured CBH and LiDAR derived CBH (3.13.4) is given in Figure 33. The R^2 for the LiDAR derived CBH was 0.73 with RMSE=0.86 m. A correlation of field measured CBH with other extracted parameters such as height and average CPA height was also tested. CBH showed significant correlation with average CPA height ($R^2=0.72$, RMSE=0.88 m), while with height it was ($R^2=0.62$, RMSE=1.0 m).

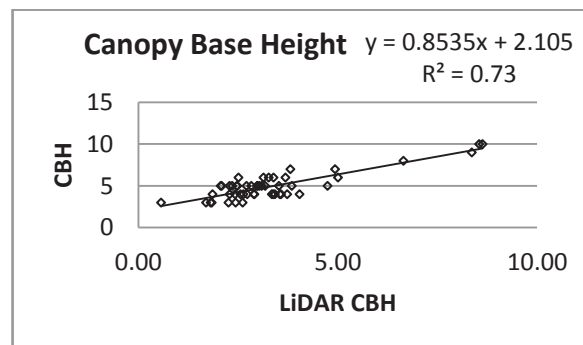


Figure 33. R^2 for LiDAR derived CBH

4.6. CPA

Coefficient of determination, R² and root mean square error (RMSE) for CPA obtained from Region growing and Thiessen polygons segmentation approaches are given in Table 11. The relation of Region growing CPA with manually delineated CPA is shown in Figure 34.

Table 11. Accuracies of CPA obtained from Region growing and Thiessen polygons segmentation approaches

CPA	n	Mean	Std. deviation	R ²	RMSE (m ²)
Field (manually digitised)	262	10.157	10.031		
Region growing segmentation	262	10.460	9.669	0.868	3.653
Region growing segmentation (smooth)	262	10.214	9.708	0.867	3.671
Thiessen polygons segmentation (smooth)	262	9.961	8.753	0.901	3.161

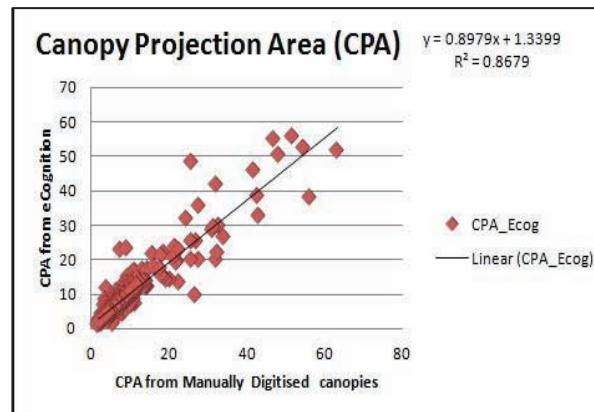


Figure 34. Relation of Region Growing CPA with manually delineated CPA

4.7. Canopy tilt

Coefficient of determination, R² for canopy tilt with field measured tree tilt at 2 m is given in Figure 35. A subset of extracted point cloud of trees with canopy tilt less < 70 degree is given in Figure 36.

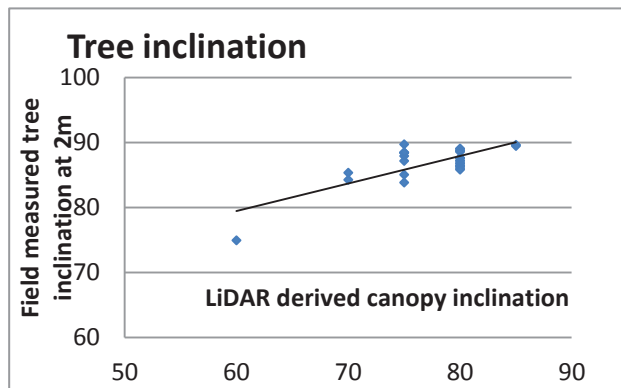


Figure 35. Scatter plot of canopy tilt and field measured tree tilt at 2 m from base of tree.



Figure 36. Extracted point cloud of tilted trees with canopy tilt < 70 degree

4.8. Application of inventory data

4.8.1. Open canopies

Using local canopy gaps (3.13.14) parameter in the inventory, trees having less than 50 % local canopy gaps were identified in landslide and non-landslide zones. In landslide zone 10.4 % trees had open canopies while in non-landslide zone 7.7 % tree had open canopies Table 12. Map showing distribution of trees with open canopies is given in Figure 37.

Table 12. Open canopy distribution.

Open Canopies in different Zones			
Zone	No of trees	Gap%>50	%
Landslide Zone	75690	7887	10.4
Nonlandslide Zone	45778	3512	7.7

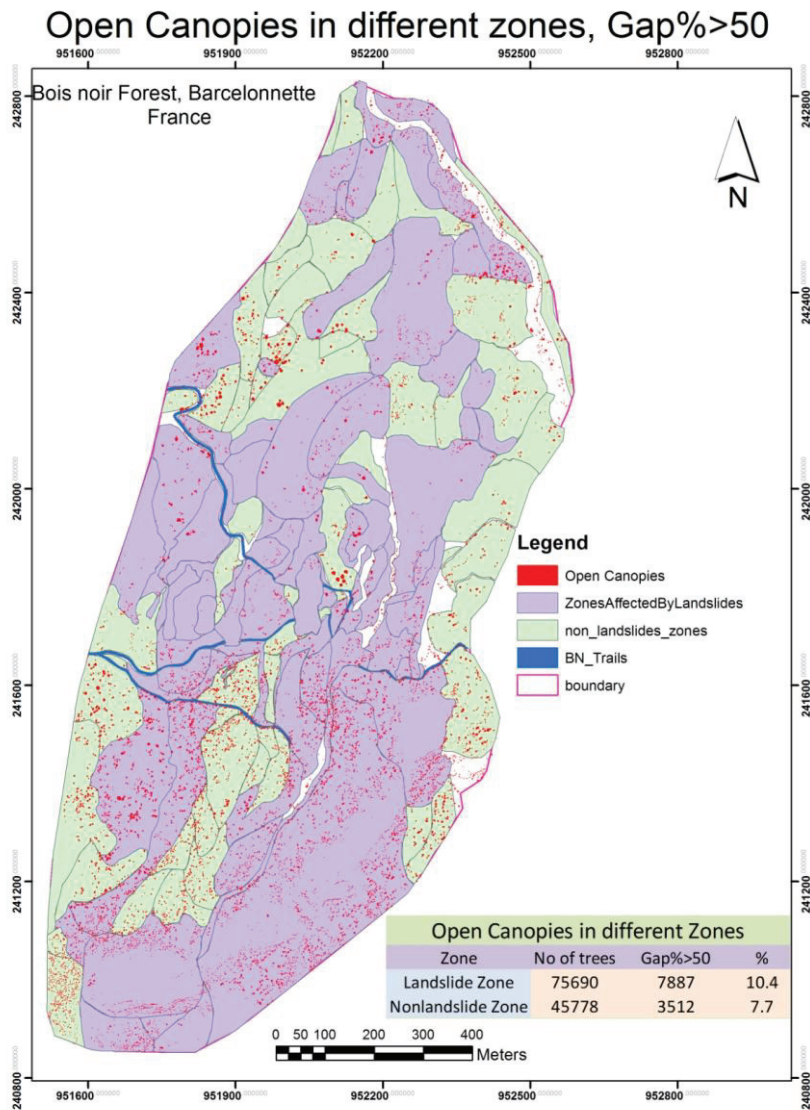


Figure 37. Open canopies in landslide and non-landslide zones

4.8.2. Close canopies

Using local canopy gaps (3.13.14) parameter in the inventory, trees having no inter canopies gaps were identified in landslide and non-landslide zones in the study area. In landslide zone 38.8 % trees had open canopies while in non-landslide zone 37.4 % tree had open canopies (

Table 13). Map showing distribution of trees with open canopies is given in Figure 38.

Close canopies in different zones

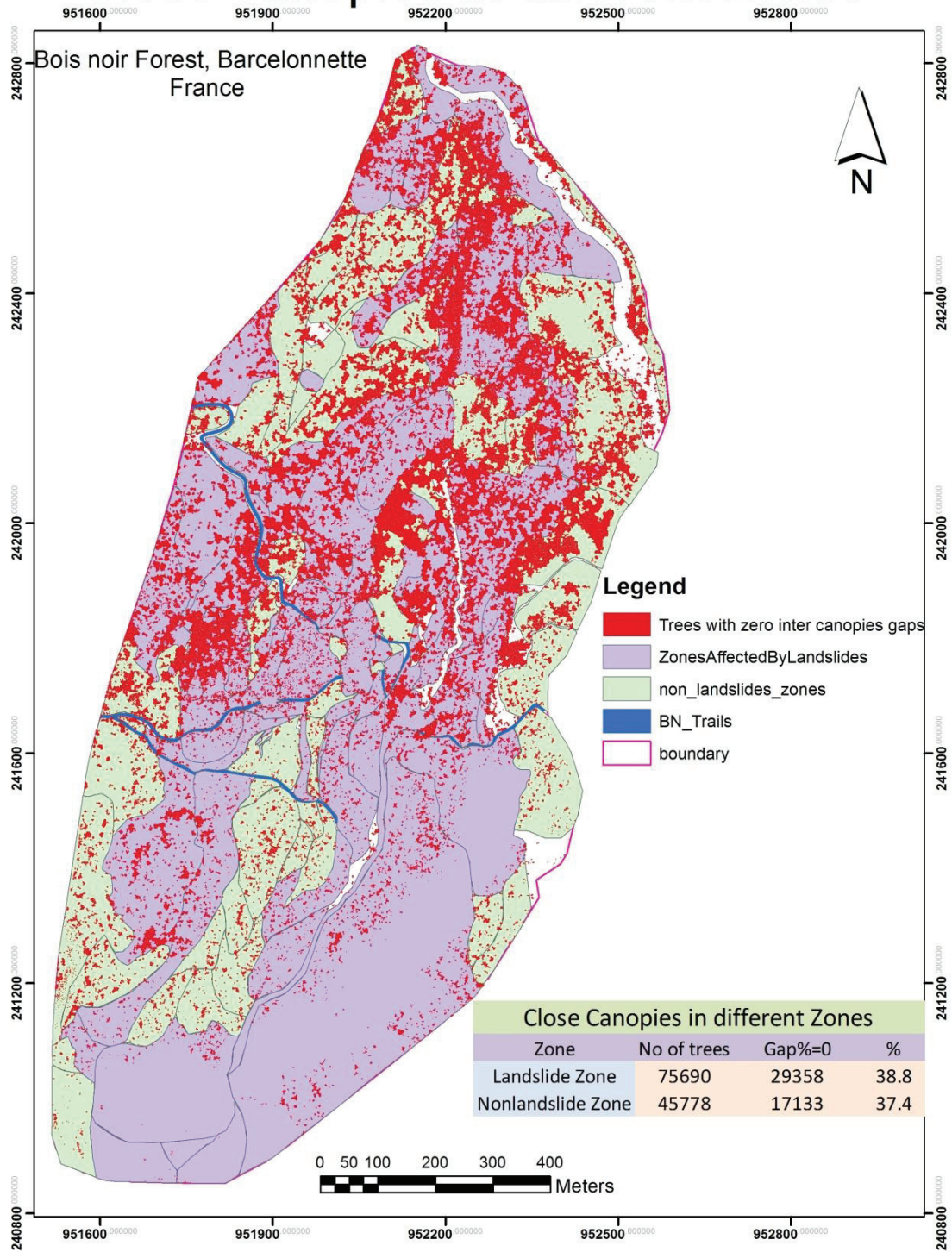


Figure 38. Close canopies in landslide and non-landslide zones.

Table 13. Distribution of trees with close canopies

Close Canopies in different Zones			
Zone	No of trees	Gap ⁰ =0	%
Landslide Zone	75690	29358	38.8
Non-landslide Zone	45778	17133	37.4

4.8.3. Canopy tilt

Using canopy tilt parameter in the geospatial inventory, trees having tilt less than 70 degree were identified in landslide and non-landslide zones. Landslide zone and non-landslide zone had 1303 and 673 tilted trees respectively. Map showing distribution of tilted trees is given in Figure 39.

Table 14. Distribution of tilted trees

Canopy tilt<70 degrees in different Zones			
Zone	No of trees	Tilt<70 degree	%
Landslide Zone	75,690	1303	1.7
Non-landslide Zone	45,778	673	1.5

4.8.4. Variation in tree parameters due to aspect

Using aspect parameter in the geospatial inventory, trees were identified in the northern and southern aspect. Their mean height and CPA in both aspect is given in Table 15. Map showing spatial distribution these trees is given in Figure 40.

Table 15. Mean height and CPA of trees in Northern and Southern aspect.

Variation in Tree Parameters due to aspect			
ASPECT	No of trees	Mean Height (m)	Mean CPA (m ²)
Northern	79,168	9.9	6.3
Southern	49,015	9.6	7.4

Canopy tilt : Tilt<70 degree

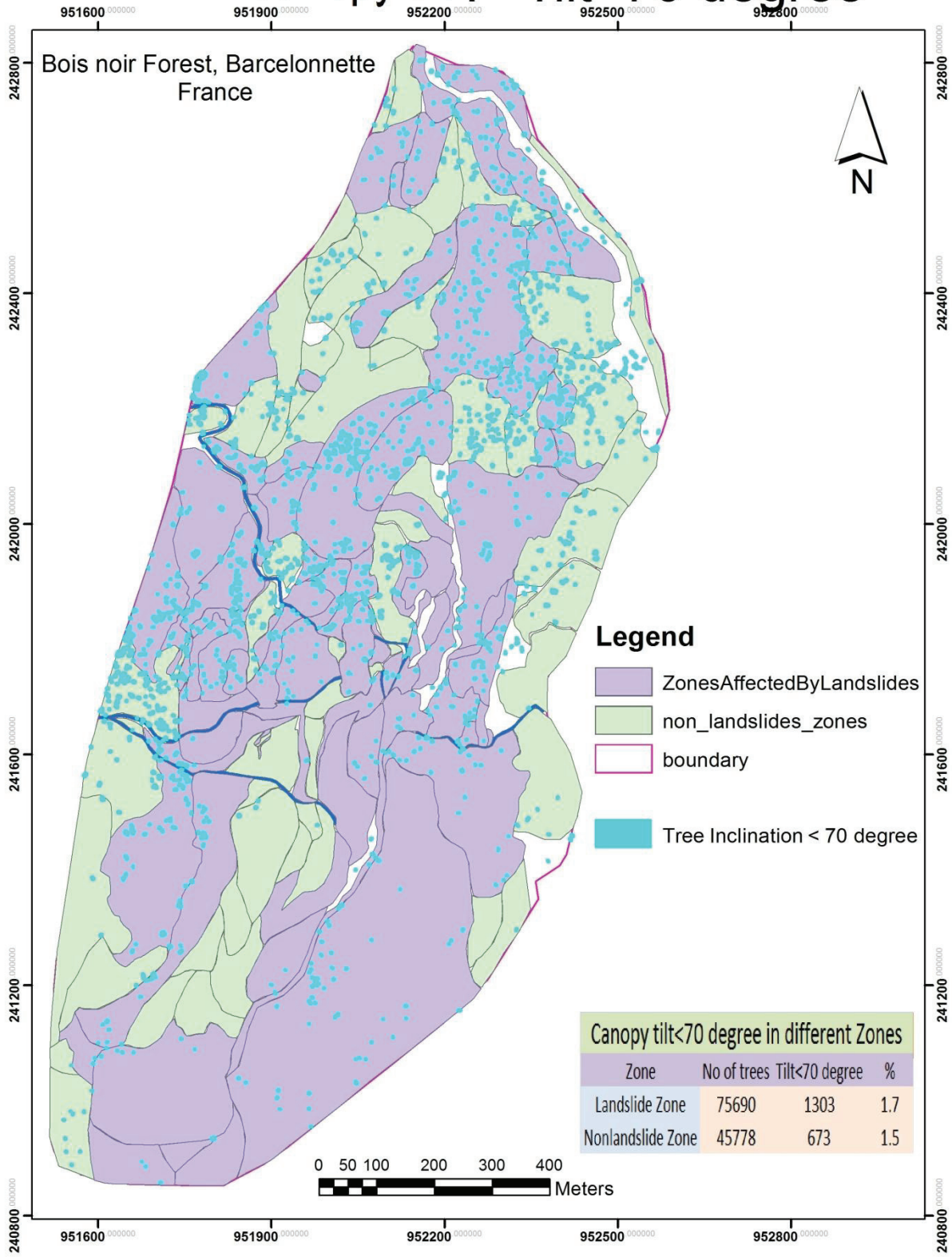


Figure 39. Distribution of tilted trees.

Variation in Tree parameters due to Aspect

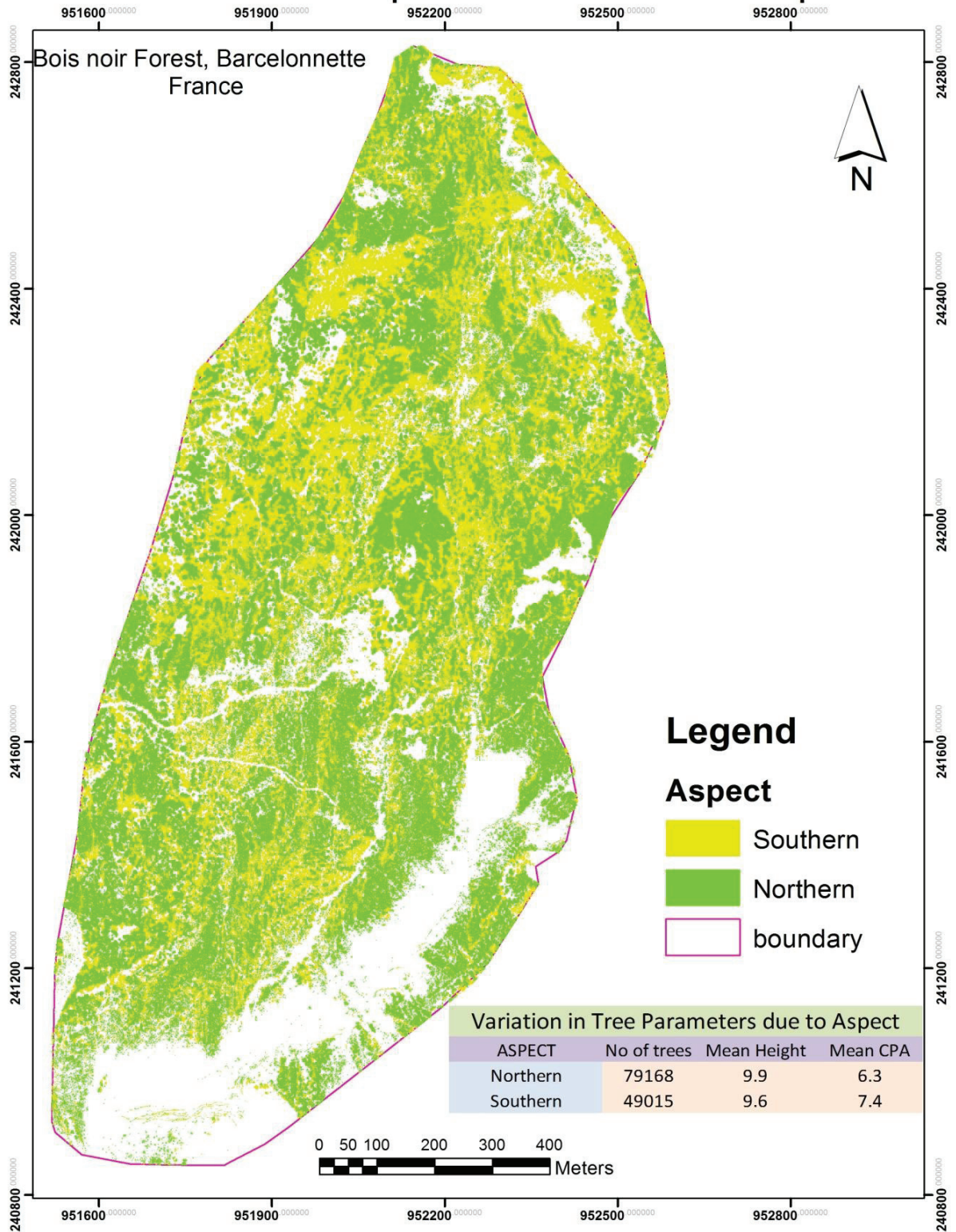


Figure 40. Variation in tree parameters due to aspect

4.9. Descriptive statistics of study area from inventory data

Descriptive statistics of extracted parameters is given in Table 16. Trees falling within 2 m from the study area boundary were excluded due to incomplete crowns.

Table 16. Descriptive Statistics of extracted parameters in the study area.

Variable	n	Minimum	Maximum	Mean	Std. deviation
CHM height	126,653	0.03	34.53	9.82	4.12
CPA	126,653	0.32	108.79	6.73	5.47
Avg CPA height	126,653	2	26.53	7.69	3.39
Canopy Volume	126,653	0.05	1211.3	37.91	46.82
Crown diameter	126,653	0.63	11.77	2.74	1.03
CBH	126,653	2	14.85	2.76	1.63
CBH/Height	126,653	1.5	150.45	0.28	0.73
Tree_Inclination	126,653	8.24	89.98	84.03	4.68
SLOPE	126,653	0.9	86.91	21.07	11.11
ELEVATION	126,653	1403.35	2037.73	1632.36	123.82
TreeDensity	126,653	41.77	5259.88	1451.2	610.54
LidarHits/Area	126,653	0	1605.72	122.43	90.43
LiDAR_Pts/tree	126,653	0	55654	945.08	1407.09
CanopyDensity(LidarPts/vol)	126,653	0	1609.1	28.18	26.34
Gap_Percent	126,653	0	100	17.41	21.67
CD/Height	126,653	0.04	95.88	0.32	0.55

4.10. Tree height profile in the study area

Tree height profile for the whole study area is given in Figure 41. It is based on the CHM height (3.13.1.2) obtained from the LiDAR data.

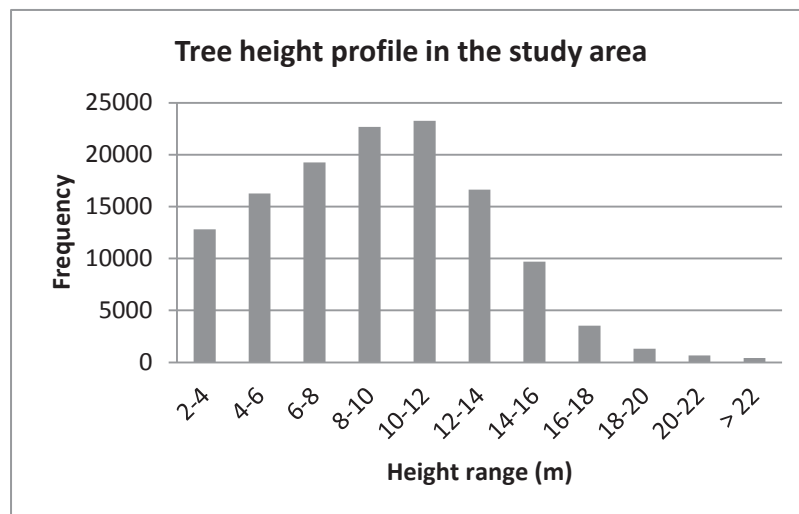


Figure 41. Tree height profile of the study area

4.11. Regression analysis

Three linear regression models were developed for the estimation of biomass/carbon in the study area based on the set of LiDAR derived tree parameters. They are described in the following sections.

4.11.1. Model 1 (CPA and Height)

In this model CPA obtained as a result of Region growing segmentation in eCognition (3.11.1) and LiDAR derived CHM height (3.13.1.2) were used as explanatory variables to get linear regression model for biomass/carbon. Summary statistics of the parameters used in modelling is given in Table 17 and their correlation matrix is given in

Table 18. Goodness of fit statistics is given Table 19. Error statistics of model coefficients is given in Table 20. Plot showing predicted carbon and reference carbon in training and validation data set is given in Figure 42.

Table 17. Summary statistics of parameters used in the model 1.

Training data					
Variable	Observations	Minimum	Maximum	Mean	Std. deviation
Carbon		25.76	264.17	107.84	49.45
Height	125	6.91	19.42	12.46	2.63
CPA		0.90	29.75	7.88	4.94
Validation data					
Carbon		34.75	305.49	107.22	68.54
Height	38	6.51	19.64	12.10	2.88
CPA		1.26	48.40	9.28	8.20

Table 18. Correlation matrix (Model 1)

Variables	Height	CPA	Carbon
Height	1.00	0.18	0.73
CPA	0.18	1.00	0.60
Carbon	0.73	0.60	1.00

Table 19. Goodness of fit statistics (Model 1)

R ²	0.757
Adjusted R ²	0.753
MSE	604.457
RMSE	24.586
MAPE	23.907

Table 20. Model 1 Parameters

Source	Value	Standard error	t	Pr > t	Lower bound (95%)	Upper bound (95%)
Intercept	-81.262	10.835	-7.500	< 0.0001	-102.710	-59.813
Height	12.125	0.854	14.202	< 0.0001	10.435	13.815
CPA	4.819	0.454	10.612	< 0.0001	3.920	5.718

Equation of the Model 1

Carbon (kg) =

$$0.5 * (-81.2618971572085 + 12.1247619660425 * \text{Height} + 4.81873720853689 * \text{CPA})$$

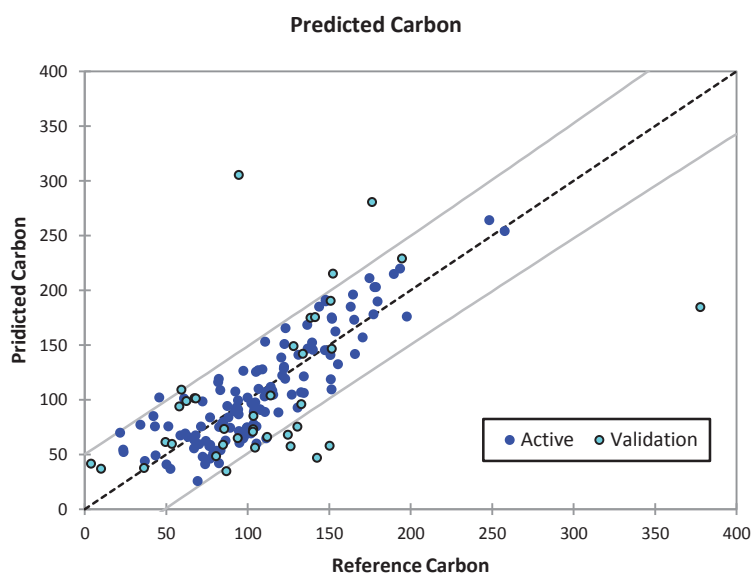


Figure 42. Reference and predicted carbon in training and validation data sets (Model 1).

4.11.2. Model 2 (Canopy Volume and Height)

In this model Canopy Volume (3.13.3) and LiDAR derived CHM height (3.13.1.2) were used as explanatory variables to get linear regression model for biomass/carbon. Summary statistics of the parameters used in modelling is given in Table 21 and their correlation matrix is given in

Table 22. Goodness of fit statistics is given in Table 23. Error statistics of model coefficients is given in Table 24. Plot showing predicted carbon and reference carbon in training and validation data set is given in Figure 43.

Table 21. Summary statistics of parameters used in the model 2.

Training data					
Variable	Observations	Minimum	Maximum	Mean	Std. deviation
Carbon		25.76	264.17	107.84	49.45
Canopy_Vol	125	5.63	199.13	45.84	29.45
Height		6.91	19.42	12.46	2.63
Validation data					
Carbon		34.75	305.49	107.22	68.54
Canopy_Vol	38	5.18	322.50	51.60	51.67
Height		6.51	19.64	12.10	2.88

Table 22. Correlation matrix (Model 2)

Variables	Canopy_Vol	Height	Carbon
Canopy_Vol	1.00	0.54	0.79
Height	0.54	1.00	0.73
Carbon	0.79	0.73	1.00

Table 23. Goodness of fit statistics (Model 2)

R ²	0.751
Adjusted R ²	0.747
MSE	618.936
RMSE	24.878
MAPE	23.732

Table 24. Model 2 Parameters

Source	Value	Standard error	t	Pr > t	Lower bound (95%)	Upper bound (95%)
Intercept	-36.438	11.136	-3.272	0.001	-58.482	-14.393
Canopy_Vol	0.929	0.090	10.350	0.0001	0.751	1.107
Height	8.158	1.006	8.106	0.0001	6.165	10.150

Equation of the model:

$$\text{Carbon (kg)} = 0.5 * (-36.4376358958664 + 0.929230749280394 * \text{Canopy_Vol} + 8.15762627104967 * \text{Height})$$

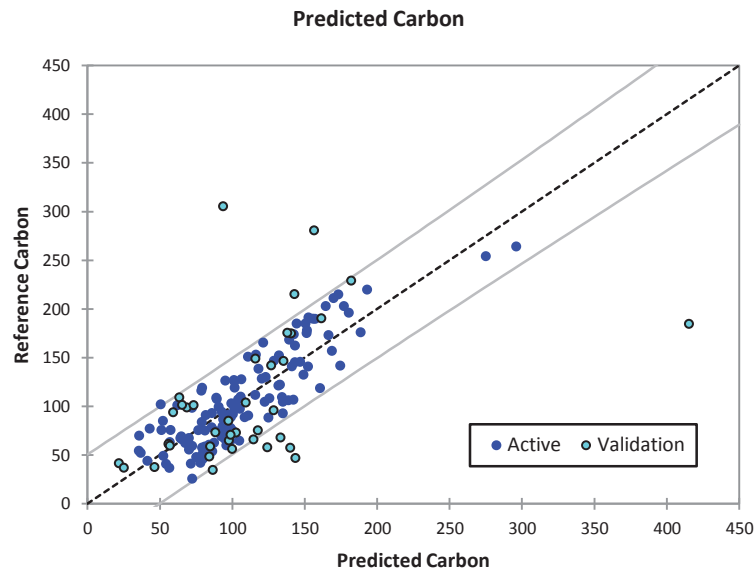


Figure 43. Reference and predicted carbon in training and validation data sets (Model 2).

4.11.3. Model 3 (CPA, Height, LTD)

In this model, additional explanatory variables like local tree density, local canopy gaps, aspect, slope were added to height and CPA to investigate the improvement in the previous models. All these explanatory variable were tested in SPSS statistical software using back elimination of parameters. The best model out of them was achieved for explanatory variables height, CPA and local tree density. This model is based on interaction of height with local tree density and CPA. The model parameters used were height, (height)x(CPA), (height)x(local tree density). Goodness of fit statistics is given in Table 25. Error statistics of model coefficients is given in

Table 26. Plot showing predicted carbon and reference carbon in training and validation data set is given in Figure 44.

Table 25. Goodness of fit statistics (Model 3)

R ²	0.787
Adjusted R ²	0.782
MSE	532.589
RMSE	23.078
MAPE	21.831

Table 26. Model 3 parameters.

Source	Value	Standard error	t	Pr > t	Lower bound (95%)	Upper bound (95%)
Intercept	-45.92	10.38	-4.42	< 0.0001	-66.47	-25.37
LTDxHeight	0.00	0.00	-2.96	0.00	0.00	0.00
Height	11.74	1.33	8.83	< 0.0001	9.11	14.37
CPAxHeight	0.30	0.04	6.66	< 0.0001	0.21	0.38

Equation of the model 3:

$$\text{Carbon (kg)} = 0.5 * (-45.923634209894 - 1.44132788781274E-03 * \text{LTDxHeight} + 11.7389720241281 * \text{Height} + 0.295287590676784 * \text{CPAxHeight})$$

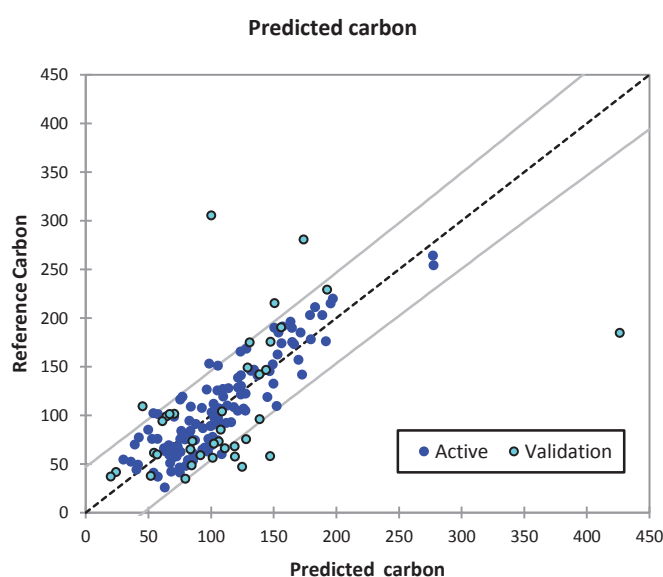


Figure 44. Reference and predicted carbon in training and validation data sets (Model 3)

4.11.4. Selecting best model for Carbon estimation

The best regression model was selected based on higher R^2 and lower RMSE. From the results, model 3 (4.11.3) was found to be the best with highest R^2 and least RMSE. Carbon was calculated based on this model for *Pinus uncinata* and *Pinus sylvestris* in the whole study area. Spatial distribution of carbon for Pines in the study is given in Figure 45. Based on the regression model, the total carbon in the study area was 3811 tons with mean carbon per tree of 33.16 kg (Table 27).

Table 27. Carbon estimation of Pines in the study area

Carbon estimation of Pines in the study area			
	Pines	Mean Carbon(Kg)/tree	Total Carbon (Tons)
Carbon	114,921	33.16	3,811

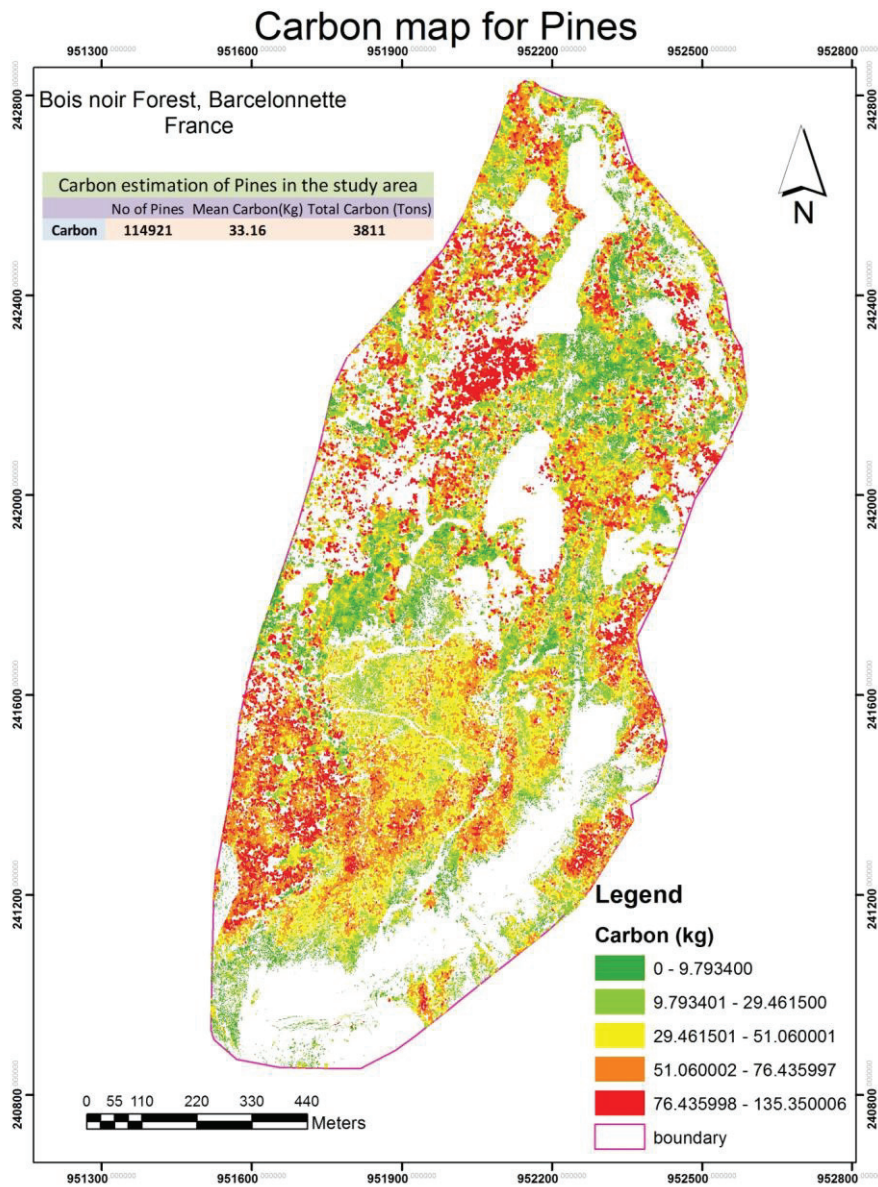


Figure 45. Carbon map for *Pinus uncinata* and *Pinus sylvestris*

5. DISCUSSION

5.1. Tree Peak identification

A precise individual tree based inventory parameter extraction leverages an accurate identification of trees. The main aim of the research was to extract inventory parameters, and such parameters cannot not be retrieved accurately unless trees are identified and delineated accurately. Therefore, much of the research efforts have gone in developing a method for tree peak detection. Tree peak detection accuracy obtained in this research was 96 % (4.2) with total number of identified tree peaks equal to 128,918 (Table 6). In comparison to previous research works, the accuracy of the result is quite statistically significant. Pitkänen et al (2004) could identify 40 % trees in CHM, Reitberger et al (2007) achieved 61 % accuracy in coniferous forests based on a stem detection algorithm using full waveform LiDAR data. Rahman & Gorte (2009) detected more than 70 % trees using density of high points in LiDAR data with sampling density of 70 points/m². Koch et al (2006) achieved 87.3 % tree detection accuracy in douglas firs by searching local maxima in a smooth CHM using LiDAR data with sampling density of 5-10 points/m². Kwak et al (2007) achieved an accuracy of 86.7 % for *P. koraiensis*, *L. leptolepis*, and *Quercus* species, by removing spurious local maxima in extended maxima transformation based on height values of local maxima using LiDAR data with a sampling density of 1.8 points/m².

Before we review the obtained accuracy of peak detection, it is pertinent to discuss how the algorithm for peak detection was developed. We had a small foot print high sampling density LiDAR data with average of 122 points per square meter on tree canopies. The density is equivalent to a point on the average in each 9 cm grid. The average number of LiDAR points on a tree were 945, the maximum LiDAR hits in a single tree was 55,654 in the study area (Figure 46). The point cloud density was good enough to give structural definition to trees. To know how well the point cloud defines the trees, the LiDAR data was thoroughly visualised in 3D using software such as Quick Terrain Modeler and MARS (Figure 47). It was found that trees were structurally well defined with distinctive peaks (Conifers show distinctive peaks). The very next question was, how to identify these trees. Whether to look for tree peaks, tree stems or for density of point clouds around peaks. We chose the first option as tree stem information was missing in large number of trees in the point cloud, the density of peak was not reliable as the LiDAR data was over sampled with multiple flights (overlapping flight tracks or intersection of tracks will show high density of point clouds).

Earlier research of tree peak detection is based on finding local maxima in CHM or smooth CHM or CHM with varying degree of smoothness in a fixed or variable size search windows. We wanted to know the best method for our study area and to improvise it for higher accuracy.

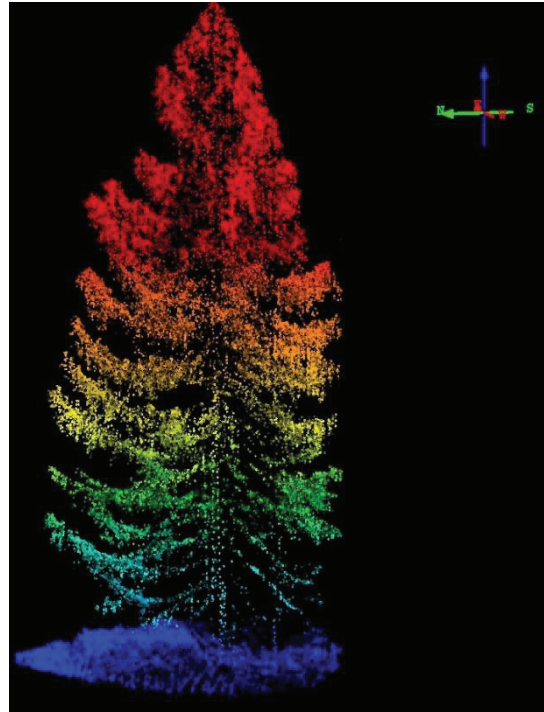


Figure 46. *Larix* tree with 55,654 LiDAR hits

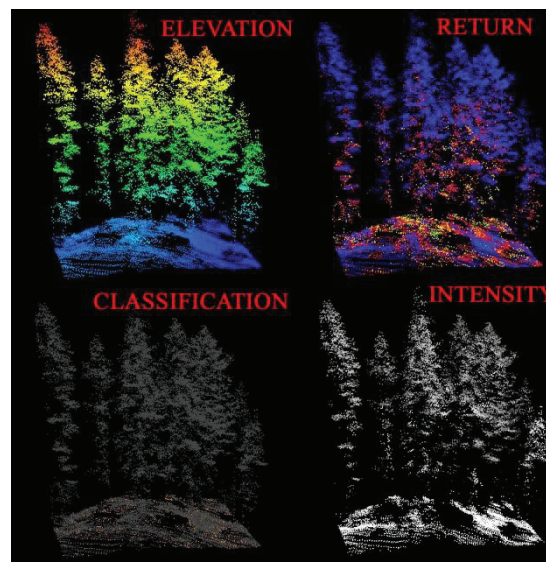


Figure 47. Point cloud visualisation on the basis of elevation, returns, classification and intensity

5.1.1. Fixed size window

In a fixed size search window the size of the window is decided on the basis of mean crown diameter of trees. eCognition based Region growing segmentation also gets the seeds by identifying local maxima in a fixed window size unless they are provided separately in a thematic layer. Fixed size window works best with the homogeneous, monoculture plantations as the standard deviation in the crown diameter is less. However, it is difficult to obtain accurate results of tree detection in a fixed size window in a mixed forests because of varying crown sizes resulting into a high error of omission .

5.1.2. Variable size window

Popescu and Wynne (2004) suggested variable search window for locating tree maxima and showed the improvement in accuracy in comparison to fixed size window. However, it requires a prior knowledge of height and CPA relation in the forests. Variable window will show a high error of omission if there doesn't exist a fixed relation between tree height and crown size. For this reason TreVaw (developed by Popescu) could identify only 76,000 trees in the study area, whereas we detected 128,918 trees.

5.1.3. Reasons for good accuracy

It is difficult to compare the obtained accuracy of tree detection with the previous research results due to variation in point cloud densities, methods adopted and type of forests (coniferous or broadleaved). However, error involved in similar methods may be analysed. Both fix window and variable window methods do not take into account individual tree structural information but are based on mean crown diameter or height and crown diameter relation. While variable smoothing method takes into account each pixel of CHM to get a smooth CHM. The smoothing effect depends on the shape of individual tree and the degree of smoothing. A small fixed size window (45 cm) makes sure that there is only one local maxima within search window, reducing error of omissions. Since in the adopted approach smoothing is height retaining or in other words, it makes an enveloping surface over the tree (convex hull), merging of tree canopies due to flattening of tree canopies during smoothing is substantially reduced. Further, the merging effect of smoothing is controlled by varying degree of smoothing based on height. Care is required to select height cut off for a particular degree of smoothing. It is fine tuned in successive results by observing error of omission and commission to reach to optimal values for height cut off. Error of commission is reduced firstly due to coniferous forests (trees with distinctive peaks) and secondly for using high density LiDAR data where on the average each 9 cm apart there is a LiDAR hit. Figure xx shows how different local maxima based peak detection algorithm works.

5.1.4. Limitation of the method

- i. The method requires *a priori* about height and crown size relation.
- ii. It is based on identifying local maxima in smooth CHM, therefore tree tops not appearing as local maxima in the smooth CHM may not be detected e.g. trees with top broken, deciduous trees with flatten top, trees with their top merging with neighbouring tree canopies, fallen trees.

5.1.5. Sources of error

- i. Close spacing of tree tops (< 45 cm (search window size)).
- ii. Small trees in the neighbourhood of large trees resulting in canopy merging.
- iii. Low point cloud density. (i.e. a point cloud density insufficient to give a point in the search window for a tree)

5.2. Delineation of tree crowns

The results of segmentation are given in Section 4.3. Tree crown delineation using Region growing approach resulted in D value of 0.16 (84 % accurate) with 93.5 % accuracy of 1:1. For segmentation using Thiessen polygon approach, the D value is 0.21 (79 % accuracy) with 94.2 % accuracy of 1:1 correspondence. Both segmentation approaches have performed well. High crown delineation accuracy is attributed to accurate identification of tree peaks and inter canopy gaps. Overall segmentation accuracy in both approaches was marginally increased when segmentation was smoothed with polygon smoothing. In Region growing the improvement in segmentation accuracy was 3% while in Thiessen polygons it was 1%. Region growing segmentation had jagged edges due to low resolution (60 cm) supported by eCognition while Thiessen segmentation was prepared in ArcGIS and had better resolution (15 cm). Therefore, the improvement in segmentation accuracy in Thiessen approach was negligible due to segmentation smoothing.

It was observed that for open canopies, both approaches gave almost similar segmentation (Figure 49). This is attributed to the fact that we used the same information of seeds (tree peaks) and gaps in both approaches. With the fixation of tree peaks (seeds), the segmentation strategy for any algorithm is the allocation of space to each seed. Region growing works on the principle that it grows more towards the direction of homogeneity of pixel and stops at minima (Ke & Quackenbush, 2008). Whereas, Thiessen polygon works on the principle of allocating space to each node (tree peaks) such that any point in the polygon is closest to its node than to any other node. In case of open canopies, the accuracy of delineation comes from the well delineated inter canopy gaps. This is due to the fact that in both approaches for open canopies, the adjacent gap boundary becomes the common boundary as a result of segmentation. But in case of close canopies where inter canopy gaps cannot help the delineation process, Region growing

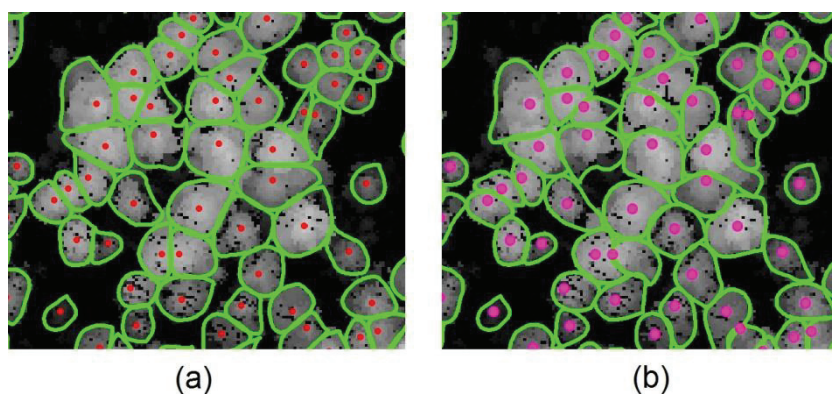


Figure 48. (a) Region growing segmentation (b) Thiessen segmentation

approach was observed to perform better. Better performance of Region growing may be explained in term of information it is using for delineation. Thiessen polygons approach only uses the information of tree seed (tree location) which puts a restriction of growth of a node due to presence of surrounding nodes. However, Region growing approach, besides making use of tree location information (seed), uses

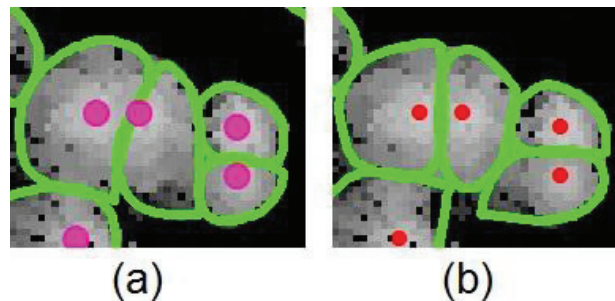


Figure 49. (a) Thiessen segmentation (b) Region growing segmentation

tree structural information of canopy slopes and canopy intersection (minima). In case of homogenous forest stand, the Thiessen polygons perform well but in mixed forest where a large tree stands near a small tree. The Thiessen Polygons approach does over segmentation of small tree and under segmentation of large tree (Figure 48). However, Region growing approach has proven to be effective for the more complex forest structure of naturally regenerating forests (F. Gougeon, 1995).

Thiessen polygons and Region growing approaches have showed similar results in 1:1 correspondence. It is attributed to the fact in both approaches the segmentation grew from the same set of seed information (tree peaks).

For the assessment of segmentation accuracies, crowns are manually delineated. In case of intermingled trees, the manual delineation is difficult and subjected to human error.

5.2.1. Visualising segmented trees in point cloud

Validation of segmentation suffers from human bias due to manual delineation of reference segments. In case of intermingled trees it is difficult to delineate crown. Extraction of point cloud of segmented trees gives a visual result of the accuracy. Error of omission is clearly visible in a high density point cloud data. It has also helped in cross checking the accuracy of manually delineated crowns. Future research is required to develop it into an independent segmentation validation method.

5.3. Species classification

Conventionally, tree species information is extracted from hyper spectral images or high resolution colour infrared aerial photographs (Brandtberg et al., 2003; Hyyppä et al., 2008). LiDAR data has also been used

to classify tree species. Holmgren and Persson (2004) tested species classification of Scots pine in Norway with classification accuracy of 96 %. Moffiet et al (2005) suggested that LiDAR singular returns is an important criterion for tree species classification. Brandtberg et al (2003) used LiDAR data under leaf off conditions (data taken in leaf fall season for broadleaved) for species classification. Persson et al (2002) used fusion of high resolution multi-spectral image with high density LiDAR data for species classification. Liang et al (2007) used a simple technique, the difference of first and last return under the leaf off condition to discriminate between deciduous and coniferous trees.

Species classification based on individual tree parameters is a new topic of research. We obtained an overall accuracy of 97 % of species classification by identifying *Pines* and *Larix* in the study area, based on tree structural and spatial parameters. *Larix decidua* trees which were interspersed with other species and well distributed in the study area, were identified purely on structural information and had a classification accuracy of 77 %. The obtained overall accuracy of species classification (97 %) will be misleading to quantify LiDAR capacity to classify species with this accuracy on structural differences in mixed conditions. It is increased due to accurate classification of *Pinus uncinata* and *Pinus sylvestris* which were distributed strictly on elevation basis. However, accuracy of *Larix decidua* is indicative of LiDAR potential to identify species in mix conditions using structural information. Korpela et al (2010) studied the effects of stand and tree parameters for tree species classification using LiDAR data. Holmgren and Persson (2004) used CBH as strong separating factor between pine and spruce.

5.3.1. Limitation

In complex mixed forest, LiDAR derived structural and spatial parameters cannot fully explain the differences in species. Similarly, in sub-species having similar structural formation, use of LiDAR data only cannot suffice for classification. LiDAR cannot replace the hyper-spectral optical images for species classification. Therefore, fusion of LiDAR with high resolution spectral images has been frequently used to exploit both spectral and structural information for species classification. There have been attempts to use intensity data of LiDAR for species classification (Kim et al.). Korpela et al (2010) indicated that use of intensity of first-or-only echoes is optimal for use in species classification. Intensity of LiDAR return depends on various factors such as target emitter distance, beam divergence (there is a loss of intensity with the diverging beam), the laser footprint size, angle of incidence, atmospheric attenuation and signal processing. Moreover, canopy may contain different scatterers e.g. bark, needles, cones, flowers, twigs, all of which vary in reflectance. It makes difficult to use intensity with explanatory power in species classification.

5.4. Extracted parameters

5.4.1. Height

The height was estimated in four ways as described in the Section (3.13.1). The result of accuracies of LiDAR derived heights is given in Section (4.4). The best R^2 (0.86) for LiDAR derived heights was achieved for CHM height. There was no significant change in R^2 (0.85) when it was measured in smooth CHM. However, some research show better correlation of smooth CHM height with field measured height (Hyypä et al., 2008). We wanted to investigate whether taking maximum pixel value in a tree crown segment is appropriate for a measure of tree height. It was observed that in Region growing as well as in Thiessen polygon segmentation, some crown segments overlap with a neighbouring crown. In such cases, the selection of maximum pixel value as a tree height can be inaccurate due to influence of neighbouring crown pixels. It was found that height accuracy for eCognition CHM height ($R^2=0.81$) and eCognition smooth CHM height ($R^2=0.81$) was less than the accuracy of the CHM height. Therefore, CHM height and smooth CHM height proved to be a somewhat better estimator for field measured height.

The obtained accuracy of height does not commensurate with the quality of LiDAR data we had. The past research shows better results with lesser sampling density than the data used in this research. The purpose of the research was not to assess the height estimation capacity of LiDAR. Several research have already been done to prove this point. Heurich et al (2004) estimated accuracy at 0.96 for coniferous and 0.98 for deciduous trees. However, to assess the accuracy of LiDAR derived height, we need comparable technology to measure trees in the field. The Laser range finder used for height measurement has a standard error of 0.5 m. Furthermore, it requires a minimum distance from the object for accurate measurement. It also requires unobstructed line of sight to tree base and tree top. We observed a variation up to 3 m in reading for the same tree when measured by different people. It was difficult to measure height with the laser rangefinder due to high density of forest with steep slopes, for this reason the accuracy of laser range finder was adversely affected. Therefore, a certain degree of error for difficult trees cannot be negated in measured heights. Andersen et al (2006) did a rigorous assessment of tree height measurement obtained from LiDAR and conventional field methods. He acquired an accuracy of (<2 cm error) in measurement of tree heights using total station survey. It was shown that keeping into account the DTM error and missing tree top error, the overall height error was $-.073(\text{DTM}) \pm 0.43$ m (missing tree top).

Causes of error in height

Error in LiDAR derived height is combination of error due to tree top detection and error in the DTM at the base of the tree. Andersen et al (2006) showed that for point cloud density of 6 points/m² the error contribution of DTM was 10 to 20 cm for relatively flat surface but in case of steep slopes DTM error contribution would be more. Yu et al. (2004b) and Hyypä et al (2009) showed that flight altitude, point density and footprint size, all have effect on canopy height. With increase in flight height the accuracy decreases. Point density had the more influence on estimation of tree height than the footprint size. Our LiDAR dataset is quite dense therefore error of top detecting as well as error in DTM generation should be relatively low.

5.4.2. CPA

For eCognition derived CPA (4.6) the accuracy is 0.87 (R²), while for Thiessen polygon derived CPA the accuracy is 0.9 (R²). It shows that Thiessen polygon based segmentation is a good estimator for CPA assessment. The Thiessen polygon approach is relatively simpler and quicker to achieve. However, the accuracy in this approach is dependent on accurate detection of tree peaks and inter canopy gaps information from the LiDAR data.

5.4.3. Canopy Volume

Canopy volume was assessed in this study to see its usefulness as explanatory variable for estimation of forest biomass/carbon in a regression model. Canopy volume was found equally important explanatory variable in comparison to CPA. The set of explanatory variables (CPA, height) and (Canopy volume, height) had the same R² = .75. The measurement of Canopy volume in the field is complex, therefore its validation from field observed data is not assessed.

5.4.4. Canopy base height

CBH showed good correlation with average CPA height of smooth CHM, R² = 0.77 It indicates a possibility of regression model of CBH using LiDAR derived average CPA height which is relatively easy to measure..

5.4.5. Canopy tilt

Measuring tilt of a tree from LiDAR point cloud is a new topic of research. Bucksch et al (2009) developed an algorithm, SkelTre to measure individual tree dimensions as well as tree tilt and orientation from individual tree point cloud data. Measuring tree tilt at forest level using LiDAR data has not been tried. Folkesson et al (2006) developed an automatic detection method of wind thrown trees in forest using VHF SAR images. We developed a method to extract canopy tilt at forest level using LiDAR data.

We did not have data of canopy tilt from the field but we had the data of tree tilt at 2 m from the base. It was shown that variation in tree tilt at 2 m could be explained by LiDAR derived canopy tilt with an accuracy of 0.57 (R^2). The validation of our result from field measured canopy tilt is subject to future research. However, identified tilted trees were extracted from the point cloud using eCognition based segmentation shape file. The result is shown in Figure 36.

Limitation

- i. The canopy tilt algorithm requires a precise delineation of tree crowns.
- ii. It is based on the assumption that trees are symmetrical objects with centroids of the crown segments coinciding with the tree trunks.
- iii. Canopy tilt was measured from the smooth CHM peak and the centroid of CPA segment. Therefore, malformed trees with broken tops or broken branches will show a shift of tree peaks from the centroid. Consequently, such trees will show a false tilt. However, a new insight is obtained for identification of malformed trees to assess forest disturbance. This may be studied in future research.

5.5. Forest inventory

We endeavoured to generate a detailed geospatial forest inventory by extracting structural tree parameters and spatial terrain information from LiDAR data. Forest inventory information has been crucial with respect to forest management. In addition, for sustainable forest management, the information is needed, not only for planning future forest management, but also for recording the previous status of the forested area (Koch et al., 2006). Moreover, single-tree-level forest information has been essential for various forest applications, such as monitoring forest regeneration, forest inventory, and evaluating forest damage (Chen et al., 2006). Therefore, detailed forest information, such as tree counts, tree heights, crown base heights, canopy volume, canopy tilt and forest biomass, are critical for the effective management and quantitative analysis of forests. We tested some applications of forest inventory with a view to show its importance as a decision support tool for forest managers.

5.5.1. Open canopies

Status of open canopies in the forest is important as an indicator of forest disturbance as well to know the potential area for regeneration. We identified trees having local canopy gaps percentage more than 50 %. Result (4.8.1) show that in the landslide zone the percentage of open canopies was 10.4 % while that in non-landslide zone was 7.7%. A greater canopy opening in the landslide zone may be an indication of forest disturbance in the zone but it needs further validation from the field data.

5.5.2. Close canopies

Close canopies with no inter canopy gaps in the study area were identified. Results are shown in (0). It is found that about 38% trees in the study area have close canopies. It is an indication of closely packed forest. This information is important for forest managers for carrying out silvicultural operation like thinning or selective felling. The result show no difference in percentage of open canopies in landslide zone and non-landslide zone.

5.6. Descriptive statistics of extracted parameters

Descriptive statistics of some of the important parameters is given in the Section 4.9. Results provide a broad understanding of the forest area. The mean height of the trees in the study area is 9.82 m while average CPA is 6.73 m², average crown diameter is 2.74 and average canopy volume is 46.82 m³. Here trees with height less than 2 m have not been considered. The study area is mainly a coniferous forests and not subjected to any felling for last the 100 years. Results show that the forest has poor growth as tall trees are of small size. Average CBH is 2.76 m, it indicates that most of the leaves biomass is above this height. The average ratio of CBH with height is 0.28, it means on the average CBH starts at about one third of the height of a tree. Average tree tilt is 84 degree, indicating trees area mostly straight. Average local tree density is 1451 trees per ha and average local canopy gaps percentage is 17.4 % which indicates high density of forests. Average point density of LiDAR on tree canopies is 122 points/m², while the average is 164 points/m². It shows LiDAR backscattering is reduced due to vegetation. The average canopy diameter to height ratio is 0.32 implying conical canopy shape (Table 5), indicating coniferous forests.

5.7. Carbon Modelling

Carbon modelling done for pair of explanatory variable (CPA, height) and (Canopy volume, height) gave almost similar results of R² equal to 0.757 and 0.751 with RMSE of 24.59 kg and 24.88 kg respectively. In previous research, Lefsky et al (2002) obtained R² of 92 % for above ground biomass. Heurich et al. (2004) was able to estimate timber volume in coniferous forests with an accuracy of 0.87-0.95. However, getting a poor regression is not uncommon. Popescu et al. (2003) got the maximum R² of 0.33 for deciduous forests. Biomass is well explained by dbh and height. But direct measurement of dbh with LiDAR data at forest level is still not possible. Therefore accuracy of biomass estimation largely depends on how good the explanatory variables explain the biomass.

We did not have measured biomass but calculated allometric equation of uncertain accuracy. We had the impression that we will get the local biomass equations for *Pinus uncinata* and *Pinus sylvestris* from the forest department France. Unfortunately allometric equations were not available. We have used allometric equation for *Pinus nigra* from Netherlands. Tree biomass is species and area dependent. There is a difference of climate, soil and specie for the equation used. Moreover, the forest is anomalous with

abandoned unthinned plantations. This is the reason that we did not get good accuracy despite the fact that explanatory variables had significant accuracy.

Popescu et al. (2003) showed that crown diameter alone could explain 83 % of the variation associated with biomass in coniferous forests in the south-eastern US. However, for our study area the crown diameter alone explains 36 % of the variation in biomass. We found a dbh anomaly with height as well as with CPA, where same dbh shows variation in height as well as in CPA. To improve the model we tried to include additional explanatory variables such as local tree density, local gap percentage, aspect, elevation, canopy volume, canopy density. Using backward elimination method in SPSS statistical software. The best model we could get was with explanatory variables height, CPA and local tree density. The model was based on the interaction of height with local tree density and CPA. The R^2 was 0.79 with RMSE of 23 kg for carbon. The model was improved in terms of R^2 as well as RMSE, although the improvement was not very significant. The improvement may be explained in terms of tree behaviour in high tree density. Due to high tree density conditions, trees tend to grow vertically because of unavailability of lateral space. It results into higher height and lower CPA .

6. CONCLUSIONS AND RECOMMENDATIONS

6.1. Conclusion

How accurately the tree peaks can be detected in Canopy Height Model of high density airborne LiDAR data?

Tree peaks could be detected with an accuracy of 96 %. The new adaptive approach for tree detection tested in this research has performed well. High density LiDAR point cloud with an average point density of 122 points/m² for trees has also contributed in improving the peak detection accuracy.

What is the difference in segmentation methods by Object based image analysis and Thiessen polygons using airborne LiDAR data with prior knowledge of tree peaks and inter canopy gaps.?

The performances of two crown delineation approaches were compared. The result indicated that both approaches provided useful results in delineating tree crowns in mixed dense coniferous forest. The Region growing approach resulted in delineation accuracy of 84% with 93.5 % 1:1 correspondence while, Thiessen polygons approach resulted in tree crowns delineation accuracy of 79% with 94.2% 1:1 correspondence. Thiessen approach in comparison to Region growing is much simpler. Thiessen segmentation showed marginally better R² with manually delineated segments and proved to be a significant estimator for CPA.

How accurately the tree structural parameters such as tree height, CPA, canopy base height, tree tilt can be estimated from LiDAR point cloud data?

Tree height and canopy base height could be achieved with significant accuracy, (for CHM height, R²=0.86), (Canopy base height, R² = 0.73), however, tree tilt could not be fully validated for want of relevant field data. Canopy tilt was compared with tree tilt at 2 m from the base. The extracted canopy tilt could explain the variation in tree tilt (at 2 m) with an accuracy of , R² = 0.56

What is the accuracy of Biomass/carbon obtained from (CPA + Height) and (Canopy Volume + Height) as pair of explanatory variables in regression analysis?

For explanatory variables CPA and Height of biomass/carbon, the coefficient of determination R² was 0.757 and Root Mean Square Error, RMSE was 24.586 kg, while for explanatory variables Canopy Volume and Height, the R² was 0.751 with RMSE of 24.878 kg

What is the accuracy of Biomass/carbon obtained from CPA, height with additional variables such as local tree density and local canopy gaps?

The best model we could achieve with inclusion of additional explanatory variables for determination of biomass/carbon, was achieved in interaction model approach. The model had three explanatory variables namely Height, (Tree Density)*Height, CPA*Height. The R² for this model was 0.787 with RMSE of 23.078 kg.

What is the accuracy of species classification in the study area?

The overall accuracy of species classification at the tree crown level was 97%. For *Larix decidua* it was 77% while for *Pinus uncinata* and *Pinus sylvestris* it was 98% and 100% respectively.

What is the relationship between CPA, height and biomass/Carbon?

Biomass (kg) = a + b.CPA + c.Height

Carbon (kg) = 0.5.(a + b.CPA + c.Height)

Where, $a = -81.2618971572$, $b = 4.8187372085$, $c = 12.1247619660$

What is the relationship between canopy volume, height and biomass/Carbon?

Biomass (kg) = $a + b \cdot \text{CanopyVolume} + c \cdot \text{Height}$

Carbon (kg) = $0.5 \cdot (a + b \cdot \text{CanopyVolume} + c \cdot \text{Height})$

Where, $a = -36.4376358959$, $b = 0.9292307493$, $c = 8.1576262710$

What is the amount of biomass/carbon stock for pines in the study area?

Biomass = 7622 tons, Carbon = 3811 tons

6.2. Recommendation

LiDAR is full of possibilities to fulfil the needs of precision forestry. High density LiDAR is capable of recording enough structural information for enabling accurate inventory parameter extraction. Future research is required to extract tree tilt and orientation to address the issues of forest disturbance. The effectiveness of crown delineation was tried in dense unthinned plantations mixed with natural regeneration, this approach is recommended to be used in other natural mixed forests and plantation forests.

LIST OF REFERENCES

- Andersen, H. E., et al. (2003). Estimating forest structure parameters on Fort Lewis Military Reservation using airborne laser scanner (LIDAR) data. *PRECISION FORESTRY*, 45.
- Beaudoin, A., et al. (1994). Retrieval of forest biomass from SAR data. *International Journal of Remote Sensing*, 15(14), 2777-2796.
- Beucher, S., et al. (1979). Use of watersheds in contour detection.
- Bortolot, Z. J. (2006). Using tree clusters to derive forest properties from small footprint LiDAR data. *Photogrammetric Engineering and Remote Sensing*, 72(12), 1389.
- Boudreau, J., et al. (2008). Regional aboveground forest biomass using airborne and spaceborne LiDAR in Québec. *Remote Sensing of Environment*, 112(10), 3876-3890.
- Brandtberg, T., et al. (1998). Automated delineation of individual tree crowns in high spatial resolution aerial images by multiple-scale analysis. *Machine Vision and Applications*, 11(2), 64-73.
- Brandtberg, T., et al. (2003). Detection and analysis of individual leaf-off tree crowns in small footprint, high sampling density lidar data from the eastern deciduous forest in North America. *Remote Sensing of Environment*, 85(3), 290-303.
- Brown, S., et al. (1995). Use of forest inventories and geographic information systems to estimate biomass density of tropical forests: Application to tropical Africa. *Environmental Monitoring and Assessment*, 38(2-3), 157-168.
- Bucksch, A., et al. (2008). CAMPINO — A skeletonization method for point cloud processing. *ISPRS journal of photogrammetry and remote sensing*, 63(1), 115-127.
- Castel, T., et al. (2002). Retrieval biomass of a large Venezuelan pine plantation using JERS-1 SAR data. Analysis of forest structure impact on radar signature. *Remote Sensing of Environment*, 79(1), 30-41.
- Chen, L. C., et al. (2005). Fusion of LIDAR data and high resolution images for forest canopy modelling. *Proc. 26th Asian Conf. on Remote Sensing*.
- Chen, Q., et al. (2006). Isolating individual trees in a savanna woodland using small footprint lidar data. *Photogrammetric Engineering and Remote Sensing*, 72(8), 923-932.
- Danson, F., et al. (2008). *Terrestrial laser scanners to measure forest canopy gap fraction*.
- Deng, F., et al. (2007). A methodology for fusion LIDAR and digital images - art. no. 67952C. *Second International Conference on Space Information Technology, Pts 1-3*, 6795, C7952-C7952.
- Drake, J. B., et al. (2001). Relationship between lidar metrics and aboveground biomass in closed-canopy neotropical forests. *International Archives of*.
- Dralle, K., et al. (1996). Stem number estimation by kernel smoothing of aerial photos. *Canadian Journal of Forest Research*, 26(7), 1228-1236.
- El-Sheimy, N., et al. (2005). *Digital terrain modeling: acquisition, manipulation, and applications*: Artech House.
- Erdody, T. L., et al. (2010). Fusion of LiDAR and imagery for estimating forest canopy fuels. *Remote Sensing of Environment*, 114(4), 725-737.
- FAO. (2010). *Global Forest Resources Assessment 2010*. Rome.
- Gibbs, H. K., et al. (2007). Monitoring and estimating tropical forest carbon stocks: making REDD a reality. *Environmental Research Letters*, 2(4), 045023.
- Goetz, S. J., et al. (2009). Mapping and monitoring carbon stocks with satellite observations: a comparison of methods. *Carbon Balance and Management*, 4(1), 2.
- Gougeon, F. A. (1995). A crown-following approach to the automatic delineation of individual tree crowns in high spatial resolution aerial images. *Canadian Journal of Remote Sensing*, 21(3), 274-284.
- Harding, D., et al. (2001). Laser altimeter canopy height profiles: Methods and validation for closed-canopy, broadleaf forests. *Remote Sensing of Environment*, 76(3), 283-297.
- Heinzel, J. N., et al. (2008). Full automatic detection of tree species based on delineated single tree crowns a data fusion approach for airborne laser scanning data and aerial photographs. *on LiDAR*.
- Heritage, G. L., et al. (Eds.). (2009). *Laser scanning for the environmental sciences*. US: Wiley-Blackwell.
- Hill, R., et al. (2005). Mapping woodland species composition and structure using airborne spectral and LiDAR data. *International Journal of Remote Sensing*, 26(17), 3763-3779.
- Holmgren, J., et al. (2004). Identifying species of individual trees using airborne laser scanner. *Remote Sensing of Environment*, 90(4), 415-423.
- Hopkinson, C., et al. (2004). Assessing forest metrics with a ground-based scanning lidar. *Canadian Journal of Forest Research*, 34(3), 573-583.

- Houghton, R. A. (2005). Aboveground Forest Biomass and the Global Carbon Balance. *Global Change Biology*, 11(6), 945-958.
- Huber, M., et al. (2003). Fusion of LIDAR data and aerial imagery for automatic reconstruction of building surfaces. *2nd Grss/Isprs Joint Workshop on Remote Sensing and Data Fusion over Urban Areas*, 82-86.
- Hudak, A. T., et al. (2002). Integration of lidar and Landsat ETM+ data for estimating and mapping forest canopy height. *Remote Sensing of Environment*, 82(2-3), 397-416.
- Hussin, Y., et al. (1991). Estimating splash pine biomass using radar backscatter. *Geoscience and Remote Sensing, IEEE Transactions on*, 29(3), 427-431.
- Hyypä, J., et al. (2008). Review of methods of small-footprint airborne laser scanning for extracting forest inventory data in boreal forests. *International Journal of Remote Sensing*, 29(5), 1339-1366.
- Hyypä, J., et al. (2009). Forest inventory using small-footprint airborne LiDAR. *Topographic Laser Ranging and Scanning: Principles and Processing*, 335-370.
- Innes, J. L., et al. (1998). Forest biodiversity and its assessment by remote sensing. *Global Ecology and Biogeography Letters*, 397-419.
- Ke, Y., et al. (2010). Synergistic use of QuickBird multispectral imagery and LIDAR data for object-based forest species classification. *Remote Sensing of Environment*, 114(6), 1141-1154.
- Kebiao, H., et al. (2010, 18-20 June 2010). *Regional aboveground forest biomass estimation using airborne and spaceborne LiDAR fusion with optical data in the Southwest of China*. Paper presented at the Geoinformatics, 2010 18th International Conference on.
- Kim, S. R., et al. (2010). Estimation of carbon storage based on individual tree detection in Pinus densiflora stands using a fusion of aerial photography and LiDAR data. *Science China-Life Sciences*, 53(7), 885-897.
- Koch, B. (2010). Status and future of laser scanning, synthetic aperture radar and hyperspectral remote sensing data for forest biomass assessment. *Isprs Journal of Photogrammetry and Remote Sensing*, 65(6), 581-590.
- Koch, B., et al. (2006). Detection of individual tree crowns in airborne lidar data. *Photogrammetric Engineering and Remote Sensing*, 72(4), 357-363.
- Large, A. R. G., et al. (2009). Laser Scanning: The Future. *Laser Scanning for the Environmental Sciences*, 262-271.
- Le Toan, T., et al. (1992). Relating forest biomass to SAR data. *Geoscience and Remote Sensing, IEEE Transactions on*, 30(2), 403-411.
- Le Wang, P. G., et al. (2004). Individual tree-crown delineation and treetop detection in high-spatial-resolution aerial imagery. *Photogrammetric Engineering & Remote Sensing*, 70(3), 351-357.
- Leckie, D., et al. (1998). Forestry applications using imaging radar. *Principles and Applications of Imaging Radar*, 2, 435-509.
- Lefsky, M. A., et al. (1999). Lidar remote sensing of the canopy structure and biophysical properties of Douglas-fir western hemlock forests. *Remote Sensing of Environment*, 70(3), 339-361.
- Lefsky, M. A., et al. (2001). Lidar remote sensing of aboveground biomass in three biomes. *International archives of photogrammetry remote sensing and spatial information sciences.*, 34(3/W4), 155-162.
- Lefsky, M. A., et al. (2002). Lidar remote sensing for ecosystem studies. *BioScience*, 52(1), 19-30.
- Lefsky, M. A., et al. (2005). Estimates of forest canopy height and aboveground biomass using ICESat. *Geophysical Research Letters*, 32(22), L22S02.
- Li, Y. (2009). *Towards Small-footprint Airborne LiDAR-assisted Large Scale Operational Forest Inventory*. University of Washington.
- Lim, K., et al. (2003). LiDAR remote sensing of forest structure. *Progress in Physical Geography*, 27(1), 88-106.
- Litkey, P., et al. (2008). *Single-scan TLS methods for forest parameter retrieval*.
- Lu, D. (2006). The potential and challenge of remote sensing-based biomass estimation. *International Journal of Remote Sensing*, 27(7), 1297-1328.
- Lucas, R., et al. (2008). Classification of Australian forest communities using aerial photography, CASI and HyMap data. *Remote Sensing of Environment*, 112(5), 2088-2103.
- Luckman, A., et al. (1997). A study of the relationship between radar backscatter and regenerating tropical forest biomass for spaceborne SAR instruments. *Remote Sensing of Environment*, 60(1), 1-13.
- Mallet, C., et al. (2009). Full-waveform topographic lidar: State-of-the-art. *ISPRS journal of photogrammetry and remote sensing*, 64(1), 1-16.
- Maltamo, M., et al. (2009). Predicting tree attributes and quality characteristics of Scots pine using airborne laser scanning data. *Silva Fennica*, 43(3), 507-521.

- McGaughey, R. J., et al. (2003). Fusing LIDAR data, photographs, and other data using 2D and 3D visualization techniques. *Proceedings of Terrain Data: Applications and Visualization—Making the Connection*, 28-30.
- Means, J. E., et al. (1999). Use of large-footprint scanning airborne lidar to estimate forest stand characteristics in the Western Cascades of Oregon. *Remote Sensing of Environment*, 67(3), 298-308.
- Meyer, F., et al. (1990). Morphological segmentation. *Journal of visual communication and image representation*, 1(1), 21-46.
- Moskal, L. M., et al. Lidar Applications in Precision Forestry.
- Mumtaz, S. A., et al. (2008). Fusion of High Resolution Lidar and Aerial Images for Object Extraction. *Icast 2008: Proceedings of 2nd International Conference on Advances in Space Technologies*, 163-168.
- Næsset, E. (2007). Airborne laser scanning as a method in operational forest inventory: Status of accuracy assessments accomplished in Scandinavia. *Scandinavian Journal of Forest Research*, 22(5), 433-442.
- Næsset, E., et al. (2004). Laser scanning of forest resources: the Nordic experience. *Scand. J. For. Res.*, 19(6), 482-499.
- Nelson, R., et al. (1988). Estimating forest biomass and volume using airborne laser data. *Remote Sensing of Environment*, 24(2), 247-267.
- NSIDC. (2011). DAAC Data Projects: LIDAR. *National Snow and Ice Data Centre*. Retrieved 23rd August, 2011, from <http://nsidc.org/daac/projects/lidar/glas.html>
- Pang, Y., et al. (2006). *Model based terrain effect analyses on ICESat GLAS waveforms*.
- Patenaude, G., et al. (2005). Synthesis of remote sensing approaches for forest carbon estimation: reporting to the Kyoto Protocol. *Environmental Science & Policy*, 8(2), 161-178.
- Persson, A., et al. (2002). Detecting and measuring individual trees using an airborne laser scanner. *PE & RS- Photogrammetric Engineering & Remote Sensing*, 68(9), 925-932.
- Pflugmacher, D., et al. (2008). Regional applicability of forest height and aboveground biomass models for the geoscience laser altimeter system. *Forest Science*, 54(6), 647-657.
- Pilger, N. (2008). *Coupling LiDAR and high-resolution digital imagery for biomass estimation in mixed wood forest environments*. Paper presented at the ASPRS 2008 Annual Conference.
- Pollock, R. J., et al. (1996). The automatic recognition of individual trees in aerial images of forests based on a synthetic tree crown image model. *The University of British Columbia (Canada)*.
- Popescu, S. C. (2007). Estimating biomass of individual pine trees using airborne lidar. *Biomass and Bioenergy*, 31(9), 646-655.
- Popescu, S. C., et al. (2004). Seeing the trees in the forest: using lidar and multispectral data fusion with local filtering and variable window size for estimating tree height. *Photogrammetric Engineering and Remote Sensing*, 70(5), 589-604.
- Popescu, S. C., et al. (2003). Measuring individual tree crown diameter with lidar and assessing its influence on estimating forest volume and biomass. *Canadian Journal of Remote Sensing*, 29(5), 564-577.
- Popescu, S. C., et al. (2004). Fusion of small-footprint lidar and multispectral data to estimate plot-level volume and biomass in deciduous and pine forests in Virginia, USA. *Forest Science*, 50(4), 551-565.
- Pyysalo, U., et al. (2002). Reconstructing tree crowns from laser scanner data for feature extraction. *INTERNATIONAL ARCHIVES OF PHOTOGRAMMETRY REMOTE SENSING AND SPATIAL INFORMATION SCIENCES*, 34(3/B), 218-221.
- Reitberger, J., et al. (2007). Single tree detection in forest areas with high-density LiDAR data. *International Archives of Photogrammetry, Remote Sensing and Spatial Information Sciences*, 36, 139-144.
- Reutebuch, S. E., et al. (2003). Accuracy of a high-resolution lidar terrain model under a conifer forest canopy. *Canadian Journal of Remote Sensing*, 29(5), 527-535.
- Rosenqvist, Å., et al. (2003). A review of remote sensing technology in support of the Kyoto Protocol. *Environmental Science & Policy*, 6(5), 441-455.
- Sader, S. A. (1987). Forest biomass, canopy structure, and species composition relationships with multipolarization L-band synthetic aperture radar data. *Photogrammetric engineering and remote sensing (USA)*.
- Samberg, A., et al. (1999). *Assessing tree attributes from the laser scanner data- The high-scan case*.
- Santos, J., et al. (2002). Savanna and tropical rainforest biomass estimation and spatialization using JERS-1 data. *International Journal of Remote Sensing*, 23(7), 1217-1229.
- Schardt, M., et al. (2002). Assessment of forest parameters by means of laser scanning. *International archives of photogrammetry remote sensing and spatial information sciences*, 34(3/A), 302-309.
- Schutz, B., et al. (2005). Overview of the ICESat mission. *Geophys. Res. Lett.*, 32(21).

- Sheng, Y., et al. (2001). Model-based conifer-crown surface reconstruction from high-resolution aerial images. *PE & RS- Photogrammetric Engineering and Remote Sensing*, 67(8), 957-965.
- Soille, P. (2003). *Morphological Image Analysis: Principles and Applications*. 2003.
- Straub, C., et al. (2009). Using airborne laser scanner data and CIR orthophotos to estimate the stem volume of forest stands. *Photogrammetrie-Fernerkundung-Geoinformation*, 2009(3), 277-287.
- Sun, G., et al. (2002). Radiometric slope correction for forest biomass estimation from SAR data in the Western Sayani Mountains, Siberia. *Remote Sensing of Environment*, 79(2), 279-287.
- Thierry, Y., et al. (2007). Landslide susceptibility assessment by bivariate methods at large scales: Application to a complex mountainous environment. *Geomorphology*, 92(1-2), 38-59.
- Tiede, D., et al. (2008). Domain-specific class modelling for one-level representation of single trees. *Object-Based Image Analysis*, 133-151.
- Treuhaft, R. N., et al. (2004). Forest attributes from radar interferometric structure and its fusion with optical remote sensing. *BioScience*, 54(6), 561-571.
- Wagner, W., et al. (2006). Gaussian decomposition and calibration of a novel small-footprint full-waveform digitising airborne laser scanner. *ISPRS journal of photogrammetry and remote sensing*, 60(2), 100-112.
- Wang, C., et al. (2009). Integrating LIDAR intensity and elevation data for terrain characterization in a forested area. *Geoscience and Remote Sensing Letters, IEEE*, 6(3), 463-466.
- Wang, Y., et al. (2008). A lidar point cloud based procedure for vertical canopy structure analysis and 3D single tree modelling in forest. *Sensors*, 8(6), 3938-3951.
- Wang, Y., et al. (2008). Lidar point cloud based fully automatic 3D single tree modelling in forest and evaluations of the procedure. *International Archives of Photogrammetry, Remote Sensing and Spatial Information Sciences*, 37, 45-51.
- Wulder, M., et al. (2000). Local maximum filtering for the extraction of tree locations and basal area from high spatial resolution imagery. *Remote Sensing of Environment*, 73(1), 103-114.
- Zaremba, M. B., et al. (2006). Fusion of high-resolution satellite and LIDAR data for individual tree recognition. *2006 Canadian Conference on Electrical and Computer Engineering, Vols 1-5*, 1237-1240.
- Zianis, D., et al. (2005). Biomass and stem volume equations for tree species in Europe. *Silva Fennica Monographs*, 4(Monographs 4), 1-63.
- Andersen, H. E., et al. (2003). Estimating forest structure parameters on Fort Lewis Military Reservation using airborne laser scanner (LIDAR) data. *PRECISION FORESTRY*, 45.
- Andersen, H. E., et al. (2006). A rigorous assessment of tree height measurements obtained using airborne lidar and conventional field methods. *Canadian Journal of Remote Sensing*, 32(5), 355-366.
- ASPRS. (2008). Superseded ASPRS LAS 1.2 Format Specification, September 2, 2008 *ASPRS Standards Committee*, from http://www.asprs.org/a/society/committees/standards/lidar_exchange_format.html
- Azahari Razak, K., et al. (2010). Use of high resolution Airborne Laser Scanning data for landslide interpretation under mixed forest and tropical rainforest: case study in Barcelonnette, France and Cameron Highlands, Malaysia. *EGU General Assembly 2010, held 2-7 May, 2010 in Vienna, Austria, p. 7184, 12, 7184*.
- Beaudoin, A., et al. (1994). Retrieval of forest biomass from SAR data. *International Journal of Remote Sensing*, 15(14), 2777-2796.
- Beucher, S., et al. (1979). Use of watersheds in contour detection.
- Bortolot, Z. J. (2006). Using tree clusters to derive forest properties from small footprint LiDAR data. *Photogrammetric Engineering and Remote Sensing*, 72(12), 1389.
- Boudreau, J., et al. (2008). Regional aboveground forest biomass using airborne and spaceborne LiDAR in Québec. *Remote Sensing of Environment*, 112(10), 3876-3890.
- Brandtberg, T., et al. (1998). Automated delineation of individual tree crowns in high spatial resolution aerial images by multiple-scale analysis. *Machine Vision and Applications*, 11(2), 64-73.
- Brandtberg, T., et al. (2003). Detection and analysis of individual leaf-off tree crowns in small footprint, high sampling density lidar data from the eastern deciduous forest in North America. *Remote Sensing of Environment*, 85(3), 290-303.
- Brown, S., et al. (1995). Use of forest inventories and geographic information systems to estimate biomass density of tropical forests: Application to tropical Africa. *Environmental Monitoring and Assessment*, 38(2-3), 157-168.

- Bucksch, A., et al. (2008). CAMPINO — A skeletonization method for point cloud processing. *ISPRS journal of photogrammetry and remote sensing*, 63(1), 115-127.
- Bucksch, A., et al. (2009). SkelTre. *The Visual Computer*, 1-18.
- Castel, T., et al. (2002). Retrieval biomass of a large Venezuelan pine plantation using JERS-1 SAR data. Analysis of forest structure impact on radar signature. *Remote Sensing of Environment*, 79(1), 30-41.
- Chen, L. C., et al. (2005). Fusion of LIDAR data and high resolution images for forest canopy modelling. *Proc. 26th Asian Conf. on Remote Sensing*.
- Chen, Q., et al. (2006). Isolating individual trees in a savanna woodland using small footprint lidar data. *Photogrammetric Engineering and Remote Sensing*, 72(8), 923-932.
- Clinton, N., et al. (2010). Accuracy Assessment Measures for Object-based Image Segmentation Goodness. *Photogrammetric Engineering and Remote Sensing*, 76(3), 289-299.
- Coillie, F. M. B., et al. (2008). Semi-automated forest stand delineation using wavelet based segmentation of very high resolution optical imagery. In T. Blaschke, S. Lang & G. J. Hay (Eds.), *Object-Based Image Analysis* (pp. 237-256): Springer Berlin Heidelberg.
- Culvenor, D. S. (2002). TIDA: an algorithm for the delineation of tree crowns in high spatial resolution remotely sensed imagery. *Computers & Geosciences*, 28(1), 33-44.
- Danson, F., et al. (2008). *Terrestrial laser scanners to measure forest canopy gap fraction*.
- Definiens (2009). *eCognition Developer 8, reference book*. Munchen, Germany.
- Deng, F., et al. (2007). A methodology for fusion LIDAR and digital images - art. no. 67952C. *Second International Conference on Space Information Technology, Pts 1-3, 6795, C7952-C7952*.
- Drake, J. B., et al. (2001). Relationship between lidar metrics and aboveground biomass in closed-canopy neotropical forests. *International Archives of*.
- Dralle, K., et al. (1996). Stem number estimation by kernel smoothing of aerial photos. *Canadian Journal of Forest Research*, 26(7), 1228-1236.
- El-Sheimy, N., et al. (2005). *Digital terrain modeling: acquisition, manipulation, and applications*: Artech House.
- Erdody, T. L., et al. (2010). Fusion of LiDAR and imagery for estimating forest canopy fuels. *Remote Sensing of Environment*, 114(4), 725-737.
- Erikson, M., et al. (2005). Comparison of three individual tree crown detection methods. *Machine Vision and Applications*, 16(4), 258-265.
- FAO. (2010). *Global Forest Resources Assessment 2010*. Rome.
- Finney, M. A., et al. (1998). *FARSITE, Fire Area Simulator--model development and evaluation*: US Dept. of Agriculture, Forest Service, Rocky Mountain Research Station.
- Folkesson, K., et al. (2006). *Automatic detection of wind-thrown forest in VHF SAR images*.
- Gibbs, H. K., et al. (2007). Monitoring and estimating tropical forest carbon stocks: making REDD a reality. *Environmental Research Letters*, 2(4), 045023.
- Goetz, S. J., et al. (2009). Mapping and monitoring carbon stocks with satellite observations: a comparison of methods. *Carbon Balance and Management*, 4(1), 2.
- Gougeon, F., et al. (2006). The individual tree crown approach applied to Ikonos images of a coniferous plantation area. *Photogrammetric Engineering and Remote Sensing*, 72, 1287-1297.
- Gougeon, F. A. (1995). A crown-following approach to the automatic delineation of individual tree crowns in high spatial resolution aerial images. *Canadian Journal of Remote Sensing*, 21(3), 274-284.
- Hale, C. M., et al. (2004). Allometric equations for estimation of ash-free dry mass from length measurements for selected European earthworm species (Lumbricidae) in the western Great Lakes region. *The American midland naturalist*, 151(1), 179-185.
- Harding, D., et al. (2001). Laser altimeter canopy height profiles: Methods and validation for closed-canopy, broadleaf forests. *Remote Sensing of Environment*, 76(3), 283-297.
- Heinzel, J. N., et al. (2008). Full automatic detection of tree species based on delineated single tree crowns a data fusion approach for airborne laser scanning data and aerial photographs. *on LiDAR*.
- Heritage, G. L., et al. (Eds.). (2009). *Laser scanning for the environmental sciences*. US: Wiley-Blackwell.
- Heurich, M., et al. (2004). Detecting and measuring individual trees with laser scanning in mixed mountain forest of Central Europe using an algorithm developed for Swedish boreal forest conditions. *International Archives of Photogrammetry, Remote Sensing and Spatial Information Sciences*, 36, 307-312.
- Hippolyte, J. C., et al. (2000). Identification of Quaternary thrusts, folds and faults in a low seismicity area: examples in the Southern Alps (France). *Terra Nova*, 12(4), 156-162.

- Holmgren, J., et al. (2004). Identifying species of individual trees using airborne laser scanner. *Remote Sensing of Environment*, 90(4), 415-423.
- Hopkinson, C., et al. (2004). Assessing forest metrics with a ground-based scanning lidar. *Canadian Journal of Forest Research*, 34(3), 573-583.
- Houghton, R. A. (2005). Aboveground Forest Biomass and the Global Carbon Balance. *Global Change Biology*, 11(6), 945-958.
- Hu, J., et al. (2003). Approaches to large-scale urban modeling. *Computer Graphics and Applications, IEEE*, 23(6), 62-69.
- Huber, M., et al. (2003). Fusion of LIDAR data and aerial imagery for automatic reconstruction of building surfaces. *2nd Grss/Isprs Joint Workshop on Remote Sensing and Data Fusion over Urban Areas*, 82-86.
- Hudak, A. T., et al. (2002). Integration of lidar and Landsat ETM+ data for estimating and mapping forest canopy height. *Remote Sensing of Environment*, 82(2-3), 397-416.
- Husch, B., et al. (2003). *Forest mensuration* (Fourth edition ed.). Hoboken: Wiley & Sons.
- Hussin, Y., et al. (1991). Estimating splash pine biomass using radar backscatter. *Geoscience and Remote Sensing, IEEE Transactions on*, 29(3), 427-431.
- Hyypä, J., et al. (2008). Review of methods of small-footprint airborne laser scanning for extracting forest inventory data in boreal forests. *International Journal of Remote Sensing*, 29(5), 1339-1366.
- Hyypä, J., et al. (2004). Algorithms and methods of airborne laser-scanning for forest measurements. *International Archives of Photogrammetry, Remote Sensing and Spatial Information Sciences*, 36(8/W2), 82-89.
- Hyypä, J., et al. (2009). Forest inventory using small-footprint airborne LiDAR. *Topographic Laser Ranging and Scanning: Principles and Processing*, 335-370.
- Innes, J. L., et al. (1998). Forest biodiversity and its assessment by remote sensing. *Global Ecology and Biogeography Letters*, 397-419.
- Ke, Y., et al. (2008). *Comparison of individual tree crown detection and delineation methods*. Paper presented at the ASPRS Annual conference "Bridging the Horizons: New Frontiers in Geospatial Collaboration", Portland, Oregon, US.
- Ke, Y., et al. (2010). Synergistic use of QuickBird multispectral imagery and LIDAR data for object-based forest species classification. *Remote Sensing of Environment*, 114(6), 1141-1154.
- Kebiao, H., et al. (2010, 18-20 June 2010). *Regional aboveground forest biomass estimation using airborne and spaceborne LiDAR fusion with optical data in the Southwest of China*. Paper presented at the Geoinformatics, 2010 18th International Conference on.
- Kim, M., et al. (2009). Forest Type Mapping using Object-specific Texture Measures from Multispectral Ikonos Imagery: Segmentation Quality and Image Classification Issues. [Article]. *Photogrammetric Engineering and Remote Sensing*, 75(7), 819-829.
- Kim, S., et al. INDIVIDUAL TREE SPECIES IDENTIFICATION USING LIDAR INTENSITY DATA.
- Kim, S. R., et al. (2010). Estimation of carbon storage based on individual tree detection in Pinus densiflora stands using a fusion of aerial photography and LiDAR data. *Science China-Life Sciences*, 53(7), 885-897.
- Koch, B. (2010). Status and future of laser scanning, synthetic aperture radar and hyperspectral remote sensing data for forest biomass assessment. *Isprs Journal of Photogrammetry and Remote Sensing*, 65(6), 581-590.
- Koch, B., et al. (2006). Detection of individual tree crowns in airborne lidar data. *Photogrammetric Engineering and Remote Sensing*, 72(4), 357-363.
- Korpela, I., et al. (2010). Tree species classification using airborne lidar—effects of stand and tree parameters, downsizing of training set, intensity normalization, and sensor type. *Silva Fennica*, 44(2), 319-339.
- Kwak, D. A., et al. (2007). Detection of individual trees and estimation of tree height using LiDAR data. *Journal of Forest*.
- Large, A. R. G., et al. (2009). Laser Scanning: The Future. *Laser Scanning for the Environmental Sciences*, 262-271.
- Le Toan, T., et al. (1992). Relating forest biomass to SAR data. *Geoscience and Remote Sensing, IEEE Transactions on*, 30(2), 403-411.

- Le Wang, P. G., et al. (2004). Individual tree-crown delineation and treetop detection in high-spatial-resolution aerial imagery. *Photogrammetric Engineering & Remote Sensing*, 70(3), 351-357.
- Leckie, D., et al. (1998). Forestry applications using imaging radar. *Principles and Applications of Imaging Radar*, 2, 435-509.
- Leckie, D. G., et al. (2005). Automated tree recognition in old growth conifer stands with high resolution digital imagery. *Remote Sensing of Environment*, 94(3), 311-326.
- Lefsky, M. A., et al. (1999). Lidar remote sensing of the canopy structure and biophysical properties of Douglas-fir western hemlock forests. *Remote Sensing of Environment*, 70(3), 339-361.
- Lefsky, M. A., et al. (2001). Lidar remote sensing of aboveground biomass in three biomes. *International archives of photogrammetry remote sensing and spatial information sciences.*, 34(3/W4), 155-162.
- Lefsky, M. A., et al. (2002). Lidar remote sensing for ecosystem studies. *BioScience*, 52(1), 19-30.
- Lefsky, M. A., et al. (2005). Estimates of forest canopy height and aboveground biomass using ICESat. *Geophysical Research Letters*, 32(22), L22S02.
- Li, Y. (2009). *Towards Small-footprint Airborne LiDAR-assisted Large Scale Operational Forest Inventory*. University of Washington.
- Lim, K., et al. (2003). LiDAR remote sensing of forest structure. *Progress in Physical Geography*, 27(1), 88-106.
- Litkey, P., et al. (2008). *Single-scan TLS methods for forest parameter retrieval*.
- Liu, X. (2008). Airborne LiDAR for DEM generation: some critical issues. *Progress in Physical Geography*, 32(1), 31.
- Lu, D. (2006). The potential and challenge of remote sensing-based biomass estimation. *International Journal of Remote Sensing*, 27(7), 1297-1328.
- Luckman, A., et al. (1997). A study of the relationship between radar backscatter and regenerating tropical forest biomass for spaceborne SAR instruments. *Remote Sensing of Environment*, 60(1), 1-13.
- Mallet, C., et al. (2009). Full-waveform topographic lidar: State-of-the-art. *ISPRS journal of photogrammetry and remote sensing*, 64(1), 1-16.
- Maltamo, M., et al. (2009). Predicting tree attributes and quality characteristics of Scots pine using airborne laser scanning data. *Silva Fennica*, 43(3), 507-521.
- McCullagh, M. (1988). Terrain and surface modelling systems: theory and practice. *The photogrammetric record*, 12(72), 747-779.
- McGaughey, R. J., et al. (2003). Fusing LIDAR data, photographs, and other data using 2D and 3D visualization techniques. *Proceedings of Terrain Data: Applications and Visualization—Making the Connection*, 28-30.
- Means, J. E., et al. (1999). Use of large-footprint scanning airborne lidar to estimate forest stand characteristics in the Western Cascades of Oregon. *Remote Sensing of Environment*, 67(3), 298-308.
- Meyer, F., et al. (1990). Morphological segmentation. *Journal of visual communication and image representation*, 1(1), 21-46.
- Moffiet, T., et al. (2005). Airborne laser scanning: Exploratory data analysis indicates potential variables for classification of individual trees or forest stands according to species. *ISPRS journal of photogrammetry and remote sensing*, 59(5), 289-309.
- Möller, M., et al. (2007). The comparison index: A tool for assessing the accuracy of image segmentation. *International Journal of Applied Earth Observation and Geoinformation*, 9(3), 311-321.
- Moskal, L. M., et al. (2008). Lidar Applications in Precision Forestry.
- Mumtaz, S. A., et al. (2008). Fusion of High Resolution Lidar and Aerial Images for Object Extraction. *Icast 2008: Proceedings of 2nd International Conference on Advances in Space Technologies*, 163-168.
- Næsset, E. (2007). Airborne laser scanning as a method in operational forest inventory: Status of accuracy assessments accomplished in Scandinavia. *Scandinavian Journal of Forest Research*, 22(5), 433-442.
- Naesset, E., et al. (2004). Laser scanning of forest resources: the Nordic experience. *Scand. J. For. Res.*, 19(6), 482-499.
- Nelson, R., et al. (1988). Estimating forest biomass and volume using airborne laser data. *Remote Sensing of Environment*, 24(2), 247-267.
- NSIDC. (2011). DAAC Data Projects: LIDAR. *National Snow and Ice Data Centre*. Retrieved 23rd August, 2011, from <http://nsidc.org/daac/projects/lidar/glas.html>
- Pang, Y., et al. (2006). *Model based terrain effect analyses on ICESat GLAS waveforms*.
- Patenaude, G., et al. (2005). Synthesis of remote sensing approaches for forest carbon estimation: reporting to the Kyoto Protocol. *Environmental Science & Policy*, 8(2), 161-178.

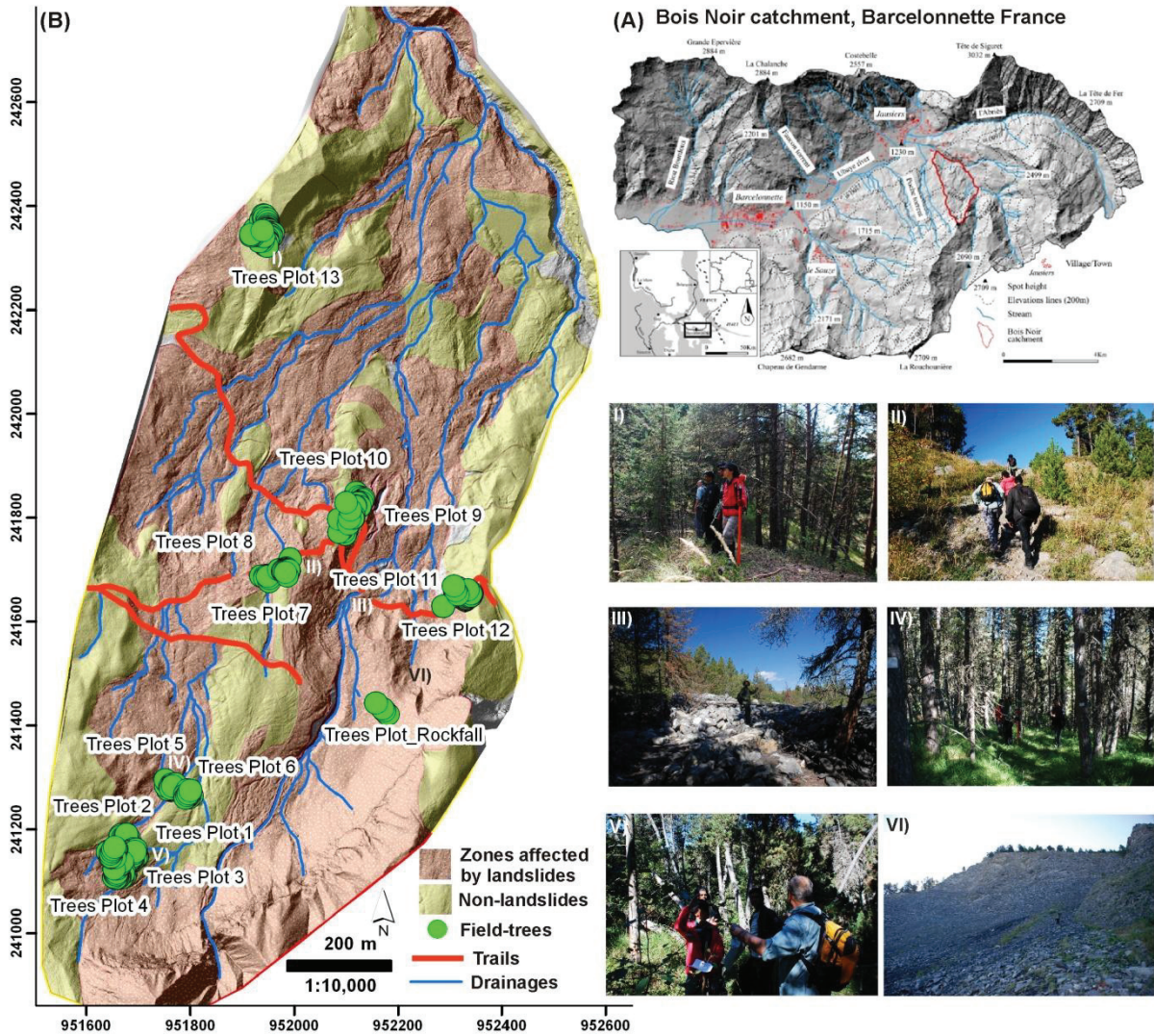
- Persson, A., et al. (2002). Detecting and measuring individual trees using an airborne laser scanner. *PE & RS- Photogrammetric Engineering & Remote Sensing*, 68(9), 925-932.
- Pflugmacher, D., et al. (2008). Regional applicability of forest height and aboveground biomass models for the geoscience laser altimeter system. *Forest Science*, 54(6), 647-657.
- Pilger, N. (2008). *Coupling LiDAR and high-resolution digital imagery for biomass estimation in mixed wood forest environments*. Paper presented at the ASPRS 2008 Annual Conference.
- Pitkänen, J., et al. (2004). Adaptive methods for individual tree detection on airborne laser based canopy height model. *International Archives of Photogrammetry, Remote Sensing and Spatial Information Sciences*, 36(8), W2.
- Pollock, R. J., et al. (1996). The automatic recognition of individual trees in aerial images of forests based on a synthetic tree crown image model. *The University of British Columbia (Canada)*.
- Popescu, S. C. (2007). Estimating biomass of individual pine trees using airborne lidar. *Biomass and Bioenergy*, 31(9), 646-655.
- Popescu, S. C., et al. (2004). Seeing the trees in the forest: using lidar and multispectral data fusion with local filtering and variable window size for estimating tree height. *Photogrammetric Engineering and Remote Sensing*, 70(5), 589-604.
- Popescu, S. C., et al. (2003). Measuring individual tree crown diameter with lidar and assessing its influence on estimating forest volume and biomass. *Canadian Journal of Remote Sensing*, 29(5), 564-577.
- Popescu, S. C., et al. (2004). Fusion of small-footprint lidar and multispectral data to estimate plot-level volume and biomass in deciduous and pine forests in Virginia, USA. *Forest Science*, 50(4), 551-565.
- Pouliot, D. A., et al. (2002). Automated tree crown detection and delineation in high-resolution digital camera imagery of coniferous forest regeneration. *Remote Sensing of Environment*, 82(2-3), 322-334.
- Pyysalo, U., et al. (2002). Reconstructing tree crowns from laser scanner data for feature extraction. *INTERNATIONAL ARCHIVES OF PHOTOGRAMMETRY REMOTE SENSING AND SPATIAL INFORMATION SCIENCES*, 34(3/B), 218-221.
- Rahman, M., et al. (2009). *Tree crown delineation from high resolution airborne lidar based on densities of high points*.
- Reitberger, J., et al. (2007). Single tree detection in forest areas with high-density LiDAR data. *International Archives of Photogrammetry, Remote Sensing and Spatial Information Sciences*, 36, 139-144.
- Reutebuch, S. E., et al. (2003). Accuracy of a high-resolution lidar terrain model under a conifer forest canopy. *Canadian Journal of Remote Sensing*, 29(5), 527-535.
- Rosenqvist, Å., et al. (2003). A review of remote sensing technology in support of the Kyoto Protocol. *Environmental Science & Policy*, 6(5), 441-455.
- Sader, S. A. (1987). Forest biomass, canopy structure, and species composition relationships with multipolarization L-band synthetic aperture radar data. *Photogrammetric engineering and remote sensing (USA)*.
- Samberg, A., et al. (1999). *Assessing tree attributes from the laser scanner data- The high-scan case*.
- Santos, J., et al. (2002). Savanna and tropical rainforest biomass estimation and spatialization using JERS-1 data. *International Journal of Remote Sensing*, 23(7), 1217-1229.
- Schardt, M., et al. (2002). Assessment of forest parameters by means of laser scanning. *International archives of photogrammetry remote sensing and spatial information sciences*, 34(3/A), 302-309.
- Schutz, B., et al. (2005). Overview of the ICESat mission. *Geophys. Res. Lett.*, 32(21).
- Scott, J. H., et al. (2002). Estimating canopy fuels in conifer forests. *Fire Management Today*, 62(4), 45-50.
- Sheng, Y., et al. (2001). Model-based conifer-crown surface reconstruction from high-resolution aerial images. *PE & RS- Photogrammetric Engineering and Remote Sensing*, 67(8), 957-965.
- Soille, P. (2003). *Morphological Image Analysis: Principles and Applications*. 2003.
- Straub, C., et al. (2009). Using airborne laser scanner data and CIR orthophotos to estimate the stem volume of forest stands. *Photogrammetrie-Fernerkundung-Geoinformation*, 2009(3), 277-287.
- Sun, G., et al. (2002). Radiometric slope correction for forest biomass estimation from SAR data in the Western Sayani Mountains, Siberia. *Remote Sensing of Environment*, 79(2), 279-287.
- Thiery, Y., et al. (2007). Landslide susceptibility assessment by bivariate methods at large scales: Application to a complex mountainous environment. *Geomorphology*, 92(1-2), 38-59.
- Thiery, Y., et al. (2003). Towards the construction of a spatial database to manage landslides with GIS in mountainous environment. *Proceedings of the 6th AGILE 2003: The science behind the infrastructure*, 37-44.

- Treuhaff, R. N., et al. (2004). Forest attributes from radar interferometric structure and its fusion with optical remote sensing. *BioScience*, 54(6), 561-571.
- USGS. Rocky Mountain Mapping Center. from http://rockyweb.cr.usgs.gov/elevation/dpi_dem.html
- Wang, L., et al. (2004). Individual Tree-Crown Delineation and Treetop Detection in High Spatial Resolution Areal Imagery. *Photogrammetric Engineering and Remote Sensing*, 70(3), 351-357.
- Wang, Y., et al. (2008). A lidar point cloud based procedure for vertical canopy structure analysis and 3D single tree modelling in forest. *Sensors*, 8(6), 3938-3951.
- Wulder, M., et al. (2000). Local maximum filtering for the extraction of tree locations and basal area from high spatial resolution imagery. *Remote Sensing of Environment*, 73(1), 103-114.
- Z Li, et al. (2009). *Towards Automatic Tree Crown Detection and Delineation in Spectral Feature Space Using PCNN and Morphological Reconstruction*. Paper presented at the *IEEE 16th International Conference on Image Processing ICIP 2009*, Cairo, Egypt.
- Zaremba, M. B., et al. (2006). Fusion of high-resolution satellite and LIDAR data for individual tree recognition. *2006 Canadian Conference on Electrical and Computer Engineering, Vols 1-5*, 1237-1240.
- Zhan, Q. M., et al. (2005). Quality assessment for geo-spatial objects derived from remotely sensed data. [Proceedings Paper]. *International Journal of Remote Sensing*, 26(14), 2953-2974.

APPENDICES

Appendix 1. Barcelonnette catchment, (B). Location of field plots for tree sampling in Bois noir forests, Barcelonnette, France. I to VI: Field photographs (source: (Azahari Razak et al., 2010))

Sample plots in Bois noir Forests, Barcelonnette France



Appendix 2. Ruleset for Region Growing in eCognition

- chess board: 4 creating 'New Level'
 - unclassified with Mean Layer 1 < 0.5 at New Level: Gap
 - Gap with Border to unclassified > 1 Pxl at New Level: Bgap
 - Gap at New Level: merge region
 - Bgap at New Level: chess board: 2
 - Bgap with Mean Layer 1 < 0.4 at New Level: Gap
 - Gap at New Level: merge region
 - Bgap at New Level: chess board: 1
 - Bgap with Mean Layer 1 < 0.3 at New Level: Gap
 - Gap at New Level: merge region
 - Bgap, unclassified at New Level: assign class by thematic layer using TreeTop
 - unclassified with Border to 99 > 1 Pxl at New Level: TreeTop
 - TreeTop at New Level: chess board: 2
 - 99 with Existence of minima (0) < 1 and Mean Diff. to neighbors Layer 2 (0) >= 0 at New Level: <- TreeTop, unclassified Mean diff. to brighter neighbors Layer 2 < 3
 - 99 with Existence of minima (0) < 1 and Mean Diff. to neighbors Layer 2 (0) >= 0 at New Level: <- TreeTop, unclassified Mean diff. to brighter neighbors Layer 2 < 0.5
 - Bgap, TreeTop, unclassified at New Level: assign class by thematic layer using GRIDCODE
 - 0 with Border to unclassified > 1 Pxl at New Level: Bgap
 - 0 with Border to 99 >= 1 Pxl at New Level: Bgap
 - 0 at New Level: Gap
 - Gap at New Level: merge region
 - Bgap at New Level: <- unclassified Mean Layer 1 < 2.5
 - Bgap at New Level: chess board: 2
 - Bgap with Mean Layer 1 < 2 at New Level: Gap
 - Gap at New Level: merge region
 - Bgap with Mean Layer 1 < 2 at New Level: Gap
 - Gap at New Level: merge region
 - TreeTop, unclassified at New Level: Tree
 - Bgap, Tree at New Level: min Layer 1 : minima
- grow region
 - minima with Existence of 99 (0) >= 1 at New Level: Tree
 - 2x: 99 with Existence of minima (0) < 1 and Rel. border to Gap < 1 at New Level: <- Bgap, Tree Mean diff. to brighter neighbors Layer 2 < 1
 - 2x: 99 with Existence of minima (0) < 1 and Rel. border to Gap < 1 at New Level: <- Bgap, Tree Mean diff. to brighter neighbors Layer 2 < 1
 - 2x: 99 with Existence of minima (0) < 1 and Rel. border to Gap < 1 at New Level: <- Bgap, Tree Mean diff. to brighter neighbors Layer 2 < 2
 - minima with Existence of 99 (0) >= 1 at New Level: Tree
 - 2x: 99 with Existence of minima (0) < 1 and Mean Diff. to neighbors Layer 2 (0) >= 0 at New Level: <- Bgap, Tree Mean diff. to brighter neighbors Layer 2 < 2
 - minima with Existence of 99 (0) >= 1 at New Level: Tree
 - 4x: 99 with Existence of minima (0) < 1 and Mean Diff. to neighbors Layer 2 (0) >= -1 at New Level: <- Bgap, Tree Mean diff. to brighter neighbors Layer 2 < 2
 - minima at New Level: chess board: 2
 - minima with Mean Layer 1 < 2 at New Level: Gap
 - minima with Existence of 99 (0) >= 1 at New Level: Tree
 - 4x: 99 with Existence of minima (0) < 1 and Mean Diff. to neighbors Layer 2 (0) >= -1 at New Level: <- Bgap, Tree Mean diff. to brighter neighbors Layer 2 < 3
 - minima with Existence of 99 (0) >= 1 at New Level: Tree
 - 4x: 99 with Existence of minima (0) < 1 and Mean Diff. to neighbors Layer 2 (0) >= -1 at New Level: <- Bgap, Tree Mean diff. to brighter neighbors Layer 2 < 3
 - minima with Existence of 99 (0) >= 1 at New Level: Tree
 - 4x: 99 with Existence of minima (0) < 1 and Mean Diff. to neighbors Layer 2 (0) >= -1 at New Level: <- Bgap, Tree Mean diff. to brighter neighbors Layer 2 < 3
 - Bgap at New Level: chess board: 1
 - Bgap with Mean Layer 1 < 2 at New Level: Gap
 - Gap at New Level: merge region
 - minima with Existence of 99 (0) >= 1 at New Level: Tree
 - 12x: 99 with Existence of minima (0) < 1 and Mean Diff. to neighbors Layer 2 (0) >= -1 at New Level: <- Bgap, Tree Mean diff. to brighter neighbors Layer 2 < 5
 - minima at New Level: chess board: 1
 - minima with Mean Layer 1 < 2 at New Level: Gap
 - Gap at New Level: merge region
 - minima at New Level: Tree
 - 12x: 99 with Existence of minima (0) < 1 and Mean Diff. to neighbors Layer 2 (0) >= -1 at New Level: <- Bgap, Tree Mean diff. to brighter neighbors Layer 2 < 5
 - 4x: 99 with Existence of minima (0) < 1 and Mean Diff. to neighbors Layer 2 (0) >= -2 at New Level: <- Bgap, Tree Mean diff. to brighter neighbors Layer 2 < 7
 - Bgap at New Level: Gap
 - Gap at New Level: merge region
 - Tree at New Level: max Layer 1 : TreeTop
 - TreeTop at New Level: merge region
 - 12x: TreeTop with Existence of minima (0) < 1 and Mean Diff. to neighbors Layer 2 (0) >= 0 at New Level: <- Tree Mean Layer 1 > 0.3
 - TreeTop with Area <= 16 Pxl at New Level: Gap
 - Gap with Area <= 16 Pxl at New Level: unclassified
 - 4x: TreeTop, 99 at New Level: <- Tree, unclassified
 - Tree at New Level: Gap
 - unclassified at New Level: Gap
 - Gap at New Level: merge region
 - TreeTop at New Level: Gap
 - Gap at New Level: merge region